Characterization of the macromolecular interactions of the key NHEJ components

Thesis

CHARACTERIZATION OF THE MACROMOLECULAR INTERACTIONS OF THE KEY NHEJ COMPONENTS

Silvia Costantini

This thesis is submitted for the degree of Doctor of Philosophy

in the Faculty of Life and Biomolecular Sciences of the Open University, UK.

International Centre for Genetic Engeneering and Biotechnology (ICGEB),

Trieste, Italy

September 2006

DATE of SUBMISSION: 26 SEPTEMBER 2006
DATE of AWARD: 4 JANUARY 2007

ProQuest LLC.
789 East Eisenhower Parkway
P.O. Box 1346
Ann Arbor, MI 48106 – 1346

To all who have helped and supported me

CONTENTS

LIST OF FIGURES

LIST OF TABLES

ABSTRACT

Non-homologous end-joining (NHEJ) is a major mechanism for repairing DNA double strand breaks in mammalian cells. Six 'core' NHEJ components have been identified to date: Ku70, Ku80, the DNA dependent protein kinase catalytic subunit DNA-PKcs, DNA ligase IV, XRCC4, and XLF-Cernunnos. In this thesis, the DNA binding properties of the Ku70/80 heterodimer are characterised by means of fluorescence anisotropy and electrophoretic mobility shift assays. Studies with duplexes holding 1, 2 or 3 heterodimers allowed to develop a binding model that can be applied to analyse the interactions of Ku with duplexes of any length. In addition, salt dependent studies indicate that electrostatic interactions play a major role in the binding of Ku to nucleic acids. The interaction of the Ku heterodimer with the DNA ligase IV/XRCC4 (LX) complex and the role of DNA-PKcs in regulating the NHEJ complex assembly are investigated. Protein-protein interaction experiments show that Ku interacts with DNA ligase IV via its tandem BRCT domain and this interaction is enhanced by the presence of XRCC4 and DNA. In particular, mutagenesis studies indicate that residues 643-748 encompassing the first BRCT domain of DNA ligase IV are necessary for binding. Moreover, Ku needs to be in its heterodimeric form to bind LX and the C-terminal of Ku80 is dispensable for this interaction. The presence of DNA-PKcs favours the interaction between Ku and LX, although its kinase activity induces the disassembly of the complex. Finally, the interaction of Ku with other factors potentially involved in NHEJ such as the replication protein A, PARP-1, and the WRN helicase is investigated. Collectively, these findings provide novel information on the macromolecular interactions that regulate the NHEJ pathway.

1 GENERAL INTRODUCTION

1.1 GENOME STABILITY AND DNA DOUBLE STRAND BREAKS

The integrity of the genome is crucial for its function. However, DNA in living cells is inherently unstable and it is constantly attacked by damaging agents that threaten its integrity. DNA damage can lead to severely impaired cellular functioning, which might cause cell death, or can induce permanent changes in the DNA sequence contributing to oncogenesis, premature ageing and severe genetic disorders (Hoeijmakers, 2001; van Gent et al., 2001). Cells have developed complex signal-transduction, cell-cycle-checkpoint and repair pathways to respond to DNA damage and promote genomic stability. About 150 genes associated with DNA repair have been identified in humans to date (Wood et al., 2005). This is not surprising considering that DNA molecules can be damaged in many ways and repair systems must be able to recognize and deal with each type of damage.

DNA double-strand breaks (DSBs) are considered as the most dangerous form of DNA damage (Hoeijmakers, 2001; Khanna and Jackson, 2001; Rich et al., 2000; van Gent et al., 2001). They are generated when the two complementary strands of the DNA double helix are broken simultaneously at sites that are sufficiently close to one another that base-pairing and chromatin structure are insufficient to keep the two ends juxtaposed (Jackson, 2002). Thus, with DSBs, DNA loses physical integrity and information content on both strands, making repair more difficult to perform than that of other types of DNA damage in which the complementary strand is used as a template. Moreover, the biochemical configuration and the structure of broken DNA ends can be very diverse and they may require processing prior to ligation.

DSBs can be generated following exposure of cells to exogenous agents or can arise during endogenous processes. Ionising radiation (IR), such as X- and γ-rays, is probably the most significant exogenous agent inducing DSBs. Although IR produces a wide spectrum of DNA lesions, DSBs represent the most dangerous ones. The type of DSB introduced by IR depends on the nature of the radiation, whether it involves high or low energy transfer (Belli et al., 2002; Pouget and Mather, 2001). The breaks formed are generally complex and may have damaged bases at their termini. Moreover, IR can produce multiple, clustered sites of damage that are introduced directly by energy deposition and indirectly by the generation of reactive oxygen species (ROS) (Pouget and Mather, 2001). Other exogenous agents that can induce DSBs are radiomimetic or chemotherapeutic drugs, such as bleomycin, neocarzinostatin, etoposide and other topoisomerase inhibitors (Povirk, 1996). DSBs are generated also by endogenous agents such as ROS produced during cellular metabolism (Lieber et al., 2003; Pouget and Mather, 2001). Metabolically generated ROS species are unlikely to give rise to the clustered damage observed with IR, they produce nevertheless DSBs that are likely associated with damaged bases and sugars (Pouget and Mather, 2001). Furthermore, DSBs are produced during programmed chromosomal rearrangements, such as meiosis to initiate recombination between homologous chromosomes, V(D)J and immunoglobulin isotype class-switch recombination (Khanna and Jackson, 2001). V(D)J recombination leads to DSBs characterized by hairpin coding ends and blunt signal ends, while meiosis probably leads to 3'-OH and 5'-P directly ligatable ends (Keeney and Neale, 2006; O'Driscoll and Jeggo, 2002). Physiological DSBs can be also generated when the replication machinery meets nicks or other types of lesions, from mechanical stress on the chromosome, or at the termini of chromosomes due to defective metabolism of telomeres (d'Adda di Fagagna et al., 2004; Khanna and Jackson, 2001; Mathieu et al., 2004).

There is experimental evidence supporting a causal relationship between DSBs, genomic instability and carcinogenesis. Indeed, incorrect repair of DSBs may cause loss or amplification of chromosomal material or translocations. These events can lead to tumorigenesis if, for example, they are associated with the inactivation of tumor suppressors or activation or dysregulation of proto-oncogenes (Jackson, 2002; Khanna and Jackson, 2001). Many cancers of lymphoid origin exhibit chromosomal rearrangements that have arisen as a consequence of the defective DSB repair of V(D)J recombination intermediates (Vanasse et al., 1999). Besides, mutations in factors involved in DSB signalling and repair lead to chromosomal instability and to increased cancer predisposition in humans and in animal models (Ferguson and Alt, 2001; O'Driscoll and Jeggo, 2006). Consistent with this, experiments that involve the introduction of site-specific DSBs in mouse embryonic stem cells using I-*Sce*I endonuclease revealed that DSBs are potent inducers of chromosomal translocations (Richardson and Jasin, 2000b).

1.2 DSB RESPONSE

Exposure of mammalian cells to genotoxic agents activates an intricate network of mechanisms collectively known as the DNA damage response. This response includes DNA repair and DNA damage signalling pathways that alert the cell to the presence of DNA damage and coordinate the appropriate response (Iliakis et al., 2003; O'Driscoll and Jeggo, 2006). The DNA damage response leads to slowing or arrest of cell-cycle progression at defined checkpoints and DNA repair, but also to marked alterations in numerous physiological processes, such as an increase in cellular levels of deoxyribonucleotides, changes in chromatin structure at the site of DNA damage, changes in gene-expression profiles and probably also in protein synthesis, degradation and trafficking (Jackson, 2002; Rouse and Jackson, 2002; Shiloh, 2003). Inefficient

repair and persistence of DNA damage can result in apoptosis. All these processes play critical roles in preventing chromosomal instability caused by the induction of DSBs.

The DNA damage response has been described as a classical signal-transduction cascade that develops through a series of steps (Figure 1-1). This model depicts rapid sensing of the DNA damage, the signal, by DNA-damage binding proteins, designed sensors. The sensor and the mediator proteins then trigger the activation of the protein kinase cascade, the transducer system, which amplifies and diversifies the signal by targeting a series of downstream effectors (Iliakis et al., 2003; Jackson, 2002).

The first step in this process is the recognition of the DNA damage. Sensor proteins recognize the DNA lesion itself or possibly chromatin alterations that follow DNA breakage (Shiloh, 2003). Studies in yeast and mammals have demonstrated that human RAD1, RAD9, RAD17, HSU1, and the four small subunits of the replication factor C (RFC; RFC2, RFC3, RFC4, RFC5) are involved in the recognition of DNA damage (Griffith et al., 2002; Niida and Nakanishi, 2006). A class of proteins termed mediators have also been shown to be implicated in the DNA damage response. Mediators are required for the recognition of the damage and for the recruitment of additional proteins that facilitate downstream signalling and repair. The most likely candidates mediators are the trimolecular MRE11–RAD50–NBS1 (MRN) complex, and the four BRCA1-C-terminal domain (BRCT) containing proteins, BRCA1, TopBP1 (topoisomerase II binding protein 1), 53BP1 (P53 binding protein 1) and MDC1 (mediator of DNA damage checkpoint protein 1) (Iliakis et al., 2003).

The initial and primary transducer that responds to a DSB is ataxia telangiectasia mutated protein (ATM), although related protein kinases, members of the phosphatidylinositol-3-kinase related protein kinases (PIKK) family, such as ataxia telangiectasia and RAD3-related (ATR) are also involved (O'Driscoll and Jeggo, 2006; Shiloh, 2003). Activated ATM and ATR phosphorylate the downstream transducers

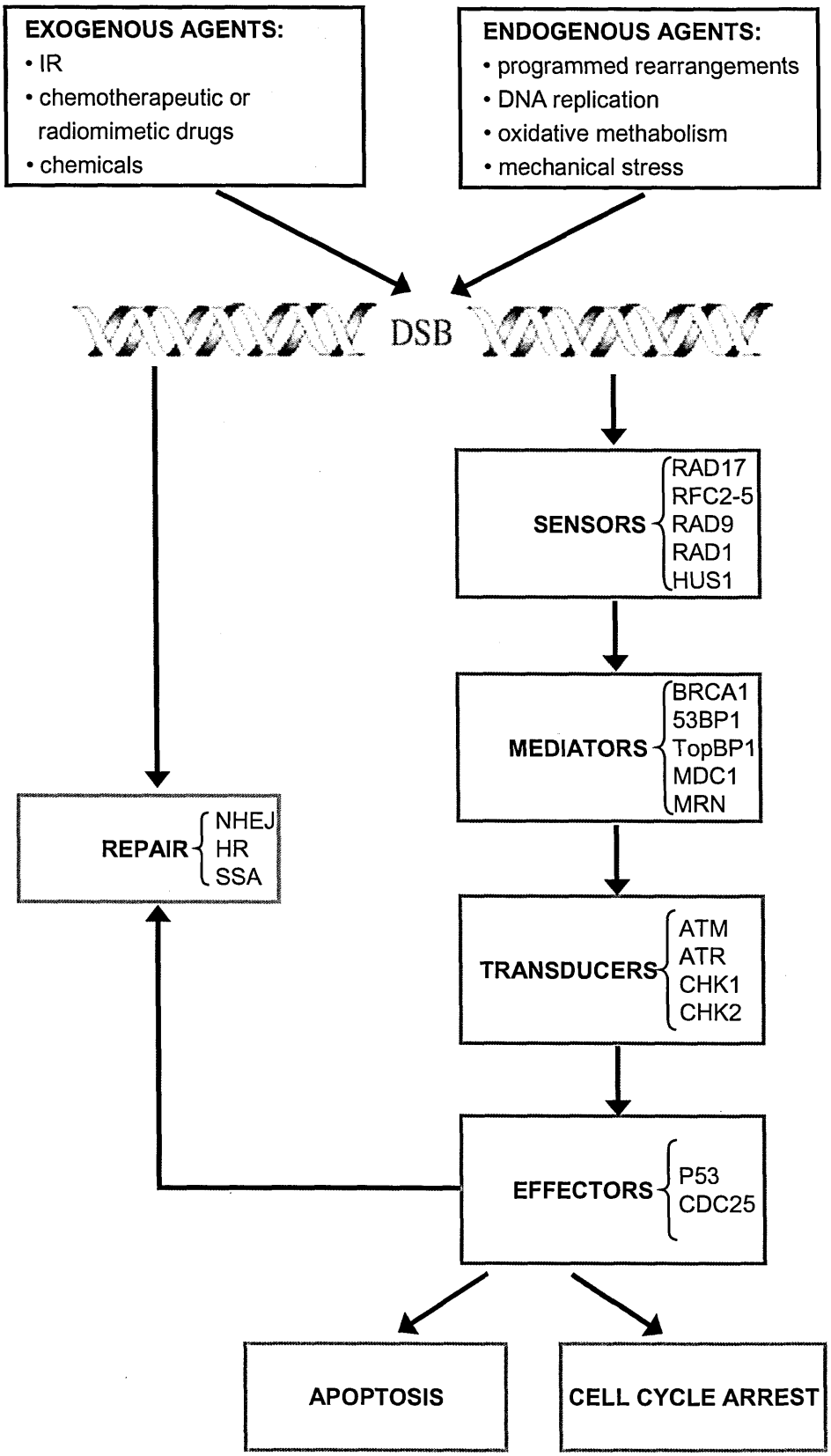

Figure 1-1 Conceptual organization of the DSB damage response. DSBs are recognized by sensor proteins and mediators that transmit the signal to transducers, which regulate the activity of effectors, thereby arresting the cell cycle, inducing repair or apoptosis.

CHK1 and CHK2. Transducers amplify the DNA damage through phosphorylation of multiple targets, most of which are effectors, such as p53 that acts as a transcription factor and the CDC25 family of phosphatases. Effectors induce cell cycle arrest, apoptosis or DNA repair (Niida and Nakanishi, 2006).

This model usefully describes the conceptual organization of the DNA damage response. However, there is a growing notion that the DSB signal might be initially amplified by means of a cyclic process in which the same proteins may have different roles at different stages of the process rather than by a series of steps with a linear hierarchy (Shiloh, 2003). An early response to DSBs that could serves as a rapid mechanism for amplifying the damage signal via repeated cycles is phosphorylation of a variant form of the histone H2A designated H2AX (Fernandez-Capetillo et al., 2004; van Attikum and Gasser, 2005). This modification is dependent on the action of three members of the PIKK family, ATM, ATR and the DNA-dependent protein kinase (DNA-PK) (Burma et al., 2001; Stiff et al., 2004; Ward and Chen, 2001). Phosphorylation occurs very rapidly in response to DNA damage on serine 139 located in an SQ motif near the C terminus of H2AX (Rogakou et al., 1998). Moreover, H2AX is massively phosphorylated in megabase chromatin domains surrounding DSBs and can be visualized as nuclear foci by immunofluorescence using antibodies against the phosphorylated form of H2AX, designed γ-H2AX (Rogakou et al., 1999). γ-H2AX foci co-localize with IR induced foci and contain DNA repair factors including mediators such as the MRN complex, 53BP1, MDC1, and BRCA1 (Celeste et al., 2002; Paull et al., 2000; Schultz et al., 2000; Stewart et al., 2003). Analysis of H2AX-deficient cells and mice have shown that H2AX is not essential for DSB repair in mammalian cells, but does appear to facilitate faithful repair (Bassing et al., 2002; Celeste et al., 2002), although the biochemical mechanism remains unclear. H2AX phosphorylation most likely promotes the retention rather than the recruitment of DNA repair and checkpoint

proteins at sites of damage, increasing the likelihood of assembling a functional repair complex (Fernandez-Capetillo et al., 2004). Another hypothesis is that multiple H2AX phosphorylation events induce a change in charge which facilitates chromatin reorganization. This rearrangement could prevent the premature separation of broken DNA ends and the focal assembly of the DNA repair/checkpoint proteins would then facilitate the synapsis of broken ends. In support of this hypothesis, H2AX-deficient cells show increased levels of translocations (Bassing et al., 2002; Celeste et al., 2002).

DNA repair and DNA damage signalling pathways are not necessarily two sequential pathways during the DNA damage response, there is instead evidence that they can occur independently (Figure 1-1). DSB repair proteins assemble at DSBs and carry out most DSB rejoining in the absence of ATM and the MRN complex (Riballo et al., 2004). Moreover, cell lines that are defective in DSB repair arrest normally at cell-cycle checkpoints in response to DSBs (O'Driscoll et al., 2001). However, in ATM-defective cell lines 10% of the DSBs fail to be rejoined, suggesting that an interplay between DNA repair and DNA damage checkpoint is required for an efficient response to DNA damage.

1.3 DSB REPAIR

The two main pathways to repair DSBs are homologous recombination (HR) and non-homologous end-joining (NHEJ) (Figure 1-2 A and B) (Jackson, 2002; Lieber et al., 2003; Valerie and Povirk, 2003). A third pathway, single-strand annealing (SSA) can be considered as a variant of HR (Figure 1-2 C). HR and NHEJ are largely distinct from one another and function in complementary ways. Their fundamental differences are the requirement for a homologous template DNA and the fidelity of DSB repair. HR relies on extensive sequence homology and involves copying the missing information from an undamaged homologous chromosome. In principle, this is error-

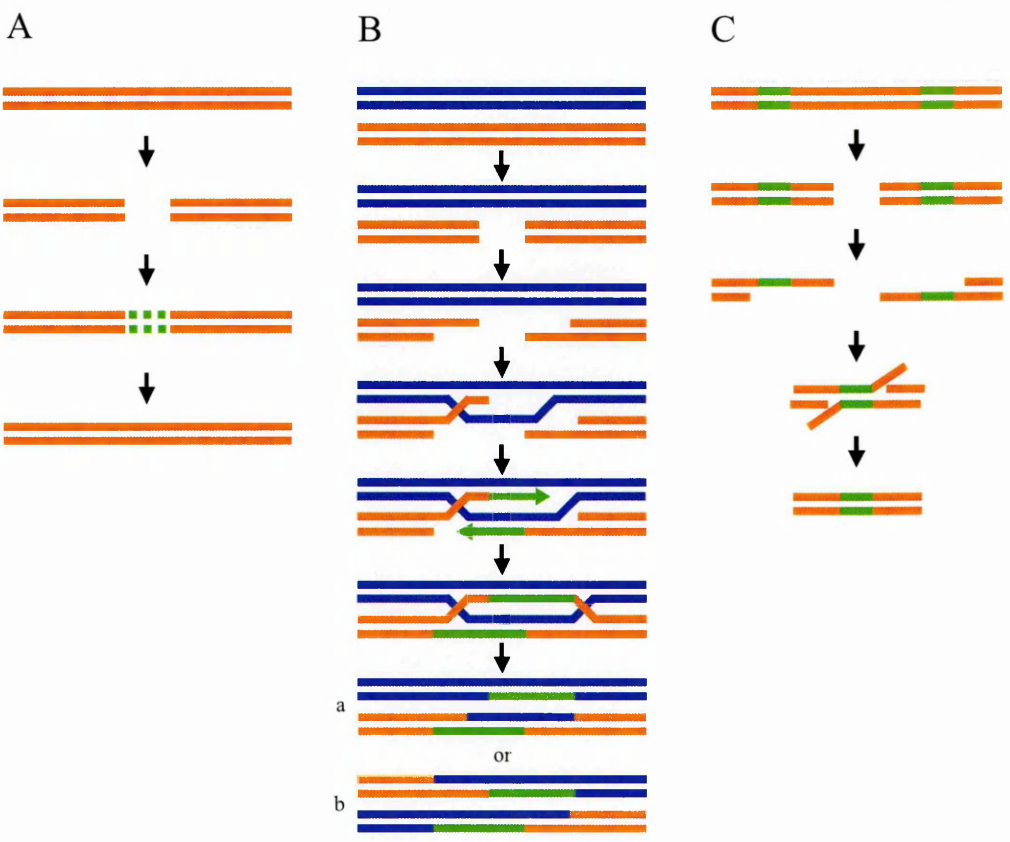

Figure 1-2 Schematic representation of the mechanisms involved in repair of DSBs (modified from (Dudas and Chovanec, 2004)). **A**, *NHEJ*. Following DSB formation, broken DNA ends are processed prior to ligation. **B**, *HR*. In this model orange and blue dsDNA represent homologous sequences. At the DSB site, dsDNA (shown in orange) is processed to form 3' single-strand ends, which invade homologous intact sequences (shown in blue). DNA strand exchange follows and generates a joint molecule between damaged and undamaged duplex DNAs. DNA synthesis fills in the break in the strand (resynthesized DNA is shown in green). Ligation and resolution of recombinant intermediates results in accurate repair of the DSB. This process can result in either non-crossover (a) or crossover (b) gene conversion products **C**, *SSA*. At the DSB site, regions of homology (shown in green) are exposed after resection of the 5'-ends and annealed. Repair of the DSB is completed by removal of non-homologous ends and ligation.

free and occurs without the loss of genetic information. Conversely, NHEJ does not require an undamaged DNA molecule and joins the broken DNA ends using little or no sequence homology. In most cases, this pathway results in the loss of a few nucleotides at the broken DNA ends. Hence, NHEJ is typically error-prone and is an imperfect process from the standpoint of preserving genomic information. SSA is similar to HR and is dependent upon homologous sequences flanking the break site. Also this process leads to loss of genetic material since the nonhomologous sequences are removed and, after annealing of the homologous sequences, ligation completes the reaction.

HR and NHEJ pathways are highly conserved throughout eukaryotic evolution but their relative importance differs from one organism to another. Simple eukaryotes such as yeasts rely mainly on HR to repair DSBs, while in higher eukaryotes NHEJ is the predominant DSB repair pathway (Jackson, 2002). This difference could be related to their genome organization. The genomes of multicellular eukaryotes have a substantial fraction of repetitive DNA (about 40% of the human genome). Therefore, the search for a homologous template DNA during HR is insurmountable when the break occurs in the portion of the genome that is repetitive and homology partners might be chosen inappropriately, except during late S, G2 and M phases, when a sister chromatid is optimally positioned physically (Lieber et al., 2003). Indeed, the relative contribution of HR and NHEJ in mammalian cells differs depending on the stage of the cell cycle. Cells defective for HR, such as RAD54 mutants, show a relative flat IR sensitivity pattern during the cell cycle and they are more IR sensitive only during the late S to G2 phases (Sonoda et al., 2006; Takata et al., 1998). Instead, cells defective for NHEJ are extremely sensitive in the G1 and early S-phases (Sonoda et al., 2006; Takata et al., 1998). This indicates that NHEJ functions throughout the cell cycle and is the predominant mechanism for DSBs repair during G0, G1 and early S phases, whereas HR is most efficient during the late S and G2 phases of the cell cycle. However, these pathways are not mutually exclusive and repair events that involve both HR and NHEJ have been detected (Richardson and Jasin, 2000a). Moreover, they are not necessarily independent and the coordinated action of both pathways is necessary in order to repair a DSB with minimal error. Indeed, studies in hamster cells have suggested that when NHEJ is impaired, HR seems to increase and *vice versa* (Allen et al., 2002; Saintigny et al., 2001).

In addition to its crucial role during G0, G1, and early S phases, the NHEJ pathway is essential to repair DSBs that occur during V(D)J recombination and Ig class-

switch recombination (CSR) in developing lymphocytes. V(D)J recombination and, likely, CSR, employ specific enzymes to initiate site-specific or region-specific genomic rearrangements events to generate a diverse repertoire of cell surface antigen receptors. These specific enzymes generate DSBs which are repaired by NHEJ (Bassing and Alt, 2004).

1.3.1 Homologous recombination

The molecular basis and genetic requirements of HR were initially defined by studies in bacteria and yeasts. Mammalian homologs of all the known proteins involved in HR in *Saccharomyces cerevisiae* have been described indicating that the basic HR pathway is conserved in higher eukaryotes (Dudas and Chovanec, 2004). However, the details of HR are likely to be considerably more complex in higher eukaryotes and in many aspects not yet elucidated. One indication of this higher complexity is the existence of several paralogues of RAD51, one of the yeast proteins important for HR, and of other proteins that lack direct homologs in yeast. A large number of proteins are involved in the HR pathway, including RAD50, RAD51, RAD52, RAD54, MRE11, NBS1, the RAD51 paralogues RAD51B, RAD51C, RAD51D, XRCC2, XRCC3 and the breast cancer susceptibility proteins BRCA1 and BRCA2 (Valerie and Povirk, 2003; West, 2003).

The first event believed to occur during HR is nucleolytic resection of the broken ends to yield single-strand overhangs. Based on analogy to yeast models, this resection is assumed to be in the 5' to 3' direction and to involve the MRN complex. However, other factors must be involved since the described nuclease activity of the MRN complex produces DNA with 5' single-stranded overhangs and not the 3' ends (Paull and Gellert, 1998; Trujillo et al., 1998; Wyman et al., 2004). The resulting 3' single-stranded overhangs are then bound by RAD51 and this process is facilitated by replication protein A (RPA), RAD52 and probably RAD54. The RPA-coated RAD51

nucleoprotein filament mediates then a search for homologous sequences on an undamaged duplex. The homologous sequence can be in the sister chromatids, in homologous chromosomes or DNA repeats. Once the homologous region is located, RAD51 initiates strand exchange in which one of the damaged DNA strands invades the homologous duplex, forming a D-loop. This stage is likely favoured by RAD54. The 3' termini then prime new DNA synthesis by polymerases that copy information from the homologous undamaged partner. The next stages of this DNA repair process are less clear and different models have been proposed. Most models involve the formation of a double Holliday junction, the point at which the strands cross over, which needs to be resolved to yield two intact DNA molecules (Figure 1-2 B). This process can result in either non-crossover or crossover gene conversion products (Figure 1-2 B, a and b respectively), depending on the mode by which the Holliday junctions are resolved.

1.3.2 Single strand annealing

This process was originally proposed on the basis of experiments in mammalian cells and subsequently in *Xenopus laevis* oocytes using specifically engineered DNA substrates (Lin et al., 1984; Maryon and Carroll, 1991). At present, there is conflicting data on its enzymology and there may be several independent SSA pathways (Sankaranarayanan and Wassom, 2005; Valerie and Povirk, 2003). SSA presumably begins with extensive 5'-3' resection of the DSB ends to generate long single strand overhangs by an exonuclease, most likely the MRN complex. RAD52 then binds to DNA ends as a heptameric ring structure and promotes the association between complementary DNA termini (Van Dyck et al., 2001). Once homology between the exposed overhangs is found, the homology is annealed, the protruding ends are trimmed by the ERCC1/XPF nuclease and the break is sealed by a DNA ligase.

1.4 NON-HOMOLOGOUS END-JOINING

1.4.1 Identification of genes required for NHEJ

It has long been evident that, in comparison with yeast, mammalian cells have a greater ability to rejoin DNA ends in the absence of any homology (Roth et al., 1985; Roth and Wilson, 1985). Studies involving the integration of exogenous DNA into mammalian genomes have shown that the majority of these events occur in the absence of any apparent homology (Lin et al., 1984). Moreover, the analysis of plasmid rejoining using extracts of *Xenopus laevis* has identified a mechanism of NHEJ (Pfeiffer et al., 1994). Research into the process of NHEJ has made a quantum leap with the identification of genes that function in this repair pathway (Jeggo, 1998). Isolation and characterization of repair defective mutant cells have led to the identification of three of the main repair genes involved in the NHEJ pathway. At least nine complementation groups of rodent mutants sensitive to IR were initially described (Jeggo et al., 1991; Thacker and Wilkinson, 1991). Members of three of these groups (IR groups 4, 5 and 7), which include the most markedly γ-ray sensitive rodent lines, showed defects in their ability to rejoin DSBs. These members shared strikingly similar phenotypes including an inability to carry out V(D)J recombination. This suggested that the proteins defined by these groups operate in a single pathway (Pergola et al., 1993; Taccioli et al., 1993). Different approaches then led to the identification of complementing genes. The human genes complementing these cells were preassigned to the *XRCC* nomenclature (X-ray cross-complementing) (Thompson and Jeggo, 1995). The *XRCC5* gene encodes for the Ku80 subunit (Cai et al., 1994; Getts and Stamato, 1994; Rathmell and Chu, 1994; Taccioli et al., 1994) of the Ku70/80 heterodimer, a protein that was originally identified as an autoantigen present in the sera of certain autoimmune patients (Mimori et al., 1981). *XRCC7* encodes for the DNA-dependent protein kinase (DNA-PK)

(Finnie et al., 1995) and *XRCC4* for the XRCC4 protein (Li et al., 1995). Rodent mutants defective in Ku70 were not isolated as radiosensitive mutants, but Ku70 knock-out cell lines subsequently constructed displayed radiosensitivity and V(D)J recombination defects (Gu et al., 1997). XRCC4 was found to be tightly associated with DNA ligase IV in mammalian cells (Critchlow et al., 1997) and the role of this ligase in DSB repair was demonstrated by gene-targeted mutation studies (Frank et al., 1998; Grawunder et al., 1998a). Recently, two other proteins have been shown to be involved in NHEJ. Artemis was discovered in 2001, as the molecular defect in children with a radiosensitive form of human severe combined immunodeficiency (SCID) (Jeggo and O'Neill, 2002; Ma et al., 2002; Moshous et al., 2001), while Cernunnos (Buck et al., 2006) or XLF (Ahnesorg et al., 2006) was identified following two different approaches in 2006.

1.4.2 Proteins involved in NHEJ

Since the discovery of the genes involved in the NHEJ process, molecular and cellular approaches have contributed to the understanding of this pathway. Moreover, studies on the structure and the biophysical properties of the codified proteins have provided insights into their biological function.

1.4.2.1 DNA-PK

DNA-PK is a serine/threonine protein kinase composed of a catalytic subunit, DNA-PKcs, and a regulatory subunit, the Ku heterodimer (Dvir et al., 1992; Gottlieb and Jackson, 1993). DNA-PKcs is a large protein (469 kDa) characterized by a C-terminal catalytic domain which bears amino acid similarity to the catalytic domain of the phosphatidylinositol 3-kinase (PI3K) family of lipid kinase (Poltoratsky et al., 1995). Unlike other members of this family, DNA-PKcs does not possess lipid kinase activity; indeed, it is a member of a subfamily of PI3K, designed phosphatidylinositol-

3-kinase related protein kinases (PIKKs) (Hartley et al., 1995; Hunter, 1995). The highly conserved PI3K catalytic domain separates two other regions of homology shared between PIKKs members: the FAT domain (so named because of the homology in this region between FRAP, ATM and TRRAP) and the FAT-C domain (C-terminal FAT) (Bosotti et al., 2000) (Figure 1-3 A). In contrast to the C-terminal catalytic region, which is of similar size in all the PIKK enzymes, the N-terminal regions show substantial variation in size and no apparent homology. The long and distinctive N-terminal region of DNA-PKcs is formed by an extended series of HEAT (huntingtin-elongation-A-subunit-TOR) and related helical repeats (Brewerton et al., 2004). This region of DNA-PKcs contains a leucine rich region (LRR) (amino acids 1503-1602) that has been shown to contribute to the intrinsic ability of DNA-PKcs to bind DNA (Fujimori et al., 2000; Gupta and Meek, 2005).

Electron microscopy (EM) studies have shown that the three dimensional (3D) structure of DNA-PKcs consists of three main regions: a globular "head" connected to a flat tubular "arm" segment terminating in a "palm" that consists of two projecting "claws" (Rivera-Calzada et al., 2005) (Figure 1-3 B). The conserved PI3K catalytic domain, the FAT and the FATC domains are all located in the head region. The N-terminal region maps into the arm region and into the palm. The distal claw probably comprises the extreme N terminus of DNA-PKcs, while the proximal claw likely contains the LRR.

The kinase activity of DNA-PKcs is stimulated by double-stranded DNA (dsDNA) ends. Although DNA-PKcs has been shown to possess DNA-binding activity, efficient activation of this kinase requires the Ku heterodimer (Dvir et al., 1992; Gottlieb and Jackson, 1993; Hammarsten and Chu, 1998; Suwa et al., 1994; West et al., 1998; Yaneva et al., 1997). Structural studies in the presence of blunt-ended dsDNA have shown that DNA binds in the open cavity between the head and the palm, with the

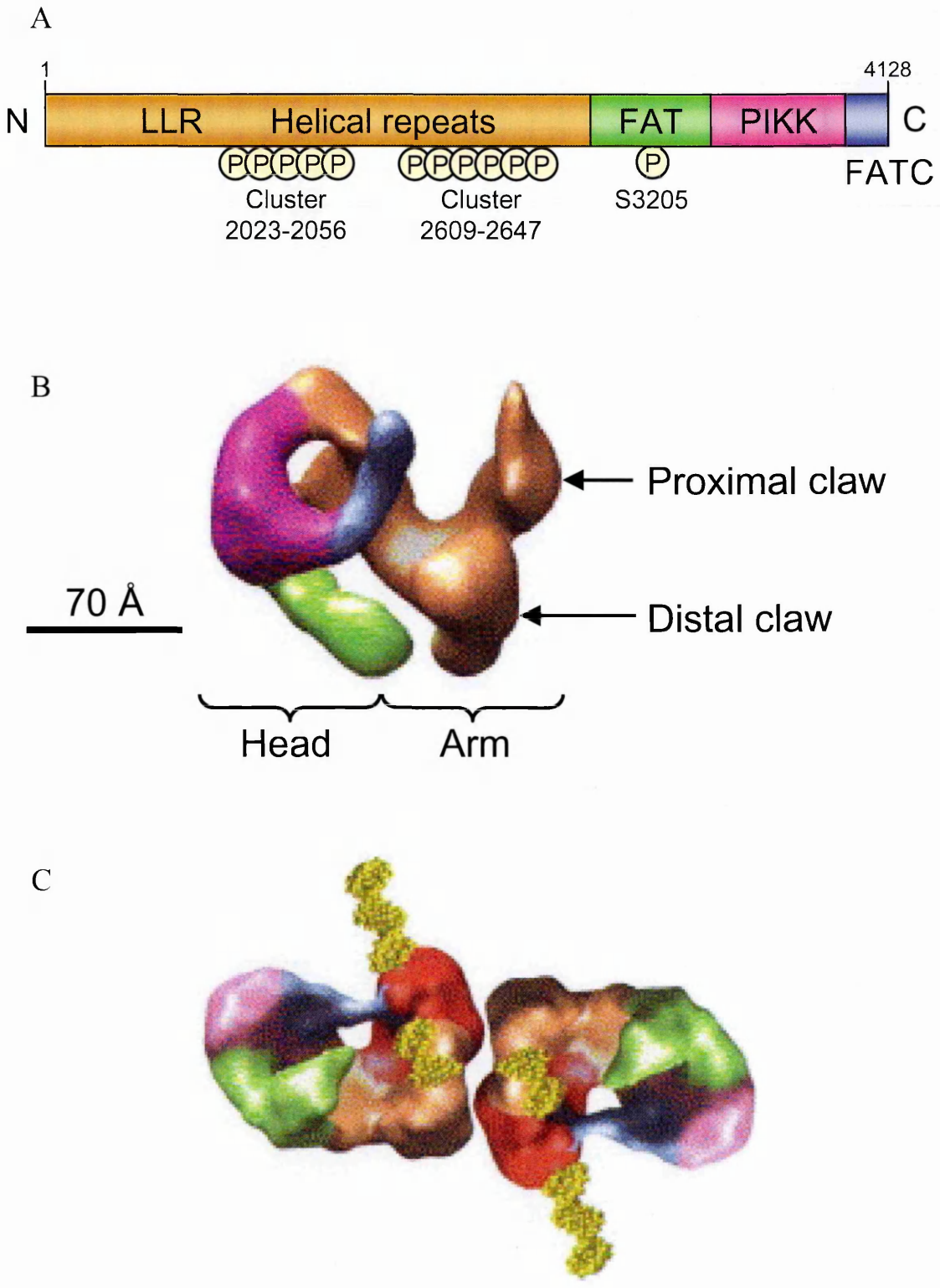

Figure 1-3 Schematic representation of the structural organization (**A**) and 3D cryo-EM structure (**B**) of DNA-PKcs (from (Rivera-Calzada et al., 2005)). Colouring depicts the assignment of domains in the sequence of DNA-PKcs (**A**) into the 3D structure according to (Rivera-Calzada et al., 2005): the N terminus in brown; the FAT domain in green; the PIKK domain in magenta and the FATC domain in blue. The scale bar represents 70 Å. The phosphorylation sites of DNA-PKcs are also evidenced (**A**). **C**, model of the putative NHEJ synaptic complex formed by DNA-PKcs, Ku70/80 (shown in red) and DNA (shown in yellow) based on the 3D structure data (from (Spagnolo et al., 2006)).

blunt end buried in the inner curved face of the palm and the edge of the head in contact with the DNA backbone. DNA binding induces a substantial change in overall conformation that triggers an interaction between initially distant palm and head regions. Conformational changes observed in the FAT and FATC domains suggest that these domains transduce DNA-induced changes to the catalytic core and regulate the kinase activity (Boskovic et al., 2003; Rivera-Calzada et al., 2005).

The precise function of DNA-PK during DNA repair and V(D)J recombination has not been completely elucidated. At the moment, there is considerable evidence that DNA-PK plays at least two roles during NHEJ which are related to its kinase activity and its large size. The essential role of the kinase activity of DNA-PK for the DSB repair process is evident by experiments with DNA-PKcs deficient cell lines. These assays have shown that DNA-PKcs harboring mutations within the kinase domain fails to complement the DSB repair or V(D)J recombination defect (Kienker et al., 2000; Kurimasa et al., 1999). Moreover, several *in vitro* and *in vivo* studies with DNA-PKcs inhibitors have confirmed that its kinase activity is required for DSB repair (Baumann and West, 1998; Chernikova et al., 1999; Rosenzweig et al., 1997). Numerous DNA-PK targets have been identified *in vitro* and *in vivo*, including a wide range of proteins involved in the DNA damage response. DNA-PKcs phosphorylates these targets preferentially on serine or threonine followed by glutamine (S/T-Q motif) or by hydrophobic residues (Anderson and Lees-Miller, 1992). However the role of these modifications is still unknown. The only substrate of DNA-PKcs that has been shown unequivocally to be functionally important for NHEJ to date is itself (Block et al., 2004; Chan et al., 2002; Ding et al., 2003). Twelve potential phosphorylation sites have been identified by mass spectrometry analysis of DNA-PKcs autophosphorylated *in vitro* and by studies with phosphorylation mutants (Cui et al., 2005; Douglas et al., 2002). One of these sites lies at the C terminus (Ser 3205) (Figure 1-3 A). Another six

phosphorylation sites are localized within a major cluster in a central region of DNA-PKcs (amino acids 2609-2647) that likely map to the arm region (Douglas et al., 2002; Rivera-Calzada et al., 2005). The autophosphorylation of this cluster likely mediates a conformational change in DNA-PK that is critical for DNA end processing and for efficient joining by the LX complex (Block et al., 2004; Ding et al., 2003; Reddy et al., 2004). Immunofluorescence analysis with phospho-specific antibodies that recognize one of these sites (Thr 2609) has demonstrated that DNA-PK is capable of phosphorylating itself *in vivo* in response to DNA damage and that DNA-PKcs phosphorylated at Thr 2609 co-localizes with DNA damage foci (Chan et al., 2002). The observation that DNA-PKcs mutants containing alanine substitutions at these autophosphorylation sites still underwent substantial autophosphorylation *in vitro* (Ding et al., 2003; Reddy et al., 2004) has led to the discovery of a new cluster of sites (between residues 2023 and 2056) (Cui et al., 2005). Separate autophosphorylation of these two major clusters probably regulates DNA end access and affects DSB repair pathway choice (Cui et al., 2005). Indeed, cells expressing DNA-PKcs that cannot autophosphorylate the cluster 2609-2647 are more radiosensitive than DNA-PKcs null cells and the HR pathway in these cells is markedly reduced (Convery et al., 2005).

Due to its extremely large size DNA-PKcs might also play a structural role in NHEJ, either by aligning DNA termini to promote their ligation or by providing a scaffold to which other proteins can be recruited. Microscopy studies have shown that DNA-PKcs facilitates the alignment or 'synapsis' of DNA broken ends (Cary et al., 1997; DeFazio et al., 2002; Yaneva et al., 1997). Although it has been observed that DNA-PKcs self-associates in the absence of Ku, recent electron microscopy data have suggested that Ku plays an indirect role in promoting synapsis, possibly regulating the conformation of DNA-PKcs (Spagnolo et al., 2006). Indeed, binding of Ku and DNA elicits conformational changes in the FAT and FATC domains of DNA-PKcs.

Moreover, structural data has shown that dimeric DNA-PK complexes interact through the N-terminal HEAT repeats of DNA-PKcs bound to DNA ends and that Ku itself is not involved in the dimeric contacts but it is positioned on the outside face of each DNA-PKcs dimer (Figure 1-3 C). This alignment or 'synapsis' of DNA ends by DNA-PK is necessary for kinase activation (DeFazio et al., 2002).

DNA-PK has been proposed to act also as a molecular scaffold for the recruitment of additional repair factors, aiding their localization to the site of damage. Many interacting proteins have been reported for DNA-PK, such as DNA ligase IV/XRCC4, DNA polymerase μ, and terminal deoxynucleotidyl transferase (TdT) (Calsou et al., 2003; Hsu et al., 2002; Leber et al., 1998; Mahajan et al., 2002; Mickelsen et al., 1999).

Cells that lack DNA-PKcs are radiosensitive and defective in DSB repair. DNA-PKcs null mice are viable but immunodeficient, due to inability to complete V(D)J recombination. Moreover, SCID mice with a defective DNA-PKcs gene and null mice possess a defective V(D)J recombination phenotype and accumulate a large number of telomeric fusions (Gilley et al., 2001) as well as shorter telomeres (Espejel et al., 2002). The only human cell line known to lack DNA-PKcs is M059J, which was isolated from a malignant glioma (Lees-Miller et al., 1995). These cells lack DNA-PK activity, due to defective mRNA turnover and a frameshift mutation in the gene (Anderson et al., 2001). Reintroduction of DNA-PKcs complements the radiosensitive defect in M059J cells, suggesting that the absence of DNA-PKcs accounts for the radiosensitive phenotype (Hoppe et al., 2000).

1.4.2.2 Ku70/80

Ku is a heterodimer made up of two subunits of 70 and 83 kDa known as Ku70 and Ku80, respectively. These two subunits show sequence similarity to each other over the length of the proteins, which suggests that they diverge from a common

ancestor (Dynan and Yoo, 1998; Gell and Jackson, 1999). The low level of sequence identity (~ 15%) among residues that contribute to the dimer interface should ensure heterodimer formation and preclude Ku70-70 or Ku80-80 homodimer formation. Identification of homologues of Ku in Archaea and Bacteria and sequence comparisons have allowed the dissection of the Ku protein sequences into three distinct domains (Aravind and Koonin, 2001). Each subunit of Ku consists of three regions: an N-terminal von Willebrand A domain (vWA), a central "core" domain and a diverged C-terminal region (Figure 1-4 A). The vWA domains and the core domains are involved in Ku heterodimerization. In Ku70, the C-terminal region contains a SAP domain, which is a derived version of a helix-extension-helix (HEH) fold and is thought to be a DNA-binding domain. The DNA-binding capability of this region (Ku70 residues 536-609) has been demonstrated by Southwestern blotting, although other groups have not detected DNA binding by either subunit on its own, which suggests that DNA binding by this domain is weak (Chou et al., 1992; Griffith et al., 1992; Ono et al., 1994). The C-terminal domain of Ku80 is longer than the C terminus of Ku70 and in higher eukaryotes contains an extension that binds DNA-PKcs.

The crystal structure of Ku has shown that Ku70 and Ku80 share a common topology comprising an N-terminal α/β domain, a central β-barrel domain and a helical C-terminal arm (Figure 1-4 B) (Walker et al., 2001). Moreover, structural studies have revealed that the two subunits form an asymmetric ring with an expansive base and a narrow bridge (Figure 1-4 C). The structure of the C terminus of Ku80 has been solved recently and shows a central structured helix-turn-helix motif flanked by an unstructured and flexible amino-terminal linker and carboxy-terminal tail (Harris et al., 2004; Zhang et al., 2004).

The eukaryotic Ku is an abundant protein (estimated at least 4 x 10^5 molecules per cell) (Mimori et al., 1986). Its localization is primarily nuclear, in agreement with

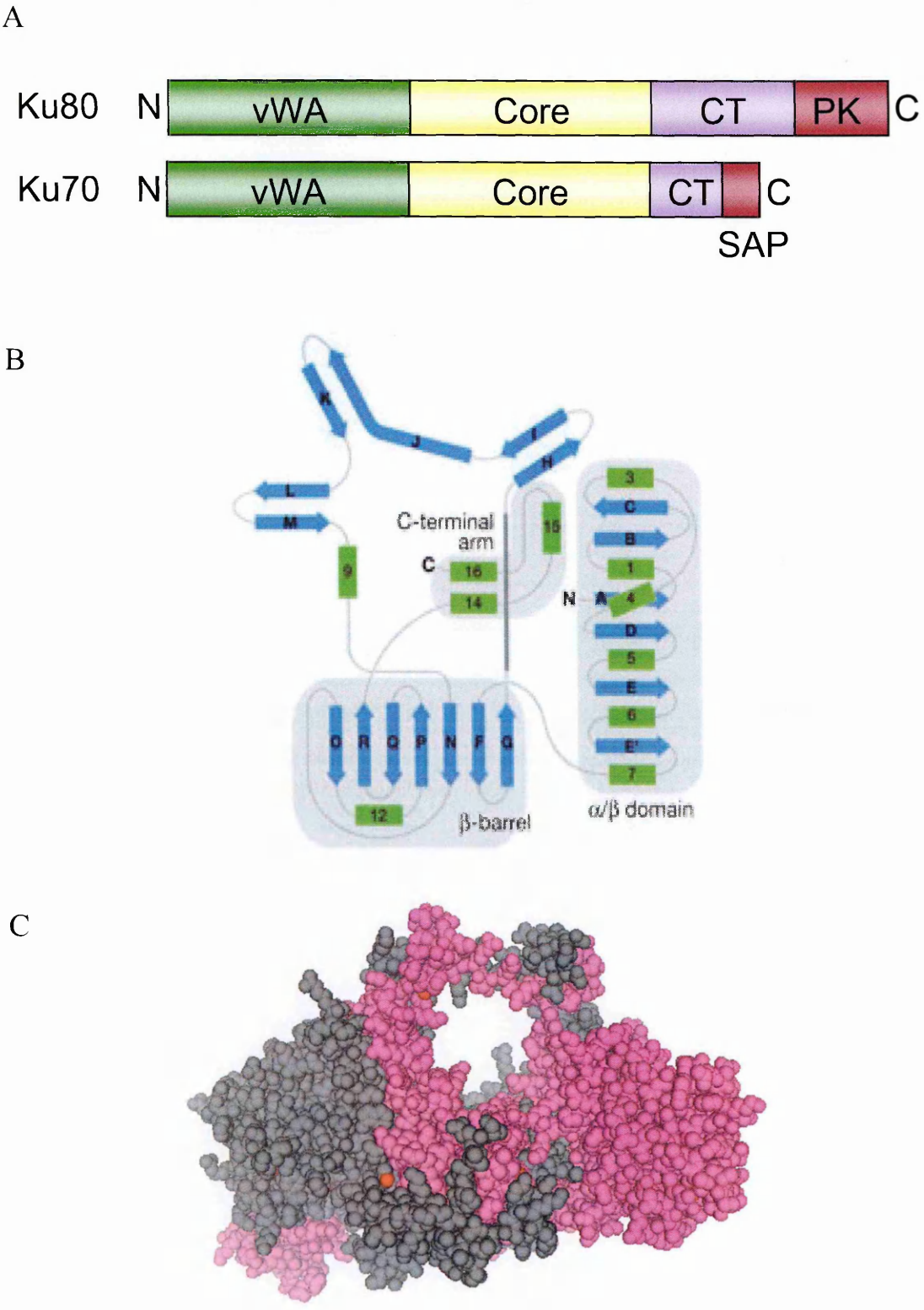

Figure 1-4 Domain organization (**A**), topology diagram showing the fold (**B**), and 3D structure (**C**) of Ku70/80. **A**, Ku subunits consist of the following regions: an N-terminal von Willebrand A domain (vWA) shown in green; a central core domain, in yellow, and a divergent C-terminal region (CT), in purple. In Ku70, the CT contains an HEH-derived SAP domain. Ku80 has a longer CT that contains a region that binds to DNA-PKcs (PK). **B**, Ku70 and Ku80 comprise an N-terminal α/β domain, a central β-barrel domain and a helical C-terminal arm. Green rods indicate α-helices, blue arrows indicate β-strands (from (Walker et al., 2001)). **C**, spacefill representation of the 3D structure of Ku70/80 drawn using the PyMol program and the atomic coordinates deposited in the Brookhaven Protein Databank (code 1JEQ). Ku80 is indicated in grey and Ku70 in violet.

the observation that both Ku70 and Ku80 contain a nuclear localization sequence (Koike, 2002). However, there is evidence that Ku is present in other subcellular locations, suggesting that Ku might have other roles elsewhere in the cell. *In vivo*, Ku is mostly found in an extremely stable heterodimeric Ku70-Ku80 complex. Ku70-deficient mice have very low levels of Ku80 and Ku80-deficient rodent cells have very low levels of Ku70 (Errami et al., 1996; Gu et al., 1997; Singleton et al., 1997). Moreover, re-introduction of Ku80 in Ku80-deficient cells restores both Ku80 and Ku70 protein levels, which implies that the heterodimeric form of Ku is the stable, and probably functional, form.

Cells that lack Ku are radiosensitive and defective in DSB repair. Animals lacking either of the Ku subunits share many characteristics with DNA-PKcs null animals, such as radiosensitivity, immune deficiency, and defective DSB repair. Moreover, Ku70 and Ku80 null animals show growth defects and premature senescence (Nussenzweig et al., 1996; Zhu et al., 1996). Mammalian cells that lack Ku, like cells that lack DNA-PKcs, exhibit end-to-end chromosomal fusions (d'Adda di Fagagna et al., 2001; Gilley et al., 2001; Hsu et al., 1999; Rebuzzini et al., 2004). Indeed, in addition to their role in DSB repair and V(D)J recombination, DNA-PKcs and Ku play an important role in the maintenance of telomeres and in prevention of chromosome end fusions.

1.4.2.3 DNA ligase IV/XRCC4

Human DNA ligase IV (LigIV) is an ATP-dependent ligase composed of 911 amino acids. In the cellular context LigIV appears unable to function alone and requires physical interaction with XRCC4 protein (Critchlow et al., 1997; Grawunder et al., 1997). The crystal structure of the LigIV/XRCC4 (LX) complex has not yet been solved and structural analysis of the ligase has relied in part on the use of other ATP-dependent DNA ligases as model systems. LigIV consists of an N terminus highly

related to those of other mammalian DNA ligases and an unique C-terminal region that contains a tandem BRCT domain (Figure 1-5 A) (Martin and MacNeill, 2002; Pascal et al., 2004; Wei et al., 1995). The conserved N-terminal region comprises the DNA-binding domain and the catalytic domain that encompasses the adenylation and the oligo-binding domain. The C-terminal part of LigIV is necessary for its interaction with XRCC4 and in particular, the region that links the two BRCT motifs was found to be sufficient for XRCC4 binding (Grawunder et al., 1998c; Sibanda et al., 2001). However, recent crystallographic studies of an XRCC4-LigIV yeast ortholog complex have revealed that XRCC4 interacts also with both BRCT domains (Dore et al., 2006).

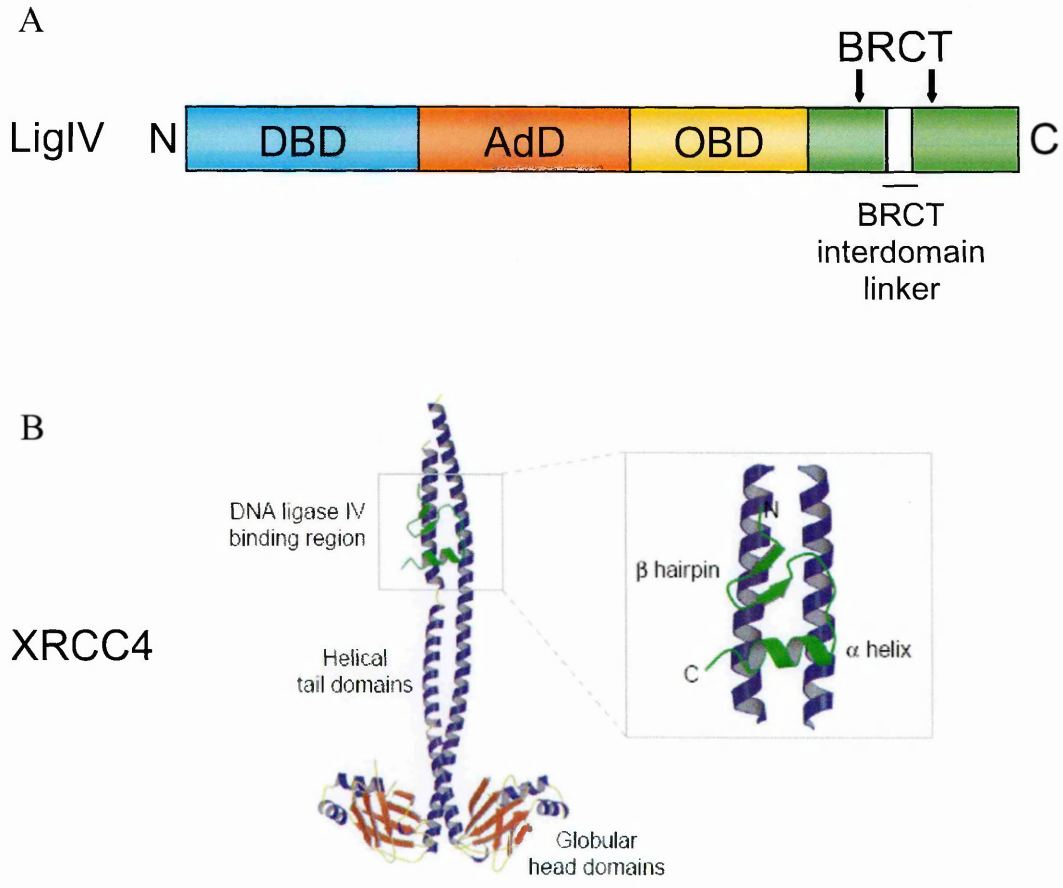

Figure 1-5 Schematic representation of the domain organization of LigIV (**A**) and 3D structure of XRCC4 (**B**). **A**, domains of LigIV are in different colours: the DNA binding domain (DBD) is indicated in blue; the adenylation domain (AdD) in orange; the oligo-binding domain (OBD) in yellow; and the BRCT domains in green. **B**, structure of a homodimer of XRCC4 bound to a short peptide corresponding to amino acids 748-784 of human LigIV (shown in green) and close-up view of the LigIV peptide bound to the helical tails of the XRCC4 dimer. The peptide comprises a β-hairpin followed by an α-helix and lies asymmetrically across both XRCC4 (modified from (Martin and MacNeill, 2002)).

Human XRCC4 is a 334-amino acid protein, characterized by a globular N-terminal head domain, that folds into a seven-stranded trumpet-shaped β-barrel, followed by a long helical tail at the C terminus (Figure 1-5 B) (Junop et al., 2000; Sibanda et al., 2001). The N-terminal head group may interact with DNA, while the C-terminal stalk is involved in binding to LigIV. Two forms of XRCC4 exist that are mutually exclusive: an XRCC4 tetramer and a dimer of XRCC4 that is complexed with LigIV (Modesti et al., 2003).

The stoichiometry of the LigIV/XRCC4 (LX) complex is apparently 1:2 (Modesti et al., 2003). This interaction is remarkably strong: the two proteins copurify over a range of chromatographic techniques, and their association withstands buffer conditions that include 2 M NaCl or 7 M urea (Sibanda et al., 2001). The interaction of LigIV with XRCC4 stimulates ligase activity (Grawunder et al., 1997). Moreover, cells that lack XRCC4 contain low levels of LigIV, suggesting that XRCC4 stabilizes the LigIV protein *in vivo* (Bryans et al., 1999).

Human LigIV is the ATP-dependent ligase required for the final joining reaction of NHEJ (Robins and Lindahl, 1996). This enzyme is unique in its ability to catalyze ligation during NHEJ, indeed it cannot be substituted by any other mammalian ligase (Grawunder et al., 1998a). The ligation reaction of the LX complex occurs through three chemical steps (Figure 1-6). During the first step, a phosphoamide bond (P-N) forms between the ε-amino group of an active site lysine and the phosphate of AMP. The formation of the ligase-adenylate complex requires a highly conserved motif, KYLGER (residues 273-278 in human LigIV), located in the N-terminal region of the protein. The activated enzyme-AMP adduct is generated in the absence of a nucleic acid substrate and it has been reported that LigIV exists as a pre-adenylated complex in mammalian cells (Robins and Lindahl, 1996). The second step of the reaction involves transfer of the AMP moiety to the phosphorylated DNA 5' end. During the last step,

ligation occurs between the 3' hydroxyl of a DNA strand and the 5' phosphorylated DNA end, then the non-adenylated ligase is released (Tomkinson et al., 2006). The three steps of the ATP-dependent ligation reaction of LigIV can be described as follows:

$$E + ATP \leftrightarrow E\text{-}AMP + PPi$$

$$E\text{-}AMP + PDNA \leftrightarrow AMP\text{-}PDNA + E$$

$$DNA + AMP\text{-}PDNA \leftrightarrow DNA\text{-}PDNA + AMP$$

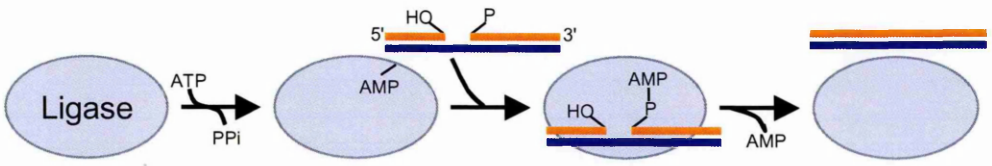

Figure 1-6 Mechanism of ligation reaction of ATP-dependent ligases (modified from (Johnson and O'Donnell, 2005)).

Both LigIV and XRCC4 are of vital importance to organisms, indeed deficiency of either LigIV or XRCC4 leads to embryonic lethality in knock-out mice due to massive neuronal apoptosis (Barnes et al., 1998; Frank et al., 1998; Gao et al., 1998). Cells that lack LigIV or XRCC4 are radiosensitive, defective in V(D)J recombination and DSBs repair.

1.4.2.4 Artemis

Artemis is a 685-amino acid protein with a mass of approximately 77 kDa. The protein sequence defines this factor as a member of the metallo-β-lactamase superfamily. Artemis has an intrinsic 5'-3' exonuclease activity. However, this protein interacts with DNA-PKcs *in vitro* and *in vivo* and this interaction converts Artemis activity to a DNA endonuclease with also DNA hairpin-opening activity, required during V(D)J recombination (Ma et al., 2002). DNA-PK is necessary to activate Artemis, although the mechanism of this activation is still unknown.

Artemis-deficient cells are mildly radiosensitive and have a defective V(D)J recombination phenotype (Moshous et al., 2001; Rooney et al., 2002). Moreover they are highly sensitive to the DSB-inducing drug bleomicin; indicating that Artemis might be required to repair a subset of NHEJ reactions that require end processing (Rooney et al., 2003).

1.4.2.5 Cernunnos-XLF

Cernunnos-XLF is a protein of 33 kDa (Ahnesorg et al., 2006; Buck et al., 2006). Computer algorithms have predicted structural similarity to XRCC4 showing that it comprises a globular N-terminal "head" domain and a C-terminal coiled-coil structure. Thus, the new gene has been designed XRCC4-like factor (XLF). The function of this newly identified factor is still unknown. Cernunnos-XLF deficient cells display similar levels of IR sensitivities and DSB-repair defects exhibited by XRCC4 or LigIV-deficient cells, suggesting that may function in all the NHEJ events.

1.4.2.6 Other factors involved in NHEJ

IR-induced DSBs are rarely blunt-ended, rather they frequently contain overhanging ends or non-ligatable ends for example, 3'-phosphate, 3'-phosphoglycolate groups, which must be modified prior to rejoining. Thus, other processing factors are required in NHEJ. Moreover, non-protein factors such as inositol hexakisphosphate (IP_6) and Mg^{2+}-ATP are also required for NHEJ. IP_6 binds to Ku and stimulates NHEJ *in vitro* (Hanakahi et al., 2000; Hanakahi and West, 2002; Ma and Lieber, 2002). Mg^{2+}-ATP is required for NHEJ *in vitro*, likely as a substrate for DNA-PK.

- ***TdT***

Human terminal deoxytransferase (TdT) catalyzes the addition of nucleotides to the junctions of coding ends during V(D)J recombination. TdT colocalizes with Ku at

sites of DNA-damage, suggesting a role in end-processing in both V(D)J recombination and DNA damage (Mahajan et al., 1999; Mickelsen et al., 1999).

- ***WRN***

The Werner syndrome protein (WRN) has both ATP-dependent helicase activity and 3'-5' exonuclease activity (Hickson, 2003). WRN interacts with Ku and it is a physiological target of DNA-PK (Karmakar et al., 2002a; Karmakar et al., 2002b; Li and Comai, 2001; Orren et al., 2001; Yannone et al., 2001). WRN negative cells have a mildly radiosensitive phenotype, suggesting a role as a DNA processing enzyme involved in NHEJ (Yannone et al., 2001).

- ***PNK***

Mammalian polynucleotide kinase (PNK), which is both a 5' DNA kinase and a 3' DNA phosphatase, functions in the processing of DSB with 5'-OH termini (Chappell et al., 2002). Recently, it has been shown that PNK interacts with the phosphorylated form of XRCC4 subunit and that this interaction is functionally important for NHEJ *in vitro* and *in vivo*. Disruption of this interaction results in increased sensitivity to IR *in vivo* and diminished DNA end joining *in vitro* (Koch et al., 2004).

- ***hTdp1***

Human tyrosyl-DNA phosphodiesterase (Tdp1) removes protein moieties from camptothecin-induced topoisomerase I-DNA structures and processes DSBs bearing 3'-phosphoglycolates (Inamdar et al., 2002). Therefore, it is possible that hTdp1, in concert with PNK, plays a role in processing of DNA ends during NHEJ.

- ***MRE11/RAD50/NBS1***

The MRN complex may be involved in NHEJ, since it has been shown to stimulate DSB rejoining in an *in vitro* end-joining assay using human cell extracts (Huang and Dynan, 2002). However, it is still unclear whether it plays a role in NHEJ *in vivo*.

- ***DNA polymerase***

Recent *in vivo* and *in vitro* biochemical studies have suggested that the mammalian Pol X family members, polymerase μ and/or λ, contribute to NHEJ function at incompatible DNA ends (Ma et al., 2004; Mahajan et al., 2002). After exposure to IR, the levels of DNA polymerase μ increase and the protein forms nuclear foci (Mahajan et al., 2002). Moreover, polymerase μ interacts with Ku and stimulates end-joining *in vitro*. DNA polymerase μ and/or λ could be recruited to the DSB and be involved in the synthesis of new DNA prior to ligation (Nick McElhinny et al., 2005). The contribution of each polymerase probably depends on the sequence and the structure of the DNA ends.

- ***53BP1***

53BP1 is amongst the earliest proteins to be recruited into IR induced nuclear foci (Bekker-Jensen et al., 2005; Mochan et al., 2004; Schultz et al., 2000). Moreover, recent genetic studies have demonstrated an epistatic relationship between 53BP1, ATM, Artemis, H2AX, NBS1, MRE11 and Ku70, demonstrating that these proteins function in a common DSB repair pathway that rejoins approximately 10% of radiation-induced DSBs (Nakamura et al., 2006; Riballo et al., 2004).

1.4.3 Current model for NHEJ

The first step in NHEJ is the detection of the DSB and binding of specific proteins to the broken DNA ends (Hefferin and Tomkinson, 2005; Lieber et al., 2003; Weterings and van Gent, 2004). This step is fundamental to limit nucleolytic degradation, which would result in the loss of genetic information. Another essential step to allow proper end-joining is the physical juxtaposition or 'synapsis' of the DNA ends. This step is mediated by protein-protein interactions between DNA end binding proteins or bridging factors bound to DNA end binding proteins. If the juxtaposed

DNA ends can be directly ligated, ligation completes the joining reaction. However, the majority of DSBs generated by exposure to DNA damaging agents must be processed to generate 3'-OH groups and 5'-P groups prior to ligation. Analysis of the DNA sequence at break sites repaired by NHEJ has suggested that many of these events involve the alignment of the broken ends by short (1-4 nucleotides) complementary sequences, microhomologies, close to the break site ends (Roth and Wilson, 1986). Therefore, after end bridging, there could be an alignment step in which the DNA sequences close to the ends are aligned. After end processing, the generation of ligatable termini allows the final ligation step.

Ku is most likely the first protein that detects and binds to the ends at a DSB, given its abundance in the nucleus and its high affinity for DNA ends (Figure 1-7). Ku is thought to be about fivefold more abundant than DNA-PKcs (Anderson and Carter, 1996) and it has been shown to enhance the affinity of DNA-PKcs for DNA (Yaneva et al., 1997). These findings suggest that DNA-PKcs is recruited on the DNA ends by Ku, which binds DNA-PKcs through the C-terminal domain of Ku80 (Gell and Jackson, 1999; Han et al., 1996; Muller and Salles, 1997; Singleton et al., 1999). The molecular mechanisms of end bridging and alignment are not clear yet. Several reports have shown that Ku has end bridging activity (Pang et al., 1997; Yaneva et al., 1997). However, since Ku recruits DNA-PKcs, it is most likely that DNA-PKcs, alone or as part of a multi-protein complex, facilitates alignment of DNA broken ends or 'synapsis' (Cary et al., 1997; DeFazio et al., 2002; Yaneva et al., 1997). In agreement with this model, structural analysis of the DNA-PK complex bound to DNA has shown that dimeric interactions between two DNA-PKcs-Ku complexes on opposing ends are mediated by DNA-PKcs (Spagnolo et al., 2006). Moreover, DNA-PKcs has been shown to promote intermolecular ligation by LX suggesting that DNA-PKcs enhances the association of DNA ends (Chen et al., 2000). In addition to its role as an alignment

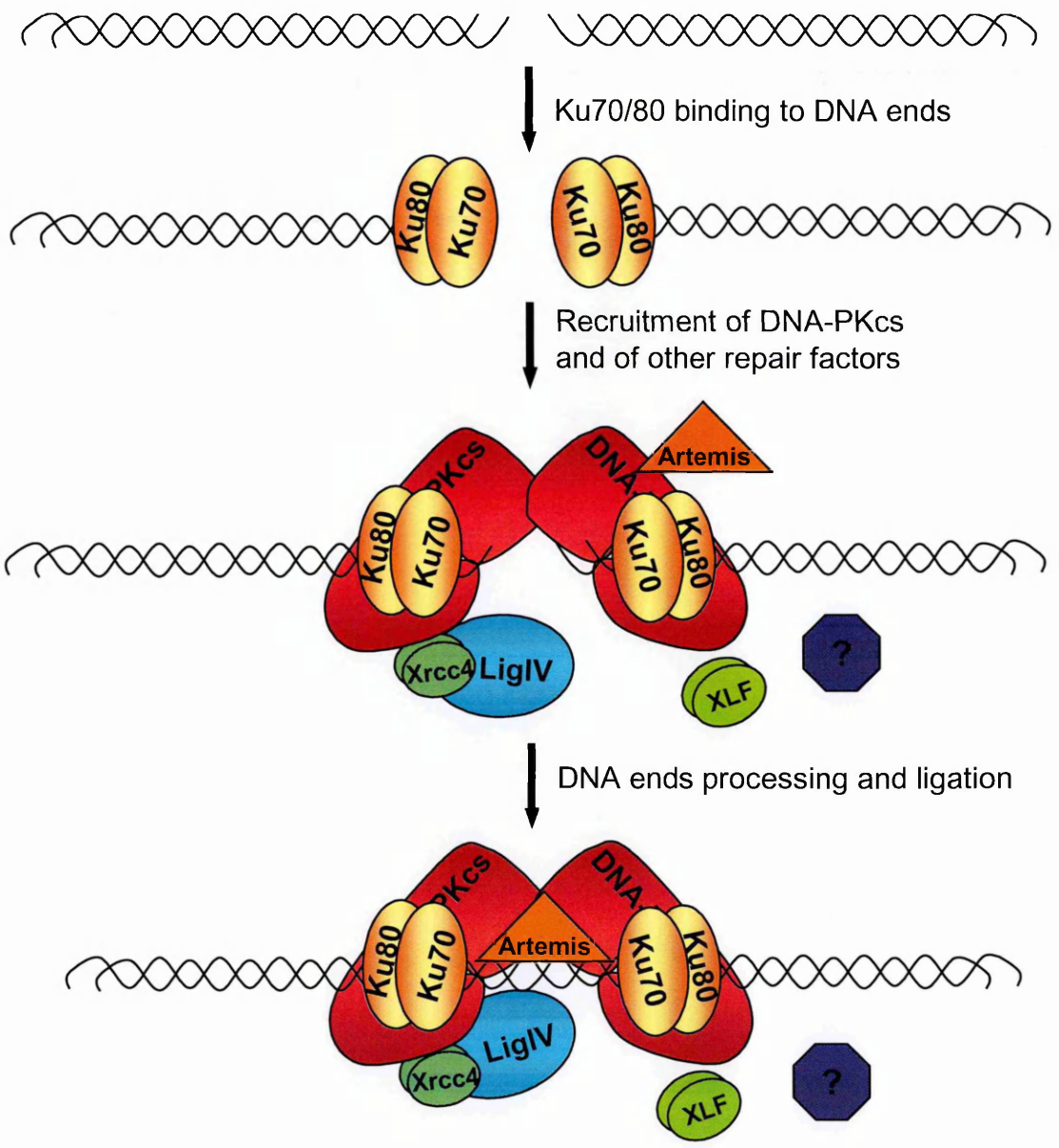

Figure 1-7 Current model of NHEJ. Ku70/80 (yellow) binds to DNA ends at DSBs and recruits DNA-PKcs (red). DNA-PKcs recruits other DNA-repair factors and facilitates DNA ends alignment and synapsis. DNA-PK regulates DNA ends processing prior to ligation by the LX complex (blue and green).

factor, DNA-PKcs most likely also prevents DNA ends degradation. Indeed, DNA-PKcs inhibitors and mutations within the autophosphorylation cluster 2609-2647 block intermolecular ligation by LX suggesting that unphosphorylated DNA-PKcs protects DNA ends (Block et al., 2004; Ding et al., 2003; Reddy et al., 2004). Once bound to DNA ends, DNA-PKcs may also act as a scaffold and recruit other repair factors

(Calsou et al., 2003; Hsu et al., 2002; Leber et al., 1998; Mahajan et al., 2002; Mickelsen et al., 1999).

The binding of DNA-PKcs to DNA and its dimerization with another DNA-PKcs activates its serine/threonine kinase activity (DeFazio et al., 2002). Activated DNA-PK phosphorylates itself and all the main components of the NHEJ, although the role of these phosphorylation events is still unknown. Autophosphorylation of DNA-PKcs has been shown to result in dissociation of the kinase from DNA-bound Ku (Chan and Lees-Miller, 1996; Merkle et al., 2002). However, recent studies with DNA-PKcs phosphorylation mutants suggest that DNA-PKcs undergoes a series of autophosphorylation-induced conformational changes that regulate access to DNA ends. Phosphorylation within the cluster sites 2609-2647 of DNA-PKcs results in a more open conformation, leaving DNA ends accessible to DNA modification and open for alignment of DNA ends. Phosphorylation of cluster 2023-2056 of DNA-PKcs induces a conformational change that probably promotes interaction with LX (Cui et al., 2005). LX is not very active in end-to end ligation itself, but requires interaction with Ku (Nick McElhinny et al., 2000). Moreover, its activity is stimulated by the presence of DNA-PKcs and other repair factors, as has been shown in a cell-free end-joining assay (Lee et al., 2000). Thus, after interaction of LX with other repair factors bound to DNA ends, the ligase can complete the joining reaction.

1.5 AIM OF THE THESIS

The binding of Ku to DNA ends at DSBs represents the first and essential step of the NHEJ pathway. Once bound, Ku interacts with other repair factors, such as DNA-PKcs and LX, and enhances their affinity for DNA. Therefore, the interaction between Ku and DNA is of central importance for the beginning and for the proper outcome of the NHEJ process. How Ku unloads from the DNA after end joining is still an open question. The first goal of this thesis was to characterise the DNA binding properties of the Ku heterodimer to gain more insight into the mechanism that regulates the Ku-DNA interaction. In particular, the thermodynamic properties of the binding of Ku to DNA were analysed by means of fluorescence spectroscopy, in order to rigorously determine the affinity of Ku for DNA ends and the eventual existence of cooperativity between heterodimers simultaneously bound to long DNA molecules. The microscopic binding constant for the binding of Ku to DNA probes of increasing lengths was measured under different solution conditions varying ionic strength and pH.

An efficient eukaryotic expression system that allowed the production of recombinant Ku70/80 (rKu70/80) with high yield was used to obtain the necessary amount of protein required for the biophysical studies. After optimisation of the expression conditions, the purity and the conformational properties of the rKu70/80 were analysed using different techniques to prove that the recombinant protein was properly expressed and the purity of the sample was sufficient for the biophysical studies.

Previous studies have suggested that the NHEJ process occurs through a series of reactions that are coordinated by protein-protein interactions. However, further biochemical studies are needed to define the molecular architecture of the protein complexes assembled on DNA ends. Therefore, the second aim of this thesis was to characterise the interactions that occur between the Ku heterodimer and the other main

components of NHEJ, such as DNA-PKcs and the LX complex. The role of nucleic acids and DNA-PKcs phosphorylation in regulating these interactions was also investigated. Moreover, the interaction between Ku and other proteins previously hypothesized to be involved in the NHEJ or in other DNA repair pathways was examined. These studies were performed to provide novel information on the mechanism of assembly of the NHEJ complex and on other factors possibly required for DNA end processing or for regulating the NHEJ process.

2 MATERIALS AND METHODS

2.1 REAGENTS AND ENZYMES

Salts were purchased from Sigma (St. Louis, MO, USA), Riedel-de Haën (Seelze, Germany), Fluka (Buchs, Switzerland) and Merk (Darmstadt, Germany). Bovine serum albumin (BSA), dithiothreitol (DTT), phenylmethylsulfonyl fluoride (PMSF), ethidium bromide (EtBr), Tween 20, Triton X-100, β-glycerol phosphate, β-mercaptoethanol were from Sigma. All DNA restriction enzymes, T4 Polynucleotide Kinase (T4 PNK) and T4 DNA Ligase were purchased from New England Biolabs (Beverly Ma USA). *Pfu* DNA Polymerase was from Promega (Promega Corporation, Madison, WI, USA). All enzymes were used following the manufacturer's instructions.

2.2 ANTIBODIES

Commercial antibodies were obtained and used as follows: mouse monoclonal antibody anti-Ku70 (A-9, sc5309, Western blotting, WB, 1:1000), anti-Ku80 (B-1, WB 1:1000), anti-DNA-PKcs (G-4, sc5282, WB 1:1000), anti c-Myc (9E10, sc40, WB 1:100) and rabbit polyclonal antibody anti-PARP (H-250, sc7150, WB 1:1000), anti-RecQ1 (H110, sc25547, WB 1:1000) were from Santa Cruz Biotechnology, Inc. (Santa Cruz, CA); mouse monoclonal (162) antibody to Ku70/80 (ab3108) and rabbit polyclonal to Werner's syndrome protein helicase (ab200, WB 1:2000), to 53BP1 (ab4564, WB 1:2000), to Artemis (ab3639, WB 1:2000) were purchased from Abcam Ltd. (Cambridge, UK); rabbit anti-human LigIV (AHP554, WB 1:1000) and anti-XRCC4 antibodies (AHP387, WB 1:1000) were purchased from Serotec (Oxford, UK); mouse monoclonal antibody anti-RPA32 (Ab-2, WB 1:1000) and anti-RPA70 (Ab-1,

WB 1:1000) were purchased from Oncogene Research Products; non-immunized mouse or rabbit IgG were purchased form Santa Cruz Biotechnology.

Goat anti-mouse, goat anti-rabbit and rabbit anti-goat horseradish peroxidase conjugated antibodies were from Pierce Biotechnology, Inc. (Rockford, USA). Horseradish peroxidase conjugated antibodies were resuspended in 50% ethylene glycol (Pierce Biotechnology). Secondary antibodies were used at a dilution of 1:10000.

2.3 OLIGONUCLEOTIDES

All oligonucleotides were chemically synthesized and purified by reverse-phase high pressure liquid chromatography (RP-HPLC) (Sigma-Aldrich, Suffolk, UK) and resuspended in Tris-EDTA (TE) buffer (10 mM Tris-HCl, pH 7.5, 1 mM EDTA, pH 8.0). Oligonucleotide sequences are reported in Table 2-1. The concentration of all oligonucleotides was measured by reading their absorbance at 260 nm and using the molar extinction coefficient calculated on the basis of their base composition with Oligo Analyzer 3.0 software. All fluorescent oligonucleotides were ~80% labelled with the fluorescein probe. The percentage of fluorescently labelled template was obtained by comparing the concentration values measured at 495 nm (fluorescein) and at 260 nm (DNA).

The blunt-ended DNA duplexes were made by annealing the oligonucleotides with their complementary strands labelled with fluorescein at the 5' end (Table 2-1 and 3-2). The annealing was performed in annealing buffer (10 mM Tris-HCl, pH 7.5, 50 mM NaCl, and 0.5 mM EDTA) by heating at 95°C for 3 min, slowly (Δ1°C/min) decreasing the temperature to 60°C or to 70°C, and waiting for 30 min at this temperature before cooling to room temperature. For the annealing reaction, the unlabelled oligonucleotides were used in 1.1-fold excess over the labelled ones. The final concentration of the annealed templates was 5 μM, and their purity was judged to

be ~90% by nondenaturing polyacrylamide gel electrophoresis (PAGE) run in Tris-borate electrophoresis (TBE) buffer (89 mM Tris-borate, 2 mM EDTA, pH 8.0). All duplex concentrations used in the DNA binding experiments were appropriately corrected for percentage of fluorescently labelled template.

Table 2-1 Oligonucleotides used in the DNA binding experiments: the 5'-3' sequence is reported; F: fluorescein.

Oligo name	Sequence 5'-3'
U20	cgtacccgatgttttcgttc
D20F	F-gaacgaaaacatcgggtacg
U25	gtcctcgtacccgatgttttcgttc
D25	gaacgaaaacatcgggtacgaggac
D25F	F-gaacgaaaacatcgggtacgaggac
U42	tgtcgtggtcagtcttcgtcctcgtacccgatgttttcgttc
D42F	F-gaacgaaaacatcgggtacgaggacgaagactgaccacgaca
U50	tgttagtatgtcgtggtcagtcttcgtcctcgtacccgatgttttcgttc
D50F	F-gaacgaaaacatcgggtacgaggacgaagactgaccacgacatactaaca
U60	gtcatgtccctgttagtatgtcgtggtcagtcttcgtcctcgtacccgatgttttcgttc
D60F	F-gaacgaaaacatcgggtacgaggacgaagactgaccacgacatactaacagggacatgac
U75	cgctctgttctgtgagtcatgtccctgttagtatgtcgtggtcagtcttcgtcctcgtacccgatgttttcgttc
D75	gaacgaaaacatcgggtacgaggacgaagactgaccacgacatactaacagggacatgactcacagaacagagcg
D75F	F-gaacgaaaacatcgggtacgaggacgaagactgaccacgacatactaacagggacatgactcacagaacagagcg

2.4 DNA CONSTRUCTS

Full-length human Ku70 cDNA with the additional region coding for the polyhistidine tag was subcloned into the *BssH*II and *Sal*I sites downstream of the PH

promoter of pFastDual, while Ku80 cDNA with the additional region coding for the polyhistidine tag was subcloned into *Xho*I and *Nsi*I sites downstream of the p10 promoter of pFastDual (Invitrogen). pcDNA3 Ku80 was a kind gift from Prof. Penny Jeggo (University of Sussex, UK). In this construct, human Ku80 cDNA was cloned into *Bam*HI sites of pcDNA3. Human Ku70 cDNA was cloned into *Bam*HI and *Xho*I sites of pcDNA3.1(+). Human $Ku80^{1-554}$ cDNA was PCR amplified with a reverse primer containing a termination codon after residue 554 followed by a *Xho*I site, pcDNA554Ku80rp (Table 2-2). Human $Ku80^{1-554}$ was then cloned into *Bam*HI and *Xho*I sites of pcDNA3.1(+).

pcDNA3.1(+) LigIV, pCI-puro(myc) LigIV and pCI-puro(myc) XRCC4 were a kind gift from Prof. Penny Jeggo. In pcDNA3.1(+), human LigIV was cloned into *BamHI* and *NotI* sites. myc cDNA encoding a single myc epitope was introduced into pCI-neo vector (Promega) at the *Nhe*I and *Xho*I restriction sites generating a pCI-neo(myc) vector. The *Hpa*I–*Bam*HI fragment, which contains the neomycin resistance gene, was replaced by a *Pvu*II–*Bam*HI fragment, containing the puromycin gene, from a pPUR vector (Clontech laboratories, Inc., CA, USA) generating a pCI-puro(myc) vector. Wild-type LigIV cDNA was then sub-cloned into the *Xho*I and *Not*I sites of the pCI-puro(myc) vector, while wild-type XRCC4 cDNA was sub-cloned into *Eco*RI and *Xba*I sites. To generate pCIpuro(myc) $LigIV^{1-643}$, pCIpuro(myc) $LigIV^{1-748}$, pCIpuro(myc) $LigIV^{1-790}$ and pCIpuro(myc) $LigIV^{R814X}$ a termination codon after residue 643, 748, 790 and 813 respectively was created by QuickChange XL Site-Directed Mutagenesis Kit (Stratagene) using Cter643LIVfp, Cter643LIVrp; Cter748LIVfp, Cter748LIVrp; Cter790LIVfp, Cter790LIVrp and R814XLIVfp, R814XLIVrp respectively (Table 2-2). pCIpuro(myc) $LigIV^{K273G}$ was obtained by site-directed mutagenesis using ligK273Gw and ligK273Gc (Table 2-2). $LigIV^{600-911}$ cDNA was PCR amplified with a forward primer containing a tail of three nucleotides at the 5'

followed by a *Xho*I site and by an ATG start codon, 600LIVBRCTfp (Table 2-2). LigIV$^{600\text{-}911}$ was then cloned into *Xho*I and *Not*I sites of the pCIpuro(myc) vector.

The entire cDNAs were analyzed by nucleotide sequencing after mutagenesis.

Table 2-2 Primers used for PCR: the 5'-3' sequence is reported.

Primer name	Sequence 5'-3'
pcDNA554Ku80rp	ctactcgagctagaaaatttcctgagcagtcac
Cter643LIVfp	gttattggaattattgagcactaaaaagcacctaaccttactaacg
Cter643LIVrp	cgttagtaaggttaggtgctttttagtgctcaataattccaataac
Cter748LIVfp	ctttatgattcatatgtgcccataaaccaaagaacattttgcccg
Cter748LIVrp	cgggcaaaatgttctttggtttatgggcacatatgaatcataaag
Cter790LIVfp	ctaacgagcagactcctgaataaatggcttctctgattgctg
Cter790LIVrp	cagcaatcagagaagccatttattcaggagtctgctcgttag
ligK273Gw	cagagtttctacatagaaaccgggctagatggtgaacgtatgc
ligK273Gc	gcatacgttcaccatctagcccggtttctatgtagaaactctg
600LIVBRCTfp	ccgctcgagatgcaacttaggggggaaggcatc
R814XLIVfp	gctctcctctcagtatgttttgacgccacaccgtttatttgg
R814XLIVrp	ccaaataaacggtgtggcgtcaaaacatactgagaggagagc

2.5 CELL CULTURE AND EXTRACTS

Escherichia coli DH5α competent cells and XL10-Gold ultracompetent cells (Stratagene, CA, USA) transformed with the appropriate plasmid were grown in Luria-Bertani medium [LB medium (per litre): 10 g bacto-tryptone, 5 g bacto-yeast extract, 10 g NaCl, (pH 7.5)] supplemented with 100 μg/ml ampicillin, overnight at 37°C. *E. coli* DH10Bac (Invitrogen) transformed with the appropriate plasmid were grown in LB

containing 50 μg/ml kanamycin, 7 μg/ml gentamicin and 10 μg/ml tetracycline, overnight at 37°C. Bacterial colonies were maintained on LB-ampicillin agar plates at 4°C for short-term storage, while for long-term storage bacteria were kept on glycerol stocks made by adding sterile glycerol to a final concentration of 20% to liquid bacterial cultures. Glycerol stocks were stored at –80°C.

The *Spodoptera frugiperda* ovary (Sf9) cells were purchased from Gibco (Invitrogen Corporation, Carlsbad, CA). Sf9 cells were maintained at 27°C in SF-900 II medium with L-glutamine (Gibco) supplemented with 10 μg/ml gentamicin and 2% heat-inactivated fetal bovine serum (FBS; Gibco). Suspension cultures were passaged when they reached a density of 2.0 x 10^6 cells/ml and diluted back to 0.7 x 10^6 cells/ml. Cells were frozen at a density of 1 x 10^7 viable cells/ml using a medium composed of 45% fresh growth medium, 45% conditioned growth medium and 10% dimethyl sulfoxide (DMSO). Cells were stored in liquid nitrogen.

Human glioma cell lines that lack (M059J) or express (M059K) DNA-PKcs were purchased from American Type Culture Collection (Manassas, VA, USA). Cells were cultured in a medium containing a 1:1 mixture of Dulbecco's Modified Eagle's Medium (D-MEM) and Ham's F12 (F12) medium, plus GlutaMAX (Gibco) supplemented with 10% FBS, 15 mM HEPES, pH 7.0, 0.05 mM non-essential amino acids and penicillin-streptomycin (Gibco) in 5% CO_2 at 37°C. 180BR and 1BR.3 human primary fibroblasts were grown in 5% CO_2 at 37°C in D-MEM plus GlutaMAX (Gibco) supplemented with 15% FBS and penicillin-streptomycin. Confluent monolayer cells were washed with phosphate-buffered saline (PBS; 137 mM NaCl, 2.7 mM KCl, 10 mM Na_2HPO_4, 1.8 mM KH_2PO_4, pH 7.4) and treated with trypsin (0.25% trypsin, 0.5 mM EDTA in PBS) at 37°C for 5 minutes or until cells were dislodged. An appropriate volume of complete growth medium was added and cells were pelleted. Cells were then resuspended in complete growth medium. Glioma cells were subcultured at a ratio of 1:6 to 1:8, while

primary fibroblasts were subcultured at 1:2 to 1:3. Cells were frozen at a density of approximately 2 x 10^6 cells/ml in complete growth medium supplemented with 10% DMSO and then stored in liquid nitrogen. To prepare whole cell extracts, ~90% confluent cells were washed with PBS, trypsinized, washed with cold PBS and lysed with lysis buffer (50 mM Tris-HCl, pH 7.5, 150 mM NaCl, 2 mM EDTA, 10 mM NaF, 10 mM β-glycerol phosphate, 0.5 % Nonidet P-40 (NP40), 10% glycerol, 1 mM DTT, 0.2 mM Na_3VO_4 and protease inhibitor cocktail from Sigma) at 4°C for 30 min. HeLa nuclear extracts were from 4C Biotech (Seneffe, Belgium). Extracts were clarified by centrifugation at 14,000 x *g* for 10 min at 4 C. Protein concentrations were estimated by Bradford protein assay (Bio-Rad GmbH Laboratories, Munchen, Germany). A standard curve was obtained using serial dilutions of BSA. Extracts were snap-frozen in small aliquots in liquid nitrogen and stored at -80°C.

2.6 PLASMID DNA PURIFICATION

Small-scale preparations of plasmid DNA from bacterial cultures were obtained using the Wizard® *Plus* SV Minipreps DNA Purification System (Promega) according to the manufacturer's instructions. In general, 10-15 µg of plasmid DNA were obtained from 5 ml of an overnight culture. Large-scale preparations of plasmid DNA were obtained using Qiagen® Plasmid Midi or Maxi Kit (Qiagen GmbH, Hilden, Germany) according to the manufacturer's instruction. In general, approximately 400 µg of plasmid DNA were obtained from 100 ml of an overnight bacterial culture. The concentration of purified plasmid DNA was determined by measuring the absorbance of DNA samples at 260 nm (A_{260}) and using an absorption coefficient of 0.02 $(\mu g/ml)^{-1}cm^{-1}$ (Ausubel, 1994). The purity of the DNA samples was estimated by reading the

absorbance at 280 nm (A_{280}) and by measuring the A_{260}/A_{280} ratio. A ratio of 1.8 or higher was obtained for most of the DNA preparations.

2.7 AGAROSE GEL ELECTROPHORESIS AND RECOVERY OF DNA FRAGMENTS

DNA samples were mixed with DNA loading buffer (6X DNA loading buffer contained 0.25% bromophenol blue, 0.25% xylene cyanol, 30% glycerol) and then analysed by agarose gel electrophoresis. Horizontal agarose gels (0.8-1% agarose in TBE) were used to analyse plasmid DNA, DNA restriction enzyme digests or to separate DNA fragments prior to gel extraction. To stain DNA, EtBr was added to 0.5 µg/ml in the gel or gels were soaked in SYBR Safe™ DNA Gel Stain (Molecular Probes, Invitrogen) diluted in TBE, for 30 min. DNA was then visualized by transillumination with ultraviolet (UV) light.

DNA fragments were purified from agarose gels using QIAquick Gel Extraction kit (Qiagen) according to the manufacturer's instructions.

2.8 EXPRESSION AND PURIFICATION OF RECOMBINANT PROTEINS

Recombinant baculoviruses expressing both polyhistidine-tagged Ku70 and Ku80 subunits were generated using the recombinant pFastBacDual Ku70/80 vector according to the manufacturer's instructions. Sf9 cells cultured in suspension were infected at a density of 1.5×10^6 cells/ml with recombinant baculovirus at a multiplicity of infection (MOI) of about 10 plaques forming units/cell (pfu/cell). Ninety-six hours after infection, cells were harvested by centrifugation, washed with PBS and resuspended in lysis buffer (50 mM Tris-HCl, pH 7.5, 5 mM β-mercaptoethanol, 1% NP40 and protease inhibitor mixture from Roche Diagnostics (Penzberg, Germany)). 1

ml of lysis buffer was used for 1.5-2 x 10^7 cells and the incubation was performed on a rolling wheel at 4°C for 15 min. Extracts were clarified by centrifugation at 1,600 x *g* for 10 min at 4°C and incubated with TALON metal affinity resin (Clontech) (1 ml of resin/ 5 mg of protein) for 2 h at 4°C. The resin was then washed with lysis buffer and with buffer (20 mM Tris-HCl, pH 7.5, 5 mM β-mercaptoethanol, 12.5 mM imidazole) containing 500 mM NaCl (three washes) and 100 mM NaCl (two washes). The polyhistidine-tagged rKu70/80 was eluted in 20 mM Tris-HCl, pH 7.5, 100 mM NaCl, 5 mM β-mercaptoethanol, 100 mM imidazole. This buffer was then changed to 20 mM Tris-HCl, pH 7.8, 100 mM NaCl, 2 mM DTT using a Vivaspin 6 ml concentrator, 100,000 MWCO from Vivascience (Hannover, Germany).

The amino acid sequence preceding each subunit of Ku is MSYYHHHHHHDYDIPTTENLYFQGAMGST and contains 6 histidines, a linker region, and a rTEV protease cleavage site. To remove the N-terminal polyhistidine sequence, rKu70/80 was incubated overnight at 4°C with rTEV protease (Invitrogen) in 50 mM Tris-HCl, pH 8.0, 0.5 mM EDTA, 1 mM DTT, and the digested sample was loaded again on the TALON column. The fraction not retained by the resin containing rKu70/80 was concentrated and stored in 20 mM Tris-HCl, pH 7.8, 100 mM NaCl, 2 mM DTT. N-terminal sequence analysis was performed as a final step to verify the removal of the polyhistidine-tag. After rTEV cleavage, 7 residues remain bound to the N terminus of each subunit.

The concentration of the rKu70/80 was determined by UV absorption measurements in 6 M guanidine hydrochloride (Gnd-HCl) and 0.02 M MES (pH 6.5) using a molar extinction coefficient of 95580 M^{-1} cm^{-1} and of 88740 M^{-1} cm^{-1} for the protein with and without the polyhistidine-tags, respectively, at 280 nm, estimated from the amino acid sequence (ProtParam; www.expasy.org). Small protein aliquots were snap-frozen in liquid nitrogen and stored at -80°C.

Recombinant LX and RPA were expressed and purified by other members of the Proteomics group (ICGEB, Trieste, Italy), as described previously (Henricksen et al., 1994; Marchetti et al., 2006).

2.9 *IN VITRO* TRANSCRIPTION/TRANSLATION SYSTEM

Purified plamids were used for *in vitro* translation/transcription reactions using TNT T7 Quick Coupled Transcription/Translation System (Promega). A 0.5-1 μg portion of each construct was used for each reaction. In the case of Ku70/80 and of the LX complex, the Ku70 construct was co-expressed with the Ku80 construct and LigIV with the XRCC4 construct, respectively. A 2-μl volume of each reaction mixture was used for Western blot analysis.

2.10 SDS POLYACRYLAMIDE GEL ELECTROPHORESIS AND DETECTION OF PROTEINS

Protein samples were heated at 95°C for 5 min in sodium dodecyl sulfate (SDS)-sample buffer (5X SDS-sample buffer contained 250 mM Tris-HCl, pH 6.8, 500 mM DTT, 10% SDS, 0.5% bromophenol blue, 50% glycerol) and then analysed by SDS-PAGE according to the standard Laemmli method (Laemmli, 1970). In general, protein samples were analyzed on 8 or 10% gel prepared using acrylamide M-BIS, 40% stock solution 29/1 (Gerbu Biotechnik GmbH, Gaiberg, Germany). SDS-PAGE was performed in SDS electrophoresis buffer (25 mM Tris, 190 mM glycine, 0.1% SDS).

Proteins were detected in the gel by Coomassie blue staining or silver staining. Coomassie blue staining was performed with 0.2% Coomassie Blue R-250 in water/methanol/acetic acid (45/45/10). Gels were then destained with water/methanol/acetic acid (65/25/10). For silver staining, proteins were first fixed in

50% methanol, 12% acetic acid and 0.05% formalin for 2 hrs or overnight. The gels were then washed three times with 35% ethanol for 20 min, sensitized with 0.02% sodium thiosulfate for 2 min, washed three times with milli-Q water for 5 min, stained with 0.2% silver nitrate, 0.076% formalin for 20 min, washed twice with milli-Q water and then developed with 6% sodium carbonate, 0.05% formalin, 0.0004% sodium thiosulfate. The reaction was stopped with 50% methanol, 12% acetic acid. The gels were then stored in 1% acetic acid at 4°C.

2.11 IN-GEL DIGESTION OF PROTEINS AND MASS SPECTROMETRY ANALYSIS

The Coomassie blue- and silver-stained bands containing Ku70, Ku80 and co-ip proteins were cut out the polyacrylamide gel and destained. Silver-stained bands were first washed with water to remove acetic acid and then treated with 15 mM potassium ferricyanide, 50 mM sodium thiosulphate until the gel slices became clear. The bands were then treated with acetonitrile for 15 min. Destained bands from silver staining and Coomassie blue-stained bands were washed with 100 mM ammonium bicarbonate and then with a 1:1 solution of 0.1 M ammonium bicarbonate and acetonitrile for 15 min. Gel slices were crushed with a Teflon stick and gel pieces were dehydrated with acetonitrile. Gel pieces were incubated with 10 mM DTT in 0.1 M ammonium bicarbonate for 1 hour at 56°C to reduce the cysteine residues and then with 50 mM iodoacetamide in 0.1 M ammonium bicarbonate at room temperature for 30 min in the dark to alkylate cysteine residues. Gel pieces were washed with 0.1 M ammonium bicarbonate for 15 min, with 20 mM ammonium bicarbonate/acetonitrile (50:50) for 15 min, dehydrated with acetonitrile for 5 min and then in a Speed Vac to complete dryness. Gel pieces were reswollen with 0.1 μg/ml porcine trypsin (Promega) in 0.1 M

ammonium bicarbonate and incubated at 37°C overnight. Peptides were extracted from the gel pieces with milli-Q water and 60% acetonitrile, 1% trifluoroacetic acid. The volume of supernatants containing the digestion products was reduced to 10 µl in a Speed Vac. The digestion products were separated by micro-HPLC and analysed by electrospray ionisation mass spectrometry (ESI-MS; Finnigan LCQ DECA, Thermo-Finnigan Corp., San Jose, CA). Proteins were identified by analysis of the peptide MS/MS data with Turbo SEQUEST (ThermoFinnigan) and MASCOT (Matrix Science).

2.12 GEL FILTRATION ANALYSIS

Gel filtration was performed on a Superdex 200 HR 10/30 column (Amersham Biosciences) equilibrated with Tris-HCl, pH 7.8, 150 mM NaCl and 2 mM DTT at a flow rate of 0.5 ml/min. Calibration was obtained using pre-mixed standard proteins of known molecular mass (Gel Filtration Calibration Kits HMW and LMW, Amersham Biosciences). The distribution coefficient (K_d) was determined from the chromatogram for pre-mixed standard proteins of known molecular mass and for the samples. K_d of each gel filtration column is defined as:

$$K_d = \frac{V_e - V_o}{V_t - V_o}$$

where V_e, V_t and V_o represent the elution, total and void column volume, respectively. The K_d values were then plotted against the logarithm of the molecular mass of the standard proteins. The standard curve obtained was used to calculate the apparent molecular mass of rKu70/80.

2.13 STEADY-STATE FLUORESCENCE AND ANISOTROPY MEASUREMENTS

Fluorescence experiments were performed with FluoroMax-3 fluorometer (Jobin Yvon, France) equipped with Glan-Thompson prism polarizer. Fluorescence anisotropy was measured at a 90° angle in a L-format. Sample temperature was controlled by a Peltier cooler (Jobin Yvon F-3004). Fluorescence spectra of rKu70/80 were acquired using 1.2 ml samples in a 1.4 ml quartz cuvette with a light path of 10 mm for excitation and 4 mm path for emission. Fluorescence anisotropy measurements were performed using 1.5 ml samples in a 4 ml quartz cuvette (10 x 10 x 45 mm; Hellma, Germany). The samples were mixed by pipetting with low retention tips (Molecular BioProducts, CA, USA), since stirring with the magnetic bar induced protein precipitation. Fluorescence emission spectra of rKu70/80 were acquired upon excitation at 278 nm and at 295 nm with a band pass of 5 nm for excitation and emission. Fluorescence excitation spectra of rKu70/80 were acquired at 349 nm with a band pass of 5 nm for excitation and 9 nm for emission. Fluorescence spectra were acquired at a protein concentration of 0.1 μM in 20 mM Tris-HCl, pH 7.5, 150 mM KCl, 2 mM DTT.

All buffers used for fluorescence measurements were filtered through 0.22 μm Millipore filters (GP Express PLUS membrane form Millipore Corporation, Billerica, MA). A small aliquot of solution was first filtered and then discarded to avoid any contaminants that might be leached from the filter. All fluorescence anisotropy measurements were performed in buffer A (20 mM Tris-HCl, pH 7.8 at 25°C, and 2 mM DTT). The concentrations of NaCl, KCl, NaBr, and NaF in this buffer ranged from 95 to 800 mM. All binding isotherms were collected at constant DNA concentration. Initially, a small aliquot (2 –20 μl) of a highly concentrated protein solution was added to reach the complete saturation of the DNA duplex. The volume in the cuvette was maintained constant thorough all the titration experiment and the protein concentration was gradually reduced performing serial dilutions with a DNA solution not containing

the Ku heterodimer. At each step, a small volume was removed from the sample cuvette and was replaced by an equal volume of solution containing the same DNA concentration. This procedure allows measurements of titration curves at constant macromolecule concentration. The anisotropy data were collected using an excitation wavelength of 495 nm and monitoring the emission at 523 nm. The band pass was 7 nm for excitation and 9 nm for emission. The integration time was 8 s. Typically, 3 to 6 measurements were collected and averaged for each point of the binding isotherm. Fluorescence intensity measurements before and after the titration experiment were made under magic angle condition setting the excitation polarizer to 0° and the emission one to 55°, and using an integration time rate of 0.4 s/nm.

2.14 SALT-BACK TITRATIONS

The 25 bp blunt-ended duplex DNA was initially titrated with the Ku heterodimer, under stoichiometric conditions, until an excess of protein was achieved. Successively, small aliquots (3-20 µl) of buffer A containing a high concentration of salt (4.9 M for NaCl and NaBr, and 3.4 M for KCl and KBr) were added. In the case of NaF, the concentration of the high salt buffer was 880 mM, due to the low solubility of this salt, and salt-back titrations were performed by replacing a fixed volume (50-400 µl) of the solution in the cuvette with the high salt buffer. The concentration of Ku and DNA were kept constant throughout the experiment. The decrease in the anisotropy signal, accompanying the dissociation of the Ku-DNA complex, was monitored as a function of the salt concentration. For all salts, the variation in the anisotropy signal due to the change in the salt concentration can be neglected since it is less the 10% of the total anisotropy change registered upon Ku binding. The validity of the method is confirmed by the fact that the k_d values obtained from salt-back titrations perfectly agree

with those determined from independent titrations performed at constant salt concentration and varying the amount of ligand.

2.15 ELECROPHORETIC MOBILITY SHIFT ASSAY

Synthetic oligonucleotides U20, U42 and U75 (Table 2-1) were labelled with [γ^{32}P]ATP (5000 Ci/mmol; Amersham Biosciences, Buckinghamshire, UK) using T4 PNK. The kinase reaction was performed in PNK buffer (70 mM Tris-HCl, pH 7.6, 10 mM $MgCl_2$, 5 mM DTT) at 37°C for 1 h and 30 min. The enzyme was heat-inactivated at 95°C for 5 min. [γ^{32}P]ATP labelled oligonucleotides were then annealed with their complementary strands labelled with fluorescein at the 5' end (D20F, D42F, D75F; Table 2-1) in annealing buffer, by heating at 95°C for 3 min and then slowly cooling to room temperature. Radiolabelled DNA duplexes were then purified using Micro Bio-Spin Chromatography Columns (Bio-Rad, Hercules, CA). Electrophoretic mobility shift assays (EMSA) were performed by incubating the purified rKu protein (1.74 μM) with [γ^{32}P] labelled dsDNA duplexes (0.4 nM) of various lengths (20, 42 and 75 bp) in 10 μl reaction mixture containing 20 mM Tris-HCl pH 7.8, 2 mM DTT, 80 μg/ml BSA, and KCl (from 100 to 275 mM). After incubation for 30 min at room temperature, 2.5 μl of 5X gel loading buffer (250 mM Tris-HCl pH 7.5, 0.2% bromophenol blue, 0.2% xylene cyanol, 40% glycerol) were added and the reaction products were separated on a 5% nondenaturing polyacrylamide gel run at 4°C in TBE buffer. Labelled DNA fragments were detected in the dried gel by autoradiography (Instant Imager, Packard Corp., Meriden, CT).

2.16 CO-IMMUNOPRECIPITATIONS ASSAY

Co-immunoprecipitation (co-ip) assays were performed using approximately 150 µg of HeLa nuclear extracts and 800 µg of M059J and M059K whole cells extracts. Ip assays with the recombinant proteins were performed using 200-300 ng of rKu and 33-150 ng of rLX. Purified recombinant proteins were pre-incubated in 20 mM HEPES, pH 7.5, 100 mM KCl, 30 mM NaCl, 0.1 mM EDTA, 2% glycerol, 0.05% Triton X-100, 0.5 mM PMSF, 2 mM DTT, 50 µg/ml BSA (IP buffer) for 30 min on ice. Co-ip assays with *in vitro* translated proteins were performed with 14 µl of each TNT reaction mixture. TNT samples were incubated for 30 min on ice. Where indicated, EtBr (50 µg/ml) or a 75 bp blunt-ended ds oligonucleotide (10 µg/ml) were added to the samples.

Anti-Ku70/80, anti-LigIV, anti-XRCC4, anti-RECQ1, normal rabbit or mouse antibodies were added to protein samples and incubation was carried out for 2 h with recombinant proteins and for 3 h with cell extracts and *in vitro* translated products. Incubation with antibodies was performed with very gently rotation on a rolling wheel at 4°C. Protein A-agarose beads, purchased from Santa Cruz Biotechnology, Inc. (Santa Cruz, CA), were washed twice in IP buffer. Fifteen microliters, for ip with recombinant proteins, or twenty-five microliters, for ip with cell extracts and *in vitro* translated proteins, of preswollen and washed protein A-agarose beads were added to the ip samples and incubation was performed for 1 h at 4°C mixing on a rolling wheel. The beads were then washed four times with 350 µl of IP buffer for 5 min at 4°C. Immunocomplexes were released from the beads by heating at 95°C for 5 min in 2X SDS-sample buffer.

2.17 DEPHOSPHORYLATION AND *IN VITRO* KINASE ASSAY

Dephosphorylation reactions were performed with HeLa nuclear extracts prior to co-ip. HeLa nuclear extracts were incubated with lambda protein phosphatase (λ–PPase; New England BioLabs) in λ–PPase buffer (50 mM Tris-HCl pH 7.5, 100 mM NaCl, 0.1 mM EGTA, 2 mM DTT, 0.01% Brij 35, 2 mM $MnCl_2$) at 30°C, for 30 min. Where indicated, HeLa nuclear extracts were preincubated with a 75 bp blunt-ended ds oligonucleotide for 30 min on ice, prior to phosphatase treatment. In control reactions, HeLa nuclear extracts were incubated in λ–PPase buffer without $MnCl_2$.

In vitro kinase assays were carried out on the immunocomplexes obtained after ip with anti-Ku70/80 antibodies in HeLa nuclear extracts. Immunoprecipitated samples were incubated with 10 mM $MgCl_2$ and 0.5 mM ATP in IP buffer without EDTA at 25°C for 30 min. Mock reactions were performed in IP buffer without EDTA. Where indicated wortmannin (Sigma-Aldrich) was added to the samples at a final concentration of 1 μM. Wortmannin stock solution was made up in 10 mM DMSO, and diluted 500-fold in water immediately before use. For control reactions, an equivalent volume of wortmannin buffer was added to the samples. Samples treated with wortmannin and controls were incubated for 10 min on ice. Then, 10 mM $MgCl_2$ and 0.5 mM ATP were added and samples were incubated at 25°C for 30 min. After incubation with ATP, beads were washed twice with IP buffer and immunocomplexes were released by heating at 95°C for 5 min in 2X SDS-sample buffer.

2.18 DEADENYLATION ASSAY

Deadenylation assays were performed on the immunocomplexes obtained with anti-Ku70/80 antibodies using HeLa nuclear extracts. Beads were washed and subsequently incubated in IP buffer with 2.5 mM sodium pyrophosphate (NaPPi;

Sigma) and 10 mM $MgCl_2$. In control reactions, the immunocomplexes were incubated in IP buffer with 10 mM $MgCl_2$. Reactions were carried out at room temperature for 15 min. After washes, the immunocomplexes were released by heating at 95°C for 5 min in 2X SDS-sample buffer.

2.19 WESTERN BLOT ANALYSIS

Protein samples were resolved by SDS-PAGE and electro-transferred onto polyvinylidene difluoride (PVDF) membrane (Amersham Biosciences) in 96 mM glycine, 12 mM Tris, 10% methanol at 4°C. Membranes were blocked with PBS containing 5% skimmed milk powder and 0.2% Tween 20, for 1 hour at room temperature or overnight at 4°C. Then membranes were probed with primary antibodies and subsequently with horseradish peroxidase conjugated secondary antibodies. Proteins were visualized by enhanced chemiluminescence (ECL) detection system (Amersham Biosciences). Successive immunoblotting were performed on the same membranes after stripping. Stripping was performed by incubating the membrane in 100 mM β-mercaptoethanol, 62.5 mM Tris-HCl pH 6.8, 2% SDS for 30 min at 55°C and washing with PBS containing 0.2% Tween 20 for 10 min. Membranes were then blocked with PBS containing 5% skimmed milk powder and 0.2% Tween 20. For data presentation, films were scanned and processed with Adobe Photoshop 7.0 software.

2.20 γ-H2AX ASSAY

MEFs grown on coverslips were irradiated at 3 Gy. After irradiation and washes, cells were fixed in PBS containing 3.7% paraformaldehyde and 2% sucrose for 15 min, washed in PBS for 3 times and permeabilized for 2 min and 40 sec with 0.2% Triton X-100 in PBS. Samples were incubated with anti-γ-H2AX antibodies (Upstate)

for 30 min at 37°C, washed in PBS three times and incubated with anti-mouse FITC conjugate antibodies (Sigma) for 20 min at 37°C, washed in PBS three times and nuclei were counterstained with DAPI. Coverslips were mounted using Vectashield (Vector Laboratories, Inc. Burlingame). For quantitative analysis foci were counted using a fluorescence microscope. Foci present in 100 cells were counted in each experiment. Data points were the mean of at least three independent experiments with SD indicated by error bars.

2.21 FAR-WESTERN ANALYSIS

Purified rKu70/80 and rRPA were resolved by 10% SDS-PAGE and then electro-transferred onto PVDF membrane. All subsequent steps were performed at 4°C. The membrane was immersed twice in denaturation buffer (6 M Gnd-HCl in PBS) for 10 min. Then, membrane was immersed 6 times in serial dilutions (1:1) of denaturation buffer supplemented with 1 mM DTT for 10 min. Membrane was blocked in PBS containing 5% skimmed milk powder and 0.3% Tween 20 for 30 min before being incubated overnight with RPA (0.8 μg/ml) in PBS supplemented with 0.25% skimmed milk powder, 0.3% Tween 20 and 1 mM DTT. Membrane was then washed for 4 times with PBS containing 0.25% skimmed milk powder and 0.3% Tween 20 for 10 min. The second wash contained 0.0001% glutaraldehyde.

3 RESULTS AND CONCLUSIONS

3.1 PRODUCTION AND CHARACTERIZATION OF RECOMBINANT KU70/80

3.1.1 Introduction

The Ku heterodimer was originally immunopurified from HeLa cell extracts using autoantibodies from patients with polymyositis-scleroderma overlap syndrome (Mimori et al., 1986). Several attempts to produce functional recombinant Ku have been largely unsuccessful until 1994, when the Ku heterodimer was expressed using the baculovirus system (Ono et al., 1994). Following studies demonstrated that the baculovirus expressed protein is functional and has properties indistinguishable from the native protein isolated form HeLa cells (Arosio et al., 2002).

The baculovirus expression system has many advantages compared to other methods, since it allows the production of large amounts of soluble protein. Moreover, being an eukaryotic expression system, the proteins produced are biologically active and undergo post-translational modifications very similar to those of their native counterparts (Patel, 1995). In addition, using the pFastBac Dual vector, two genes can be expressed simultaneously allowing the production of functional protein complexes. Therefore, this method was employed to co-express the two subunits of the Ku heterodimer. A recombinant bacmid containing both Ku70 and Ku80 cDNAs was generated and used to infect insect cells, thus avoiding simultaneous co-infection with different baculoviruses expressing the two separated subunits, as previously reported (Ono et al., 1994), and ensuring efficient production of Ku heterodimers.

To characterise the properties of rKu70/80, the purified protein was analysed by mass spectrometry, analytical gel filtration chromatography, and fluorescence spectroscopy.

3.1.2 Expression of rKu heterodimer with the baculovirus system

Full-length human Ku70 and Ku80 cDNAs with the additional regions coding for the polyhistidine tag were subcloned downstream of the two promoters of the pFastBac Dual vector. The recombinant vector was then used to generate recombinant baculoviruses necessary to infect Sf9 cells. The N-terminal polyhistidine-tagged Ku70 and Ku80 were purified by cobalt affinity resin. The purity of the recombinant complex was checked by SDS-PAGE and the gel was stained with Coomassie blue and silver staining (Figure 3-1, A and B). rKu70/80 complex migrated as two bands with a

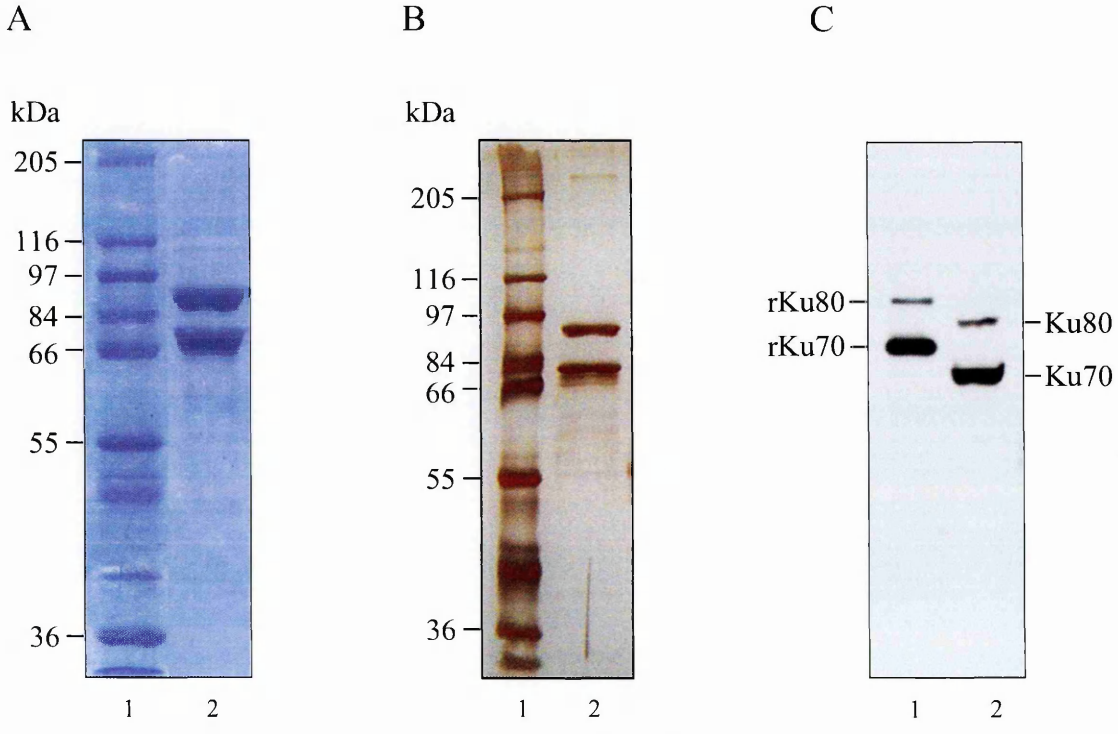

Figure 3-1 SDS-PAGE and Western blot analysis of rKu70/80. After purification by cobalt affinity resin, recombinant proteins were analysed by 8% SDS-PAGE and the gel was stained with Coomassie blue (**A**) or silver staining (**B**). **A**, lane 1, wide-range molecular weight markers; lane 2, 5 μg of rKu70/80. **B**, lane 1, wide-range molecular weight markers; lane 2, 0.8 μg of rKu70/80. **C**, Western blot analysis of purified protein with anti-Ku70 and anti-Ku80 monoclonal antibodies. Lane 1, 40 ng of rKu70/80; lane 2, 28 μg of HeLa nuclear extracts.

molecular weight of ~70 kDa and ~90 kDa corresponding to the polyhistidine-tagged Ku70 (73 kDa) and Ku80 (86 kDa). The identity of the two bands detected by SDS-PAGE was confirmed by Western blot and mass spectrometry analysis (Figure 3-1 C and Table 3-1). Maximum expression of recombinant protein occurred at 96 h post-infection using a MOI of approximately 10 pfu/ml. The amount of protein obtained was quantified by UV light absorption at 280 nm. Up to 1 mg of rKu were obtained from 2 x 10^8 infected Sf9 cells.

Table 3-1 Peptides identified by ESI-MS analysis of rKu70/80 after trypsin digestion.

	Mass (Da)			
Protein	**Found[a]**	**Calculated[b]**	**Sequence[c]**	**Pepetide[d]**
Ku70	1207.5	1206.6	DSLIFLVDASK	65-75
	787.6	1572.8	NIYVLQELDNPGAK	130-143
	960.1	1917.9	IMLFTNEDNPHGNDSAK	195-211
	710	1417.7	DTGIFLDLMHLK	224-235
	694.9	1387.87	DIISIAEDEDLR	248-259
	904.7	1806.9	TFNTSTGGLLLPSDTKR	331-347
	545.6	1088.6	IMATPEQVGK	481-490
	504.1	1006.5	LGSLVDEFK	547-555
	567.0	1699.7	KHDNEGSGSKRPK	573-585
	551.1	550.3	AYGLK	616-620
Ku80	404.7	404.2	MVR	30-32
	803.3	802.4	GITEQQK	225-231
	878.3	877.4	VDEEQMK	355-361
	408.2	814.4	YAYDKR	424-429
	772.3	771.4	SQIPLSK	555-561
	762.1	1521.7	EEASGSSVTAEEAKK	718-732
	703.4	702.4	KFLAPK	732-737

[a] Determined by ESI-MS.
[b] Molecular masses calculated form the amino acid sequence of rKu70/80.
[c] Amino acid sequence of the peptides identified by ESI-MS.
[d] Residue numbers of the peptides identified by ESI-MS of rKu70 and rKu80.

3.1.3 Analysis of rKu70/80 by gel filtration chromatography

Analytical gel filtration chromatography was performed on a Superdex 200 HR 10/30 column in the presence of 20 mM Tris-HCl, pH 7.8, 150 mM NaCl and 2 mM DTT. A single peak eluted with a distribution coefficient (K_d) of 0.2 corresponding to a molecular mass of 305 kDa (Figure 3-2). This profile indicated that the two subunits form an unique complex. Moreover, the absence of protein eluting in the void volume confirmed that the protein did not form aggregates under this buffer condition. The calculated molecular mass was much greater than the theoretical value measured for a globular protein of similar size (159.5 kDa for the recombinant protein). This result is in agreement with previous data (Mimori et al., 1981) and suggests that the Ku complex has an elongated shape in solution. Indeed, the crystal structure has revealed that Ku is an ellipsoid of ~120 x 70 x 60 Å (Walker et al., 2001). In addition, the value of the hydrodynamic radius of rKu70/80 in solution estimated by dynamic light scattering analysis was even greater than that predicted from the crystal structure indicating that the protein might be highly hydrated in solution (Arosio et al., 2002).

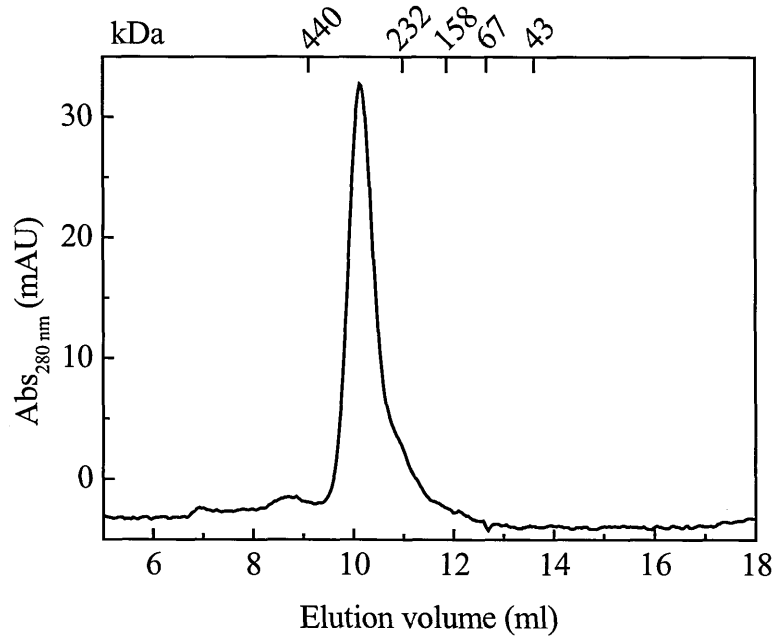

Figure 3-2 Gel filtration analysis of rKu70/80. ~ 200 µg of rKu70/80 were analysed using Superdex 200 HR 10/30 column. The numbers on the top indicate the molecular mass of protein standards.

3.1.4 Analysis of rKu70/80 by fluorescence spectroscopy

The rKu70/80 contains 42 tyrosine (Tyr), 76 phenylalanine (Phe) and 6 tryptophan (Trp) residues. Therefore, fluorescence emission spectra were acquired to investigate the conformational properties of the recombinant protein complex.

Excitation spectrum of rKu70/80 showed a single peak at 278 nm (Figure 3-3, blue curve) that corresponded to the maximum of the absorption spectrum. Upon excitation at 278 nm, emission spectrum showed a single peak near 349 nm (Figure 3-3, green curve). This spectrum reflects only the contributions of Trp and Tyr residues to emission fluorescence, since Phe residues are excited at shorter wavelengths. The value of the fluorescence emission maximum (λem_{max}) measured is consistent with the emission of Trp and indicates that these fluorophores are most likely exposed to the solvent. The λem_{max} measured in the presence and in the absence of the polyhistidine tags did not change, indicating that the tags at the N terminus of rKu70 and rKu80 do not alter the conformation of the heterodimer. Fluorescence emission spectrum of rKu was also measured at 37°C. This spectrum did not show any significant change compared with spectra obtained at 25°C, indicating that at 37°C the protein maintains the same conformation.

To dissect the contribution of Trp from that of the Tyr residues present in the molecule, emission spectra were acquired upon excitation at 295 nm. The two Trp of Ku70 lie in the N-terminal domain of the protein. In particular, the crystal structure has shown that Trp 148 is located in the α/β domain that borders the DNA-binding site of Ku (Figure 1-4 B and 3-4) (Walker et al., 2001). Structural studies have also revealed that in Ku80 Trp 247 lies in the β-barrel domain and Trp 276 in the polypeptide chain that form the channel for DNA binding, while Trp 513 is located in the C-terminal arm close to the internal ring (Figure 1-4 B and 3-4). Trp 675 lies in the C-terminal domain of Ku80. Upon excitation at 295 nm, the λem_{max} occurred at a slightly longer

wavelength, ~ 352 nm, characteristic of fully exposed Trp residues (Figure 3-3, black curve).

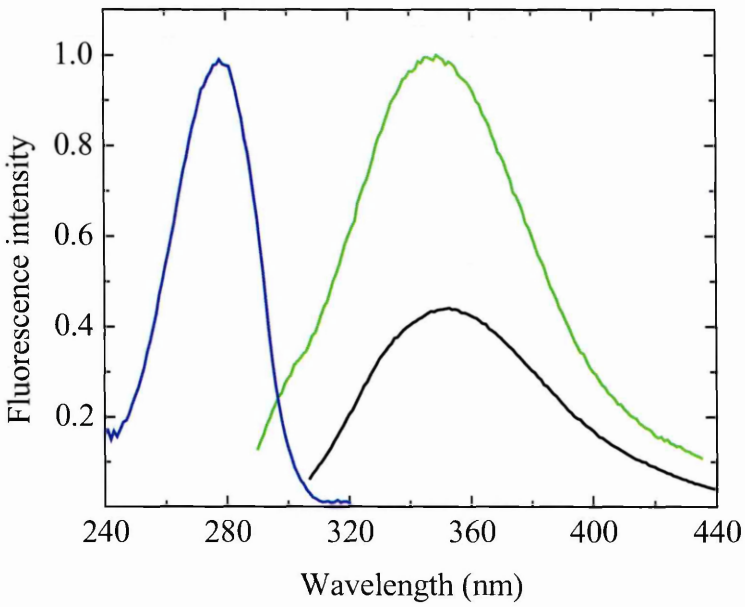

Figure 3-3 Excitation and emission spectra of rKu70/80. Excitation spectra (blue curve) were measured at 349 nm. Emission spectra were acquired upon excitation at 278 nm (green curve), and at 295 nm (black curve). Spectra were acquired in 20 mM Tris-HCl, pH 7.5, 150 mM KCl, 2 mM DTT at 25°C.

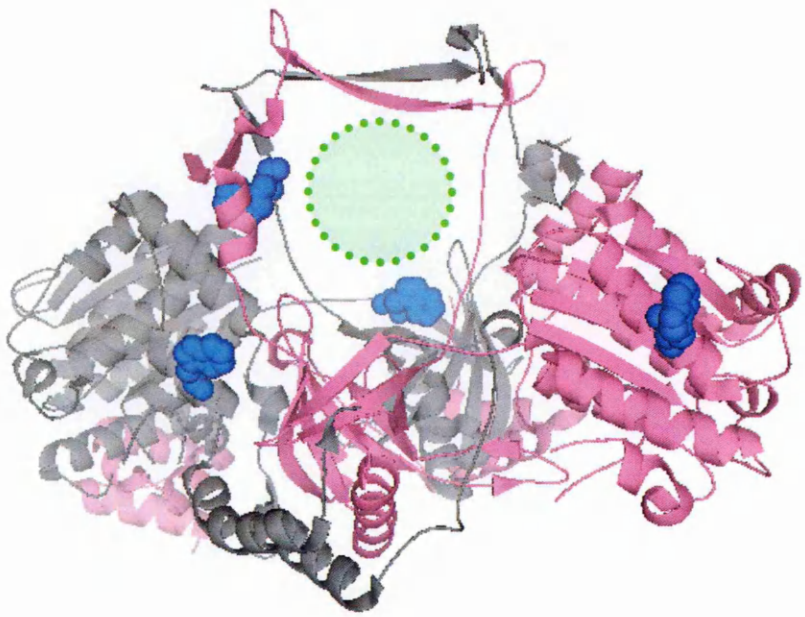

Figure 3-4 Graphic representation of the 3D structure of Ku70/80. The green circle indicates the DNA helix. The four Trp residues present in the 3D model of the protein, located close to the DNA binding site, are represented as blue spheres. The structure was drawn using the PyMol program and the atomic coordinates deposited in the Brookhaven Protein Databank (code 1JEQ).

Fluorescence spectral properties of Ku in the presence of DNA might indicate whether the molecule undergoes a conformational change upon DNA binding. Therefore, fluorescence spectrum of the rKu heterodimer bound to DNA was acquired and compared with the spectrum of the unbound protein (Figure 3-5, black and magenta curve respectively). DNA binding led to a decrease in the fluorescence emission intensity of Ku, while the λem_{max} did not change. The lower fluorescence intensity acquired could be likely related to a quenching effect due to the interaction between some fluorophores and DNA. Indeed, crystallographic studies have shown that four Trp residues present in the 3D model of Ku are close to the DNA binding site of the protein (Figure 3-4) and in particular, Trp 276 in Ku80 is involved in the interaction with the phosphates on DNA. The decrease in fluorescence intensity could also be related to a conformational change of a region of the protein upon DNA binding.

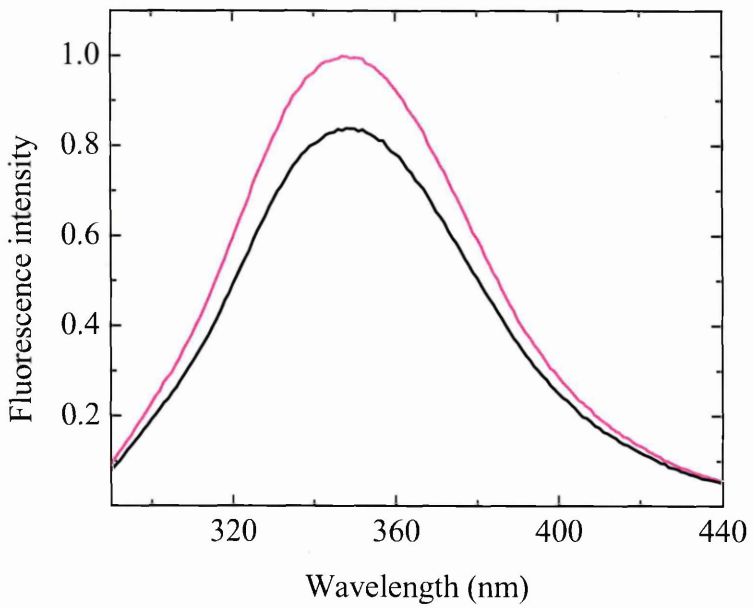

Figure 3-5 Emission spectra of rKu70/80 in the absence (magenta curve) and in the presence (black curve) of 25 bp blunt-ended dsDNA. Spectra were acquired upon excitation at 278 nm in 20 mM Tris-HCl, pH 7.8, 150 mM NaCl, 2 mM DTT at 25°C.

3.1.5 Conclusions

To characterize the DNA binding properties of the Ku heterodimer, it was necessary to produce large amounts of recombinant protein. Previous studies have reported that the Ku heterodimer can be efficiently expressed using the baculovirus system (Ono et al., 1994). This expression system was improved by co-expressing the two subunits of the Ku heterodimer using recombinant baculoviruses containing both Ku70 and Ku80 cDNAs to infect insect cells. After optimisation of the expression conditions, up to 1 mg of rKu70/80 was obtained from 2 x 10^8 infected Sf9 cells.

The biochemical and conformational properties of rKu70/80 were then analysed by SDS-PAGE, mass spectrometry, analytical gel filtration chromatography and fluorescence spectroscopy. These analyses revealed that the purity of the protein samples was sufficient for the biophysical studies. The elution profile obtained by gel filtration showed that Ku forms an unique complex. Moreover, the K_d value indicated that Ku does not have a globular shape, but rather has a more elongated shape, likely an ellipsoid. Fluorescence emission spectra of rKu70/80 showed that the signal is primarily due to the Trp residues present in the molecule. Emission spectra of Ku bound to DNA showed a decrease in the fluorescence intensity, possibly due to a quenching effect of the DNA molecule or to a conformational change of the protein upon DNA binding. The crystal structure of Ku solved in the presence of DNA has revealed that the protein maintains its conformation when bound to DNA. However, the crystallized molecule lacks the C-terminal region of Ku80, where Trp 675 lies. Additionally, many other regions of the protein have not been modelled due to weak or no associated electron density, such as the N terminus of Ku70, where Trp 4 lies. Fluorescence emission spectra of Ku bound to DNA reflect also the contribution of these fluorophores and thus a possible conformational change of these regions upon DNA binding.

3.2 ANALYSIS OF THE DNA-BINDING PROPERTIES OF KU70/80

3.2.1 Introduction

The DNA binding properties of the Ku heterodimer have been extensively investigated using different techniques (Dynan and Yoo, 1998). However, the results of these studies have been controversial. Early studies using Ku protein immunopurified from HeLa cell extracts with patient antibodies showed that Ku binds tightly to linear duplexes, whilst having much lower affinity for single-stranded DNA. Moreover, experiments with restriction enzyme cleaved plasmids provided evidence that Ku binds to DNA ends, regardless of sequence context (Mimori and Hardin, 1986). These and follow-on studies demonstrated that Ku binds to dsDNA ends with 3' or 5' overhangs, as well as to blunt ends and hairpin loops, indicating a high degree of plasticity in its ability to recognise DNA ends (Arosio et al., 2002; Falzon et al., 1993; Mimori and Hardin, 1986; Ono et al., 1994; Paillard and Strauss, 1991; Pang et al., 1997). Furthermore, Ku was shown to recognize a variety of artificial structures, including circular dsDNA molecules with nicks, single-stranded regions (gaps) or double-stranded regions of non-complementarity (bubbles) (Blier et al., 1993; Falzon et al., 1993). DNaseI footprinting analysis of Ku on DNA showed protection of sequences near the DNA ends and suggested that Ku covers approximately 25 bp (Mimori and Hardin, 1986). Subsequently, electrophoretic mobility shift assays (EMSA) demonstrated that Ku only requires short ds oligonucleotides of 14-18 bp to bind DNA (Falzon et al., 1993; Yaneva et al., 1997), whilst neutron-scattering studies showed that Ku can completely bury a 24 bp duplex DNA (Zhao et al., 1999). More recently, crystallographic studies have revealed that the DNA binding site of Ku covers about 20

bp, while encircling only the central 3-4 base pairs and leaving much of the DNA surface area exposed (Walker et al., 2001). This analysis has also shown that Ku only makes contacts with the sugar-phosphate backbone of DNA. Moreover, the crystal structure of the Ku-DNA complex has demonstrated that the Ku heterodimer binds to DNA ends in a preferred orientation. Indeed, the entrance to the DNA-binding site on one side is constructed almost entirely from Ku70 residues, and on the other side by Ku80 residues. In this complex, the free DNA end lies on the Ku70 side (Walker et al., 2001). Consistently, previous photo-crosslinking studies indicated that Ku70 is located proximal, and Ku80 distal, to the free end (Yoo et al., 1999).

Crystallographic studies on the Ku-DNA complex have provided important information about the molecular contacts that can occur within the complex (Walker et al., 2001). However, a complete understanding of the molecular basis for their function requires knowledge of their stability and of the mechanism of interaction, which can be achieved only through quantitative thermodynamic and kinetic studies (Lohman and Mascotti, 1992). The affinity of Ku for dsDNA has been measured using different methods. Binding studies reported values of the dissociation constants ranging from the low picomolar to the nanomolar range (Arosio et al., 2002; Blier et al., 1993; Falzon et al., 1993; Tuteja et al., 1994; West et al., 1998). Once bound to dsDNA, Ku can translocate along the molecule in an ATP independent manner (de Vries et al., 1989; Yaneva et al., 1997), allowing multiple subunits of Ku to bind to linear DNA. Data on the cooperativity of the interaction among the Ku molecules bound to long DNA duplexes are controversial. Ma and Lieber, reported that Ku binds to 45 bp DNA duplex in a cooperative fashion (Ma and Lieber, 2001). However, they did not see any cooperative interaction using DNA molecules of 68 or 90 bp. Conversely, Arosio and co-workers did not detect any cooperative interaction among the heterodimers that bind to DNA duplexes that can accommodate two or three Ku molecules (Arosio et al.,

2002). However, most of these DNA binding studies were not performed under true thermodynamic equilibrium conditions, thus the large discrepancy in the dissociation constant values and the contradictory findings on the presence of cooperativity are probably a result of the different experimental conditions and techniques used for the binding experiments.

This chapter reports the first rigorous quantitative analysis of the thermodynamic parameters that regulate the interaction between Ku and DNA. To study the thermodynamics of the Ku-DNA interaction, equilibrium binding constants were measured as a function of solution variables using a spectroscopic method. Preliminary fluorescence analysis of Ku bound to DNA (Figure 3-5) indicated that the change in intrinsic fluorescence of the protein upon binding to DNA is too small (~20%) for an accurate determination of the dissociation constant (k_d). To increase the sensitivity of the method, DNA duplexes were labelled with a fluorescent probe and the change in the anisotropy signal upon binding with Ku was monitored. Indeed, Ku binding to DNA resulted in an increase of the molecular volume, which led to an increase in the rotational correlation time as well as an increase in fluorescence anisotropy of the labelled dsDNA molecules. Under these conditions, the variation of the signal was more than 50%, allowing an accurate determination of the binding isotherms. Moreover, this technique is of sufficient sensitivity to allow the detection of the low concentrations of DNA necessary to study protein-DNA interactions. In addition, since it is a solution-based methodology, it provides a true equilibrium measure of the protein-nucleic acid interaction and the impact of changing solution conditions, such as ligand and oligonucleotide concentration, as well as pH, temperature and salt, can be easily studied. The effect of salt on the Ku-DNA association was analysed to obtain information on the number of cations and anions that are released upon formation of the complex as well as an estimate of the electrostatic components of the binding free

energy (Ha et al., 1992; Lohman et al., 1996; Overman and Lohman, 1994). Finally, the possible presence of cooperativity among the Ku heterodimers that bind longer duplexes was investigated using a series of DNA duplexes with increasing length (Table 3-2).

Table 3-2 List of blunt-ended DNA duplexes used in the binding studies.

Name	Structure and Sequence [a]
s20	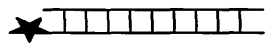 GAACGAAAACATCGGGTACG
s25	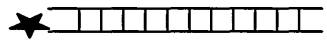 GAACGAAAACATCGGGTACGAGGAC
s42	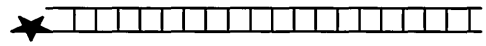 GAACGAAAACATCGGGTACGAGGACGAAGACTGACCACGACA
s50	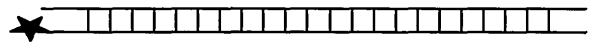 GAACGAAAACATCGGGTACGAGGACGAAGACTGACCACGACATACTAACA
s75	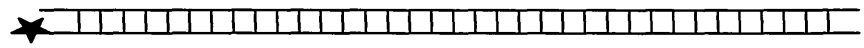 GAACGAAAACATCGGGTACGAGGACGAAGACTGACCACGACATACTAACAGGGACATGACTCACAGAACAGAGCG
ss60	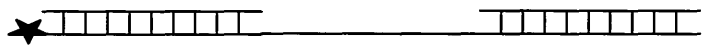 GAACGAAAACATCGGGTACGAGGACGAAGACTGACCACGACATACTAACAGGGACATGAC

[a] The star indicates the position of the fluorescein probe. The 5'-3' sequence of the fluorescein labelled DNA strand is reported.

3.2.2 Determination of the active fraction of rKu70/80

The active fraction of the purified rKu heterodimer was determined prior to DNA binding analysis (Figure 3-6). This was accomplished by titrating a solution of a 20 or 25 bp dsDNA with Ku. Crystallographic data and previous scattering studies showed that these two duplexes accommodate only one Ku molecule (Arosio et al., 2002; Walker et al., 2001; Zhao et al., 1999). Titrations were performed under

"stoichiometric conditions", where the DNA concentration was much greater (>10-fold) than the k_d. These conditions were achieved using DNA concentrations in the nanomolar range and salt concentrations below 150 mM. Under these conditions, all the added Ku molecules bound to the DNA template up to the point where all the available binding sites are saturated and the anisotropy signal reaches a plateau.

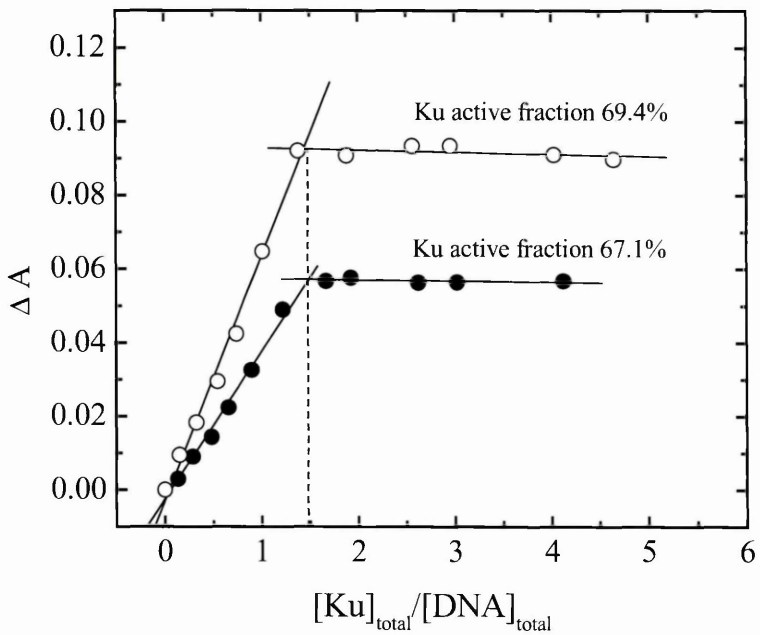

Figure 3-6 Determination of the active fraction of rKu70/80. Plot of the anisotropy changes ΔA *vs.* the ratio $[Ku]_{total}/[DNA]_{total}$. $\Delta A = A_{obs} - A_0$, where A_{obs} is the experimentally observed anisotropy signal and A_0 is the initial anisotropy signal. Data obtained respectively with the 20 (○) and 25 (●) bp duplexes (s20 and s25). Both DNA molecules were at a concentration of 5 nM (>> k_d). The experiments were performed in buffer A at 100 mM KCl and the temperature was set at 25°C. Solid lines are the linear fit of proper portion of the dataset. The active fraction is derived from the value of the crossing point of the two straight lines (1/1.490 = 0.671 x 100 = 67.1%).

The active fraction was about 70 ± 3% for most Ku preparations, with only a few exceptions where the active fraction was about 30-50%. The protein concentrations used in all the binding experiments were corrected for the active fraction. Almost identical results were obtained upon changing either the length or concentration of the duplex, or salt conditions (KCl or NaCl from 50 to 125 mM). Furthermore, the non-active protein fraction did not compromise the DNA binding studies. Indeed, for a

given DNA fragment, the same binding energy was obtained using various protein preparations with different active fractions.

3.2.3 Stoichiometry of the Ku-DNA interaction

The stoichiometry of the interaction between Ku and a series of blunt-ended DNA duplexes of different length (Table 3-2) was measured following a procedure similar to that adopted for the determination of the active fraction. Titrations were performed at DNA concentrations that ranged from 5 to 20 nM in buffer A containing 100 mM salt (Figure 3-7). All stoichiometry values were determined at 2-3 different DNA concentrations. The average values of stoichiometry are reported in Table 3-3. Blunt-ended DNA duplexes of 42 (s42) and 50 bp (s50) can accommodate two Ku heterodimers, while the 75 bp (s75) duplex is capable of binding three Ku molecules (Table 3-3). The 60 bp DNA duplex with a gap of 20 nucleotides in the middle (ss60) can bind two heterodimers, while three Ku molecules can bind to the same duplex of 60

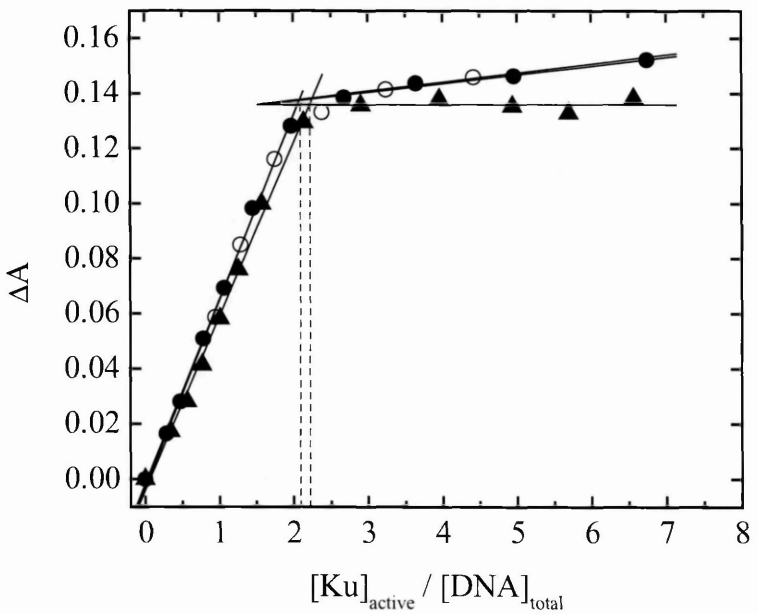

Figure 3-7 Stoichiometry determination for the s42 and s50 duplexes. Plot of the anisotropy changes *vs.* the ratio of active Ku over total DNA concentration. The duplexes used were: s50, 5 nM (▲); s42, 5 nM (○); s42, 10 nM (●). The experiments were carried out under saturating conditions $DNA_{total} >> k_d$ (<0.2 nM) in buffer A at 100 mM KCl and 25°C. The stoichiometry was calculated from the crossing point of the two straight lanes.

bp without the single stranded region. Dividing the number of base pairs (bp) of the DNA by the number of Ku molecules bound to each DNA duplex, it was estimated that Ku heterodimers cover about 22-25 bp when bound to DNA. For some of the duplexes, the stoichiometry values were also confirmed by EMSA performed at various salt concentrations (Figure 3-8). These assays demonstrated that the stoichiometry did not change at higher salt concentrations.

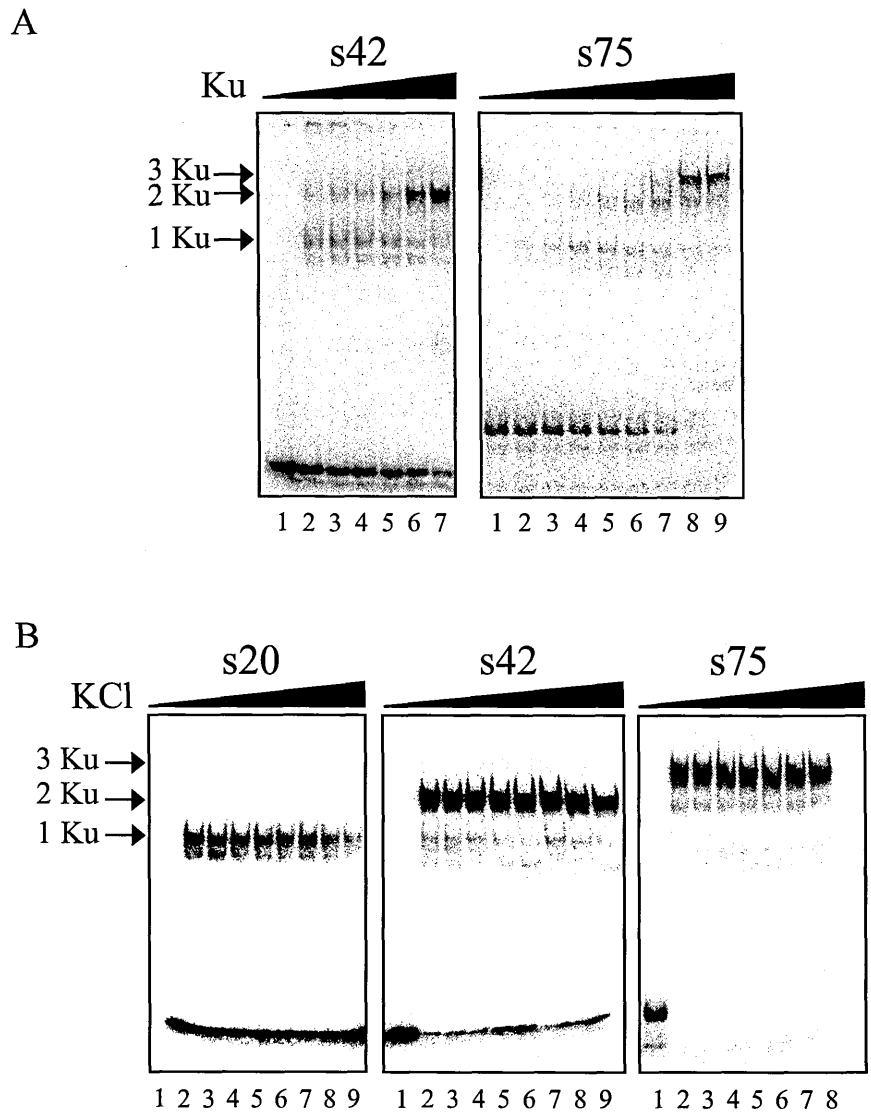

Figure 3-8 Stoichiometry determination for the s20, s42 and s75 duplexes by EMSA. **A**, the experiments were carried out with increasing amount of Ku and 0.4 nM DNA in buffer A containing 100 (s42) and 225 (s75) mM KCl and 80 μg/ml BSA. The reaction mixture was incubated for 30 min at room temperature and then reaction products were separated on a 5% non-denaturing polyacrylamide gel. Lane 1: DNA alone. Lanes 2-7 (s42): experiments performed increasing the concentration of Ku from 0.034 to 1.1 μM. Lane 2-9 (s75): experiments performed increasing the concentration of Ku from 0.2 to 4.3 μM. **B**, the experiments were carried out with 1.74 μM Ku and 0.4 nM DNA in buffer A containing different concentrations of KCl and 80 μg/ml BSA. Lane 1: DNA alone. Lanes 2-9: experiments performed increasing the concentration of KCl from 100 to 275 mM with steps of 25 mM.

Table 3-3 Stoichiometry for all the duplexes used in the binding experiments. Average values are reported.

Duplex	Stoichiometry
s20	1.01 ± 0.06
s25	0.99 ± 0.06
s42	2.08 ± 0.05
s50	2.19 ± 0.11
s75	3.20 ± 0.50
ss60	1.92 ± 0.16

3.2.4 Accuracy of the anisotropy measurements

In all the binding studies, the dsDNA duplexes were denoted as the macromolecule (*M*), while Ku was considered as the ligand. The experimentally determined anisotropy change (ΔA_{obs}) is given by Equation 1:

$$\Delta A_{obs} = A_{obs} - A_0 = \sum_{i=1}^{r}(A_i - A_0)M_i = \sum_{i=1}^{r}\Delta A_i(\nu_i / i)M_T \qquad \text{(Eq. 1)}$$

where A_{obs} is the experimentally observed anisotropy signal from the macromolecule, A_0 is the initial anisotropy signal of the free macromolecule, A_i is the anisotropy signal of the macromolecule complex with i bound Ku, M_i is the concentration of the macromolecule with i bound Ku, i is the number of the bound Ku, M_T is the total macromolecule concentration and ν_i the binding density (Lohman and Bujalowski, 1991). Equation 1 is valid as long as the macromolecular binding state does not affect the fluorescence quantum yield of the probe attached to the macromolecule. In all these measurements, the emission spectrum of the DNA-bound fluorescein did not change significantly upon Ku binding. Another requirement is that an effective linear relationship exists between the experimentally determined increase in the anisotropy

signal, ΔA_{obs}, and the average degree of binding, $\Sigma \nu_i$. To verify this condition, a series of titrations were performed at different macromolecule concentrations in buffer A at 220 mM NaCl, under conditions where the shape of the binding isotherms is dependent upon the total macromolecule concentration (Figure 3-9, A). Data were analysed following the procedure already described by Lohman *et al.* (Bujalowski and Lohman, 1989; Lohman and Bujalowski, 1991). As shown in Figure 3-9, B, the ΔA_{obs} is a linear function of the degree of binding.

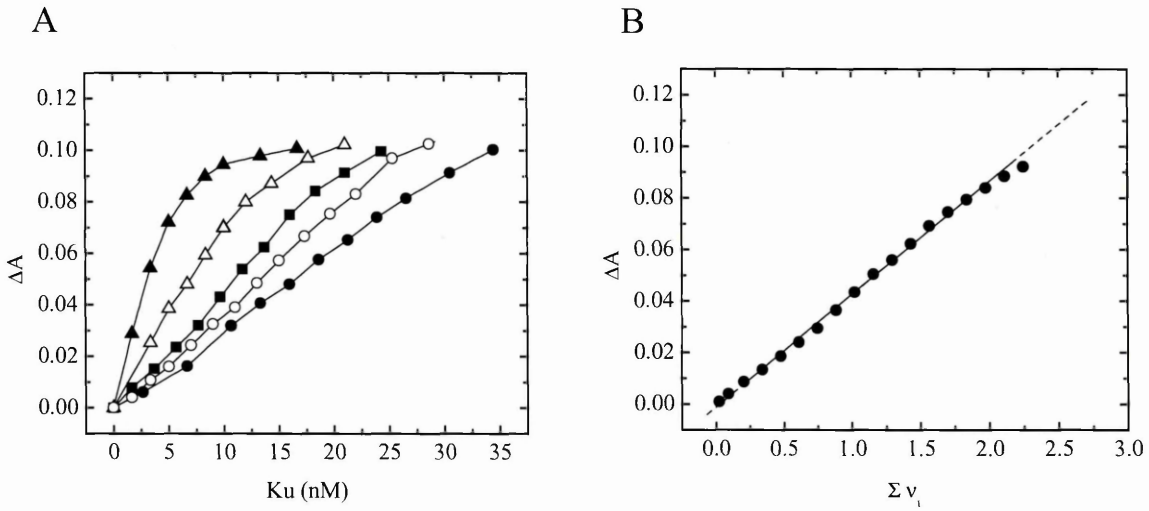

Figure 3-9 Analysis of the relationship between the signal monitored and the binding density. **A**, binding curves were collected at different macromolecule (s75) concentration: 1(▲), 3 (△), 5 (■), 7 (○), 10 (●) nM, in buffer A at 220 mM NaCl and 25°C. **B**, plot of the anisotropy values *vs.* the binding density $\nu = \sum \nu_i$ calculated with the method described by Lohman *et al.* (Lohman and Bujalowski, 1991).

Furthermore, evidence for this direct proportionality also comes from the stoichiometry studies showing that the anisotropy signal increases linearly with the fraction of ligand bound. The existence of a linear relationship between the signal measured and the degree of binding allowed fitting of the measured binding isotherms with equations of the following general form (Equation 2):

$$A_{obs} \leftarrow A_0 + \Delta A_{\max} \frac{\nu(k_1, k_2, \cdots)}{n} \qquad \text{(Eq. 2)}$$

where the fitting parameters are: the anisotropy signal of the free macromolecule A_0, the maximum change in anisotropy ΔA_{max}, the binding density v, the stoichiometry n, and a various number of binding constants (k_1, k_2...) that need to be considered depending on the binding model chosen.

3.2.5 Ku cooperativity and DSB binding affinity

Preliminary binding experiments suggested that the Ku-DNA interaction is highly salt-dependent and that the equilibrium dissociation constant (k_d) is <0.5nM at 200 mM salt. To simplify the analysis of the binding isotherms, measurements were performed at 300 mM NaCl. Under these conditions, the total ligand (Ku) concentration is almost equal to the free ligand concentration ($x_{free} \approx x_T$) and the binding isotherms are independent from the total macromolecule concentration. The equilibrium dissociation constants were determined at this salt concentration for all the duplexes listed in Table 3-2. DNA molecules with a Ku:DNA stoichiometry of 2:1 (s42 and s50) were selected to investigate the eventual presence of cooperativity between the Ku heterodimers that bind to the same DNA molecule.

Binding isotherms for s42 and s50 (Figure 3-10) were first fitted with the Adair equation for a macromolecule with two binding sites (Equation 3):

$$v = \frac{2k_1x + 2k_1k_2x^2}{1 + 2k_1x + k_1k_2x^2} \qquad \text{(Eq. 3)}$$

where k_1 and k_2 are the two sequential microscopic association constants that in this case turned out to be identical. Indeed, analogous results were obtained by fitting the data with a simple equation that considers the presence of "2" independent and identical binding sites on the macromolecule (Equation 4):

$$v = \frac{2kx}{1 + kx} = \frac{2x}{k_d + x} \qquad \text{(Eq. 4)}$$

where k_d is the microscopic dissociation constant for the single DNA end. Therefore, this analysis demonstrated the lack of cooperative interaction between Ku heterodimers. The k_d for the binding of Ku to s50 and s42 were 32 ± 2 nM and 81 ± 3 nM, respectively.

A more accurate estimate of k_d was obtained taking into account that, under these experimental conditions, the free ligand concentration (x) was still slightly dependent on the total macromolecule concentration (M_T) and could be more precisely determined using Equations 5 and 6:

$$x = x_T - \nu M_T \qquad \text{(Eq. 5)}$$

$$x = -\tfrac{1}{2}(k_d + 2M_T - x_T) + \tfrac{1}{2}\sqrt{(k_d + 2M_T - x_T)^2 + 4k_d x_T} \qquad \text{(Eq. 6)}$$

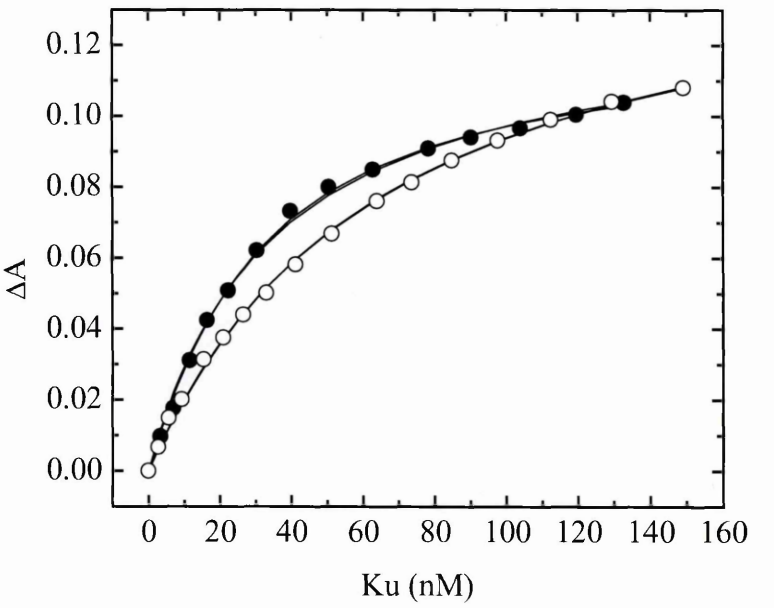

Figure 3-10 Binding isotherms for the s42 and s50 duplexes. The experiments were performed in buffer A at 300 mM NaCl and 25°C. The DNA concentration was 5 nM for the s42 (○) and 5 nM for the s50 (●). The same experiments were also repeated using a DNA concentration of 10 nM. For data analysis, the free ligand concentration (x_{free}) was derived from equation 6. The binding curves were fitted with Equation 4 and yielded k_d values of 81 ± 3 nM (s42) and 32 ± 2 nM (s50). The same analysis performed assuming $x_{free} = x_T$ produced binding curves that are basically superimposable to the previous ones.

The new fit of the data resulted in k_d = 24 ± 1 nM for the s50 duplex and k_d = 72 ± 3 nM for the s42 (Table 3-4). The same analysis was performed for the ss60 molecule containing a 20 nucleotide gap in the middle yielding a k_d value of 21 ± 1 nM.

The short duplexes (s20, s25) were analyzed differently from a simple 1:1 stoichiometry because of the presence of 2 overlapping binding sites on a single macromolecule formed by the two blunt-ends of the duplex (Figure 3-11). A degenerative factor was included into the fitting equation since only one of the two sites can be occupied by a Ku heterodimer (Equations 7 and 8):

$$v = \frac{x}{\frac{k_d}{2} + x} \qquad \text{(Eq. 7)}$$

$$x = -\tfrac{1}{2}\left(\frac{k_d}{2} + M_T - x_T\right) + \tfrac{1}{2}\sqrt{\left(\frac{k_d}{2} + M_T - x_T\right)^2 + 2k_d x_T} \qquad \text{(Eq. 8)}$$

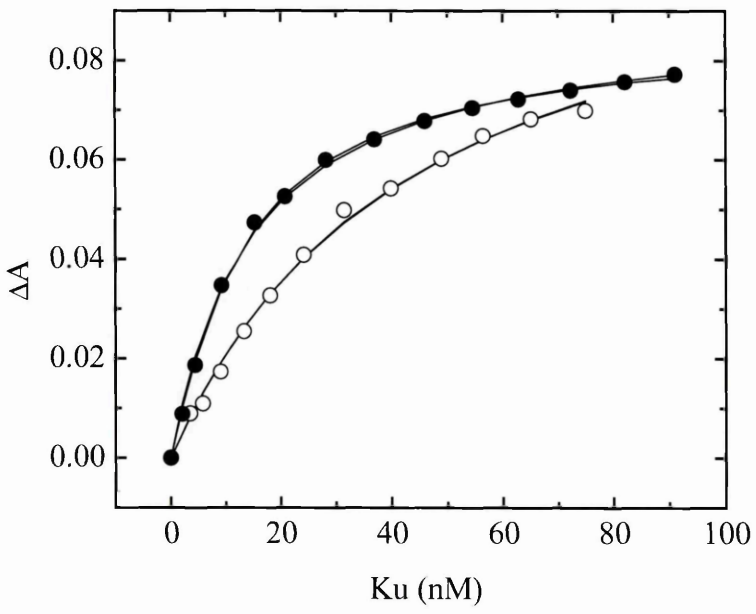

Figure 3-11 Binding isotherms for the s20 and s25 duplexes. The experiments were performed in buffer A at 300 mM NaCl and 25°C. The DNA concentration was 5 nM for the s20 (○) and 5 nM for the s25 (●). The same experiments were also repeated using a DNA concentration of 10 nM. For analysis of the binding curves, the free ligand concentration (x_{free}) was derived from equation 8. The fit of the data with equation 7 yielded k_d values of 77 ± 7 nM (s20) and 29 ± 2 nM (s25). The same analysis performed assuming $x_{free} = x_T$ produced binding curves that are basically superimposable to the previous ones.

The microscopic dissociation constants for Ku binding to the 20 and 25 bp duplexes were 77 ± 7 nM and 29 ± 2 nM, respectively (Table 3-4). The higher k_d value determined for s20 indicates that Ku needs more than 20 bp to efficiently bind DNA. Consistently, the k_d for s42 was higher than that determined for s50 suggesting that the 42 bp duplex is too short to properly accommodate two Ku molecules. The close similarity between the k_d values reported for the two shorter dsDNA (s20 and s25) and those determined for the corresponding longer duplexes (s42 and s50) confirms that the definition of the microscopic binding site, as formed by the free DNA end plus 22-25 bp, is appropriate (Table 3-4).

Table 3-4 Values of the microscopic dissociation constants (k_d) measured for all the DNA duplexes at 300 mM NaCl in buffer A.

DNA duplex	k_d (nM)
s20	77 ± 7
s25	29 ± 2
s42	72 ± 3
s50	24 ± 1
s75	22 ± 1
ss60	21 ± 1

3.2.6 Analysis of Ku binding to s75

The 75 bp duplex is able to accommodate three Ku heterodimers, two are bound at its blunt ends (sites 1 and 3) and one lies in the center of the DNA molecule (site 2). The experimental data were fitted using the Equation 9 defined for a macromolecule with three binding sites:

$$\nu = \frac{3kx + 2(1+2\omega)k^2x^2 + 3\omega^2k^3x^3}{1 + 3kx + (1+2\omega)k^2x^2 + \omega^2k^3x^3} \qquad \text{(Eq. 9)}$$

where the term $(1+2\omega)$ takes into account that the two ligands can either touch each other (if bound to sites 1,2 or sites 2,3) or interact with the two ends without touching each other (if bound to sites 1,3). In this expression, ω corresponds to a cooperativity parameter such that if $\omega > 1$ the contiguous ligands attract each other and the binding is positively cooperative, whereas if $\omega < 1$ the binding is anti cooperative and if $\omega = 1$ there is no cooperative interaction. Analysis of the binding isotherms with Equation 9 yielded a value of ω that is very close to 1 ($\omega = 1.03 \pm 0.09$) and $k_d = 33 \pm 2$ nM (Figure 3-12). A value of ω close to 1 indicates that there is no cooperative interaction

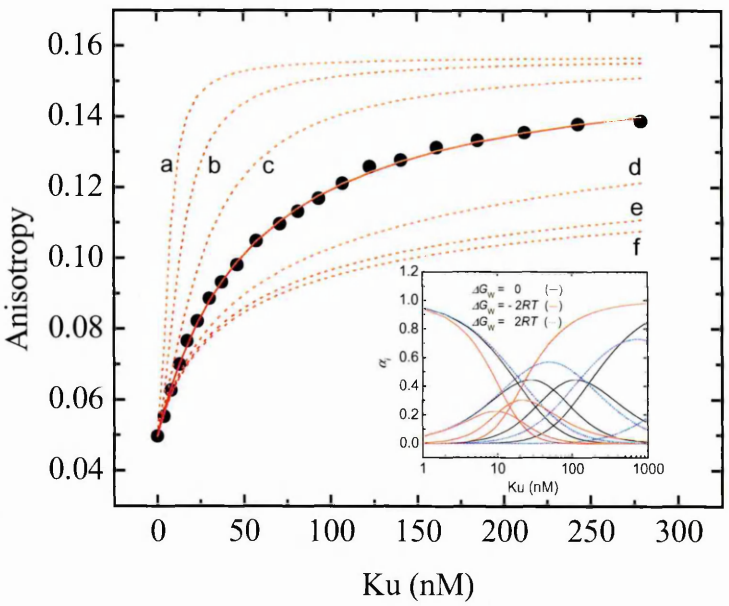

Figure 3-1 Analysis of the binding isotherm for the s75 duplex. The experiments were carried out in buffer A at 300 mM NaCl. The concentration of the DNA duplex was 5 nM while the concentration of the Ku heterodimer was varied from 0 to 300 nM. The experimental data were analyzed with equation 9 yielding a value of $\omega = 1.03 \pm 0.09$ ($\Delta G_\omega \cong 0$) and a value of $k_d = 33 \pm 2$ nM. The dotted lines refer to simulations performed using ΔG_ω values of $-3RT$ (*a*), $-2RT$ (*b*), $-RT$ (*c*), RT (*d*), $2RT$ (*e*), and $3RT$ (*f*). The inset shows the plot of the fraction of macromolecules with "*i*" ligands bound α_i *vs.* the concentration of the Ku heterodimer. The blue and red lines refer to the curves that would be obtained if $\Delta G_\omega = 2RT$ and $-2RT$, respectively.

among the nearest neighbour bound proteins and that the related free energy is almost zero ($\Delta G_\omega \cong 0$). Indeed, the relationship between the cooperativity parameter and the free energy is given by the following equation $\omega = e^{\frac{\Delta G_\omega}{RT}}$, where R and T respectively are the universal gas constant and the absolute temperature ($RT \cong 0.6$ kcal/mol at 25 °C). Computer simulations made assuming ΔG_ω values greater (RT, $2RT$, $3RT$) or smaller ($-RT$, $-2RT$, $-3RT$) than 0 clearly showed that the best fit can be obtained for ω=1 (Figure 3-12). This analysis indicates that the Ku heterodimer has the same affinity for the three binding sites of s75 confirming that the translocation of the Ku heterodimer along the double-stranded DNA molecule is energy independent. Thus, the expression for the degree of binding could be simplified into the general equation for a macromolecule with three identical and independent binding sites (Equation 10):

$$\nu = \frac{3kx}{1+kx} \qquad \text{(Eq. 10)}$$

Also in this case, the free ligand concentration could be more precisely calculated using the expression that takes into account the total macromolecule concentration (Equation 11):

$$x = -\tfrac{1}{2}(k_d + 3M_T - x_T) + \tfrac{1}{2}\sqrt{(k_d + 3M_T - x_T)^2 + 4k_d x_T} \qquad \text{(Eq. 11)}$$

Remarkably, the k_d value of 22 ± 1 calculated using Equations 10 and 11 was in good agreement with those previously measured for s50 and s25 (Table 3-4).

3.2.7 Analysis of binding isotherms considering the potential overlapping binding sites

The binding isotherms for s42, s50, and s75 were also analyzed with a model that takes into account the overlap of ligand binding sites (Di Cera and Kong, 1996; Kong, 2001). For a non-specific DNA binding protein, the potential number of

overlapping ligand binding sites on a DNA lattice is $N - m + 1$, where N is the number of base-pairs of the duplex and m is the number of consecutive residues covered by the ligand. Therefore, assuming that Ku covers 25 bp when binding to DNA, the number of overlapping binding sites for the 75 bp duplex would be equal to 51. The equations describing the binding of either non-interacting or interacting ligands to a one-dimensional linear lattice of infinite length were initially developed by McGhee and von Hippel (McGhee and von Hippel, 1974) and successively refined by several groups (Bujalowski et al., 1989; Ferrari et al., 1994; Friedman and Manning, 1984; Lohman and Mascotti, 1992; Woodbury, 1981). The binding isotherms were analysed with the method derived by Di Cera and Kong for the interaction of ligands with a linear lattice of arbitrary length and cooperativity (Di Cera and Kong, 1996; Kong, 2001). This method gives the "generating function" of all the partition functions of the model under study. By series expansion of the generating function, the partition functions of systems of any length can be obtained as the coefficients of the power series: $G(z) = 1 + P(1)\, z + P(2)\, z^2 + P(3)\, z^3 + \ldots + P(N)\, z^N + \ldots$ For a system of length N, its partition function $P(N)$ is the coefficient of z^N, where z is the auxiliary variable in the generating function. The general form of the generating function used for this analysis is shown in Equation 12:

$$G(z) = \frac{1-(\omega-1)\vartheta z^m}{1-z-\omega\vartheta z^m+(\omega-1)\vartheta z^{m+1}} \qquad \text{(Eq.12)}$$

where ω is the unitless cooperativity parameter related to the nearest-neighbour interaction among bound ligands; m is the number of binding sites covered by a bound ligand; $\vartheta = kx$, the product of the intrinsic association constant and the free ligand concentration; and z is the auxiliary variable of the generating function. The expression for the degree of binding (ν) can be simply obtained from the partition function as follows (Equation 13):

$$\nu = \frac{\vartheta}{P(m,n,\vartheta,\omega)} \frac{dP(m,n,\vartheta,\omega)}{d\vartheta} \qquad \text{(Eq. 13)}$$

where $P(m,n,\vartheta,\omega)$, derived from the generating function G(z), is the partition function of a lattice of n binding sites for a protein that covers m sites. For instance, assuming m = 25 the partition function and the degree of binding for the 75 bp duplex are given by the Equations 14 and 15:

$$P(25,75,\vartheta,\omega) = \omega^2\vartheta^3 + 26\omega\vartheta^2 + 325\vartheta^2 + 51\vartheta + 1 \qquad \text{(Eq. 14)}$$

$$\nu = \vartheta \frac{3\omega^2\vartheta^2 + 52\omega\vartheta + 650\vartheta + 51}{\omega^2\vartheta^3 + 26\omega\vartheta^2 + 325\vartheta^2 + 51\vartheta + 1} \qquad \text{(Eq.15)}$$

Analogous expressions were derived for the s42 and s50, and for other values of m. Since we do not know the precise number of base pairs that are covered by one Ku heterodimer upon DNA binding, the same analysis was repeated for m = 20, 21, 22, 23, and 24 (Figure 3-13). Equation 9 can be considered as a special case in this model, with

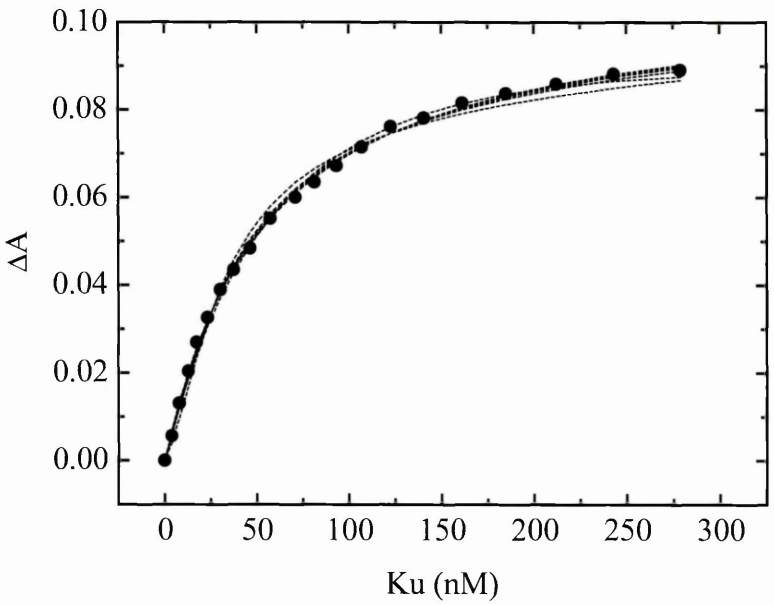

Figure 3-13 Analysis of the binding isotherm for the s75 duplex using the overlapping model and different values of m. The experiments were carried out in buffer A at 300 mM NaCl. The concentration of the DNA duplex was 5 nM while the concentration of the Ku heterodimer was varied from 0 to 300 nM. The expressions of the degree of binding for m = 20, 21, 22, 23, 24, and 25 were derived from Equation 13 as described in the text. The lines show the fit of the binding isotherm for all the different values on m.

m=1 and N=3. As expected, the results showed that the k_d values depended slightly on the value *m*, although they were all in the same range of those calculated with the previous model, after normalization of the binding sites (Table 3-5). In addition, the value of the cooperativity parameter (ω) ranged between 14 and 197 for all duplexes and *m* values (Table 3-5). The overlapping model should yield values of ω at least 10-fold higher for the cooperative interaction of proteins with DNA (Bujalowski and Lohman, 1987; Ferrari et al., 1994). Thus, this small value of the cooperative parameter confirmed that there is no significant nearest-neighbour cooperative interaction among the Ku heterodimers binding to these DNA duplexes.

Table 3-5 Values of the equilibrium dissociation constants k_d (nM) and the cooperativity parmeters (ω) calculated with the equation 13 as described in the text. The value of k_d has been normalized by the number of binding sites N-m+1 of the DNA lattice.

		***m* = 20**	***m* = 21**	***m* = 22**	***m* = 23**	***m* = 24**	***m* = 25**
	s42	15.9±0.9	22.8 ± 2	34.0 ± 2	34.0 ± 2	34.0 ± 2	34.0 ± 2
k_d	s50	20.4± 0.6	20.4±0.6	20.4±0.6	20.4±0.6	20.4±0.6	20.4±0.6
	s75	19.3± 0.6	19.7±0.6	20.4±0.7	21.4±0.7	23.2±0.8	26.8± 0.8
	s42	17 ± 4	17 ± 3	-	-	-	-
ω	s50	20 ± 2	25 ± 3	32 ± 3	44 ± 4	70 ± 7	197 ± 18
	s75	14 ± 2	17 ± 2	20 ± 3	25 ± 4	29 ± 6	16 ± 5

3.2.8 Salt dependence of the k_d for the Ku interaction with s25

The equilibrium dissociation constant for the binding of Ku to the blunt-ended DNA duplex of 25 bp was measured as a function of salt (Figure 3-14 and 3-15). Dynamic light scattering studies, performed as previously described, established that the assembly state of the Ku heterodimer is not influenced by the salt concentrations used in the experiments (Arosio et al., 2002). On the basis of the observation that the anisotropy signal of the DNA duplex was only slightly affected by [NaCl] over the concentration range used in the experiment, values of k_d were determined as a function of [NaCl] from salt-back titrations (see material and methods) (Figure 3-14).

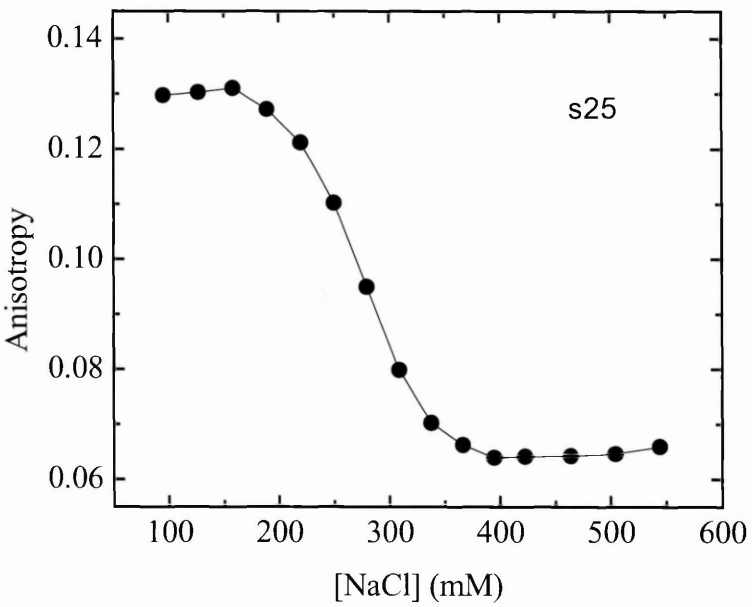

Figure 3-14 s25-Ku salt back titration. The experiments were carried out in 20 mM Tris-HCl pH 7.8, 2 mM DTT. The concentration of NaCl was gradually increased from 95 to 540 mM. The concentrations of Ku and DNA were 11.1 nM and 10 nM, respectively.

The salt back titrations were fitted using the following equations derived for 2 overlapping sites (s25) from Equations 5 and 7:

$$k_d = \frac{2(1-\nu)}{\nu}(x_T - \nu M_T) \qquad \text{(Eq. 16)}$$

$$\Delta A_i \equiv \frac{\Delta A_{obs}}{\Delta A_{max}} = \nu \qquad \text{(Eq. 17)}$$

$$k_d = \frac{2(1-\Delta A_i)}{\Delta A_i}(x_T - \Delta A_i M_T) \qquad \text{(Eq. 18)}$$

The k_d values agreed with those determined from independent titrations performed at constant salt concentration varying the amount of ligand. The equilibrium dissociation constant dramatically increased as [NaCl] was increased, indicating that there is a significant release of ions (Na^+ and/or Cl^-) upon Ku binding to DNA and a sizeable contribution of electrostatic interactions to the binding free energy (Figure 3-15). The value of the slope Γ_{salt} was 12.4 ± 0.1 indicating that approximately 12 ions are released upon complex formation (Table 3-6). In order to dissect the relative contribution of cation *versus* anion release to the slope values, the salt dependence studies were repeated using various salts that differ on the cation and anion type. For all experiments, it was first confirmed that the anisotropy signal was nearly independent of the salt concentration. The cation was changed from Na^+ to K^+. The linear fit of the data showed that there was no significant difference in the salt dependence of the k_d values measured in Na^+ and K^+ indicating that an identical number of ions is released upon formation of the Ku-DNA complex (Figure 3-15). The anions were varied from Cl^- to Br^-, and F^-. These results clearly showed that the anion type and concentration affected both the magnitude and salt dependence of the k_d (Figure 3-15). At 300 mM Na^+ (pH 7.8 at 25 °C), the equilibrium dissociation constants varied as follows: k_d (Br^-) = 33·k_d (Cl^-) = 2250·k_d (F^-) (Table 3-6).

The slopes were 12.1 ± 0.3 in NaBr and 8.8 ± 0.2 in NaF compared to 12.4 ± 0.1 in NaCl (Table 3-6). The slope in NaF was significantly smaller than in the other salts, in agreement with the observation that fluoride interacts weakly with proteins (von Hippel and Schleich, 1969), reflecting only the preferential interaction of Na^+ with nucleic acids. Therefore, the slope of 8.8 ± 0.2 measured in NaF indicates that

approximately 9 Na^+ are released from DNA upon complex formation. In addition, the difference between the slopes measured with the other anions (~12) and the slope measured in NaF (9) suggests that about 3 anions are released from the Ku heterodimer upon binding to DNA when the experiments are performed in the presence of Br^- or Cl^-.

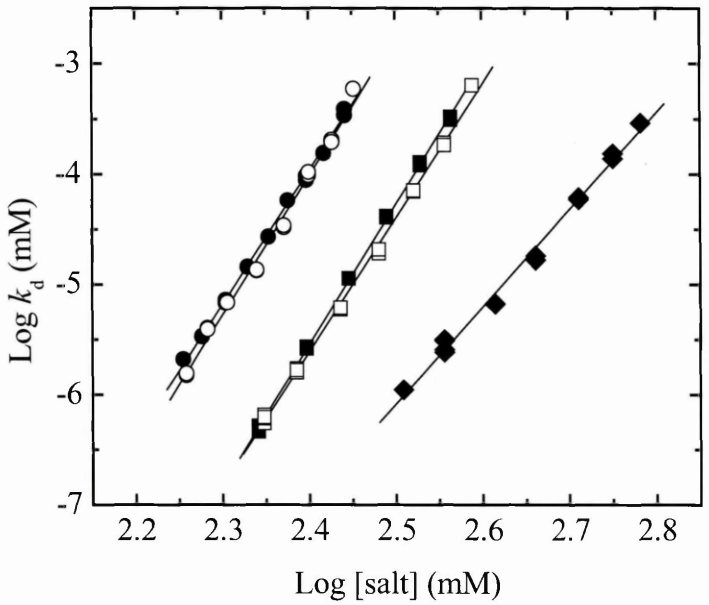

Figure 3-15 The effect of NaBr (●), KBr (○), NaCl (■), KCl (□), and NaF (◆) concentrations on the k_d for Ku binding to s25. The k_d values were obtained from the salt back titrations using the equation 15, as described in the text.

Table 3-6 Dependence of the dissociation constant on salt concentration for the interaction of Ku with the 25 bp blunt-ended DNA molecule. The slope values (Γ_{salt}) as well as the dissociation constants derived from the salt-back titrations at 220 mM and 300 mM salt are reported.

Salt	Γ_{salt}	**k_d (nM) (220 mM)**	**k_d (nM) (300 mM)**
NaBr	12.1 ± 0.3	21.6 ± 0.5	900 ± 20
KBr	12.6 ± 0.3	17.9 ± 0.4	890 ± 20
NaCl	12.4 ± 0.1	0.5 ± 0.01	26.9± 0.2
KCl	12.1 ± 0.2	0.5 ± 0.01	20.9 ± 0.3
NaF	8.8 ± 0.2	0.003 ± 0.0001	0.4 ± 0.01

3.2.9 Conclusions

The interaction of Ku with nucleic acids was quantitatively studied by following the change in fluorescence anisotropy of fluorescein-labelled DNA duplexes upon protein binding. The binding of Ku to nucleic acids occurs at DNA ends and is independent of their structure and sequence (Arosio et al., 2002; Falzon et al., 1993). After binding to the DNA termini, Ku can translocate to internal positions with a process that seems to be energy independent (de Vries et al., 1989). At first, a simple binding model that takes into account these properties of the Ku heterodimer was developed and allowed a proper analysis of the binding isotherms. Thus, the microscopic dissociation constants for DNA duplexes of various lengths was quantified under different solution conditions.

The binding studies were initially performed with two short blunt-ended DNA duplexes of 20 and 25 bp that can accommodate only one Ku heterodimer. Although these duplexes show a 1:1 stoichiometry, they were considered as macromolecules with 2 overlapping binding sites. Indeed, they possess two DNA ends and the binding of Ku to one end prevents the binding of a second molecule to the other end (see equation 7). Binding studies performed at 300 mM NaCl yielded k_d values of 77 ± 7 nM and 29 ± 2 nM for s20 and s25, respectively. The higher k_d value reported for s20 indicates that the heterodimer needs more than 20 bp to efficiently bind nucleic acids. In agreement with this conclusion, previous surface plasmon resonance (SPR) and EMSA yielded k_d values between 0.38 and 1.4 nM for the binding of recombinant Ku to an 18 bp blunt-ended dsDNA fragment and a value of 0.16 nM for the binding to a 22 bp blunt-ended duplex (Ma and Lieber, 2001). Similarly, neutron scattering studies showed that a 24 bp DNA lies almost entirely within the Ku complex and crystallographic confirmed that Ku covers approximately two turns of DNA (Walker et al., 2001; Zhao et al., 1999). However, a meaningful comparison of the affinity values reported in the literature can

be done only if the experiments are performed under similar solution conditions. In fact, the magnitude of the k_d for the Ku-DNA interaction is highly dependent on the experimental conditions used for the binding studies. For example, the dissociation constant of the 25 bp duplex, drops from 29 nM at 300 mM NaCl to <0.5 nM at 200 mM NaCl.

In an earlier work, no cooperative interaction was measured among the Ku heterodimers binding to a 50 bp duplex (Arosio et al., 2002). This result is in contrast with previous studies, where it was shown that there is positive cooperativity between two Ku molecules bound to a 45 bp blunt-ended dsDNA fragment (Ma and Lieber, 2001). A possible explanation for this discrepancy is that this 45 bp dsDNA is 5 bp shorter than the 50 bp duplex that was used in this studies. These additional 5 bp, may be responsible for the fact that the two Ku molecules bound to the 50 bp dsDNA are not close enough to interact with each other. To verify this hypothesis, the dissociation constants for the interaction of Ku with two DNA duplexes of 42 and 50 bp were compared. These results clearly show that there is no cooperative interaction between the two Ku molecules bound to both DNA templates under solution conditions used, even when the duplex is short enough to allow the contact between two adjacent heterodimers.

The analysis of the Ku interaction with a 75 bp DNA duplex, capable of accommodating three heterodimers, was performed taking into account that Ku can translocate along the duplex after binding to DSBs and bind to an internal site of the template. The binding curves yield a value of the cooperativity parameter $\omega = 1.03 \pm 0.09$ ($\Delta G_{\omega} \cong 0$). Thus, these results indicate that cooperative interactions are also absent when one of the Ku molecules is internally bound indicating that Ku has the same affinity for the three binding sites of the 75 bp duplex. This finding reinforces the previous observation on the energy independent translocation of the Ku molecule along

the DNA lattice (de Vries et al., 1989). Since $\omega \cong 1$, the binding equation reduces to the one defined for n identical and independent binding sites, where n is the stoichiometry of the DNA molecule (see Equation 10). In the case of s75, $n = 3$ and the microscopic dissociation constant is 22 ± 1 nM. This k_d value is close to that measured for s25 and s50. Thus, all the equilibrium binding data are well described by a non-interacting binding site model that considers the DNA lattice as a macromolecule with $n = N/m$ binding sites, where N is the number of base-pairs that form the duplex and m is the number of consecutive residues covered by the ligand. On the other hand, this model neglects the potential overlap of binding sites on the DNA duplexes that might need to be taken into account when studying the interaction of a non-specific DNA binding protein with nucleic acids. Previous studies have already shown the importance of applying an overlapping model to appropriately describe the interaction of non-specific DNA binding proteins with linear DNA lattices (Ferrari et al., 1994; Kowalczykowski et al., 1981; Kuil et al., 1989; McGhee and von Hippel, 1974). Thus, this model was applied also for the analysis of the Ku-DNA interaction. The binding isotherms for s42, s50, and s75 were fitted using a modified form of the McGhee and von Hippel model derived (McGhee and von Hippel, 1974) for the interaction of ligands with a linear lattice of arbitrary length and cooperativity (Di Cera and Kong, 1996; Kong, 2001). Since the precise number of base pairs covered by one Ku heterodimer is not known, the same analysis was repeated for values of m ranging from 20 to 25. The results show that the values of the dissociation constants, although slightly dependent on the value of m used for the analysis, are all in the same range of those calculated with the non-overlapping model. In addition, the values of the cooperativity parameter (ω) are always ≤ 200. These values of ω are considered small when obtained from the overlapping model and indicates that the cooperative interaction among the Ku heterodimers binding to DNA is very weak and probably negligible under the solution

conditions used. Indeed, much higher values of ω ($\geq 10^5$) have been reported for the cooperative interaction of the *E. coli* SSB tetramers with single stranded DNA in the $(SSB)_{35}$ binding mode (Ferrari et al., 1994), while values of $\omega = 420 \pm 80$ indicate the presence of a low cooperative interaction of the same protein in the $(SSB)_{65}$ binding mode (Bujalowski and Lohman, 1987). Even though the overlapping binding model might be more appropriate to describe the binding of Ku to DNA duplexes able to accommodate two or more heterodimers, both the overlapping and the non-overlapping model yield to similar conclusions and agree on the absence of cooperative interaction among the Ku molecules binding to DNA. Therefore, the same models can be most likely used to describe the interaction of Ku with DNA duplexes of any length.

After having described the mechanism of interaction, the energetic components of the binding free energy were dissected. Studies of the salt effect on protein-DNA equilibria can provide useful information on the number of cations and anions that are released upon formation of the complex as well as an estimate of the electrostatic component of the binding free energy (Anderson and Record, 1995; Dragan et al., 2003; Lohman and Mascotti, 1992). Similar studies have never been performed on any protein involved in NHEJ and, more in general, in eukaryotic DNA repair. These studies indicate that electrostatic interactions play a major role in the binding of the Ku heterodimer to nucleic acids. A change of 80 mM [salt] (in the range from 300 to 220 mM), leads to an almost 60-fold difference in the equilibrium dissociation constant. The slope (Γ_{salt}) of the plot of log k_d versus log [NaCl] is 12.4 ± 0.1. This value is among the highest reported for a protein-DNA interaction and indicates that approximately 12 ions are released upon formation of the Ku-DNA complex (Figure 3-15). An estimate of the relative contributions of anions *vs.* cations to the salt dependence of the k_d can be obtained by comparing the values of Γ_{salt} from experiments performed in different salts with a common cation, e.g. Na^+. Experiments with Cl^-, Br^-,

and F^- demonstrate that the anion type and concentration affects both the salt dependence and magnitude of the k_d. The slopes measured in NaCl and NaBr are 12.4 ± 0.1 and 12.1 ± 0.3, respectively, whereas in NaF the value of the Γ_{salt} decreases to 8.8 ± 0.2 (Table 3-6). The lower Γ_{salt} determined in NaF is consistent with the observation that fluoride appears to interact least with proteins when compared to bromide and chloride (Kowalczykowski et al., 1981; Overman et al., 1988; von Hippel and Schleich, 1969). Hence, the salt dependence in NaF should only reflect the preferential interactions of Na^+ with the negatively charged DNA molecule. In other words, the slope of 8.8 ± 0.2 in NaF indicates that approximately nine Na^+ ions are released from DNA upon formation of the Ku-DNA complex. In addition, the salt dependence studies performed in NaBr and NaCl suggest that, in these two salts, there are roughly nine Na^+ ions and three Br^- or Cl^- ions released when Ku binds to DNA. The anion effect should reflect the preferential interaction of Br^- or Cl^- with the Ku heterodimer *vs.* the DNA molecule. This conclusion is supported from previous studies on other DNA binding proteins (Kowalczykowski et al., 1981; Overman and Lohman, 1994) and from preliminary studies on the effect of pH on the Ku-DNA interaction showing that the extent of anion binding is coupled to the number of protonation sites on the Ku protein. The change in the anion type also induces a decrease in the magnitude of the k_d following the order $Br^- > Cl^- > F^-$. This hierarchy follows the so-called Hofmeister series (von Hippel and Schleich, 1969) and is due to the fact that it is harder to displace Br^- than Cl^- from the protein upon complex formation.

Interpretation of the salt dependence could be further complicated by the hidden contribution of the cation uptake component. The dependence of the k_d on monovalent salt concentration can be described by the following equation:

$$\frac{\partial \log K_d}{\partial \log[MX]} = \Delta C + \Delta A \qquad \text{(Eq. 19)}$$

This equation does not include the term due to preferential hydration since it is usually negligible at salt concentrations < 0.5 M. The terms ΔC and ΔA refer to the net release respectively of cations and anions upon formation of the complex. In general, any anion effect is due to preferential interaction with the protein, whereas the term ΔC has contribution due to the release of $z\psi$ cations from nucleic acids, as well as the uptake of b cations by the protein ($\Delta C = z\psi - b$). The symbol ψ refers to the number of counterions thermodynamically bound per phosphate and z corresponds to the number of the positively charged sites of the protein that bind to nucleic acids. In our case, $\Delta C = z\psi - b = 8.8 \approx 9$ meaning that there are $9 + b$ ions released from the nucleic acid. If b is unknown, it is only possible to calculate the minimum estimate for the number of cations that are released upon complex formation. Since $\psi = 0.88$ for double-stranded nucleic acids, the minimum estimate for z is $9/0.88 = 10.2$ meaning that at least 10 ionic interactions are formed in the complex of the Ku heterodimer with DNA. On the other hand, the cation uptake component is probably negligible in the case of the Ku-DNA interaction. Indeed, no significant effect on the magnitude of the k_d is observed as a consequence of the substitution of Na^+ with K^+. Since the affinities of Na^+ and K^+ for DNA are quite similar (Anderson et al., 1978), this result suggests that cations are simply displaced from the nucleic acid and do not interact with Ku upon complex formation. Hence, the value of 10.2 should not need to be adjusted by the cation uptake component.

The extreme sensitivity to solution conditions observed for the Ku-DNA interaction is supported by the crystallographic data on the Ku heterodimer showing a polarization of positive electrostatic charges focused on the internal surface of the Ku ring and along the DNA-binding cradle. In addition, the lack of even a single interaction of a Ku residue with a DNA base, shown in the structure of the DNA bound form, explains the reason for the absence of sequence specificity in DNA binding and

our salt dependence studies indicate that the mechanism of DNA recognition might be primarily driven by electrostatic forces. The same fundamental role of electrostatic interaction was also observed for many other DNA binding proteins previously studied by other groups. For example, values of Γ_{salt} ranging from 8 to 10 were reported for the interaction of the *E. coli* lac repressor with non-specific DNA sequences (Ha et al., 1992) and of the recA protein with single-strand DNA (Menetski and Kowalczykowski, 1985). Rigorous salt-dependence studies on the interaction of the *E. coli* single-strand binding protein (SSB) with polynucleotides and of the lambda cI repressor with DNA yielded values of Γ_{salt} between 5 and 7 depending on the type of salt and solution conditions (Overman et al., 1988; Senear and Batey, 1991). Similarly, a recent work on the binding of the *E.coli* RecQ helicase with DNA fragments of different length indicated that about 3-4 ions are released upon complex formation (Dou et al., 2004). More in general, specific ion effects are likely to control most protein-DNA interaction, especially because of the polyelectrolyte nature of nucleic acids, and should not be ignored in any quantitative analysis.

In summary, the studies presented here provide a quantitative description of the mechanism of Ku binding to DNA and clear evidence of the effects that electrostatic components of the binding free energy and specific binding of ions have on the formation of the Ku-DNA complex. These results provide important information for NHEJ and increase the knowledge about the different strategies that nonspecific DNA-binding proteins adopt to bind and translocate along the DNA lattice. Moreover, the results of the salt dependence studies can be utilized to estimate the affinity of Ku for DNA at any salt concentration and allow a proper comparison of binding data acquired under different solution conditions. These studies represent the first detailed biophysical study of a NHEJ protein. Thus, the same biophysical approach might be extended to other proteins involved in the NHEJ and to mutants that show defects in

DNA repair to evaluate the impact of these mutations on the mechanism of DNA binding.

The work described in this chapter is contained in the following article:

Arosio D, Costantini S, Kong Y & Vindigni A. Fluorescence anisotropy studies on the Ku-DNA interaction: anion and cation effects. *J Biol Chem.* 2004; 279(41):42826-35.

3.3 ANALYSIS OF THE INTERACTION BETWEEN THE DNA-PK AND LX COMPLEXES

3.3.1 Introduction

DNA-PK is a serine/threonine protein kinase composed of a catalytic subunit, DNA-PKcs, and a regulatory subunit, the Ku heterodimer (Dvir et al., 1992; Gottlieb and Jackson, 1993). Studies with DNA-PKcs deficient cell lines and with DNA-PKcs mutants demonstrated that DNA-PKcs and its kinase activity are required for NHEJ in mammalian cells (Jeggo, 1998; Kienker et al., 2000; Kurimasa et al., 1999). However, the precise function of this kinase during DSB repair has not been completely elucidated yet. Electron microscopy studies showed that DNA-PKcs facilitates alignment of DNA termini (Cary et al., 1997; DeFazio et al., 2002; Yaneva et al., 1997). Protein interaction studies suggested that DNA-PK acts as a scaffold for the recruitment of additional repair factors on the DNA (Calsou et al., 2003; Hsu et al., 2002; Leber et al., 1998; Mahajan et al., 2002; Mickelsen et al., 1999). Moreover, *in vitro* kinase assays demonstrated that DNA-PK phosphorylates all the factors known to be required for NHEJ. Some of these factors are phosphorylated by DNA-PK also *in vivo*. In particular, DNA-PKcs phosphorylates *in vitro* serine 6 of Ku70, and several amino acids in Ku80, including serines 577, 580, threonine 715 and possibly serine 579 (Chan et al., 1999). A recent work has demonstrated that these sites are phosphorylated also *in vivo*, except for serine 579 (Douglas et al., 2005). However, this study has reported that DNA-PK-mediated phosphorylation of Ku is not required for DSB repair leaving open the question of the role of these phosphorylation events *in vivo*. LigIV and XRCC4 are also substrates of DNA-PK *in vitro*, although deletion mutants analysis suggested that several potential phosphorylation sites of XRCC4 are not required for its function in

NHEJ (Mizuta et al., 1997). Similarly, Wang and co-workers reported that the phosphorylation of LigIV is not required for DNA end joining (Wang et al., 2004). However, *in vitro* and *in vivo* assays demonstrated that DNA-PKcs inhibitors block intermolecular ligation by LX, indicating that DNA-PK phosphorylation is required for LX function in NHEJ (Baumann and West, 1998; Chernikova et al., 1999; Rosenzweig et al., 1997). Moreover, Gellert and colleagues showed that phosphorylated XRCC4 does not bind to DNA (Modesti et al., 1999), while Wang and co-workers found that DNA-PK negatively regulate LigIV stability (Wang et al., 2004).

LigIV is the ATP-dependent ligase required for the final joining reaction of NHEJ (Robins and Lindahl, 1996). In cells, LigIV forms a complex with XRCC4, upon which it depends for stability and activity (Critchlow et al., 1997; Grawunder et al., 1997; Grawunder et al., 1998b). Deletion analysis of LigIV and structural analysis of XRCC4 bound to a peptide of LigIV demonstrated that the interaction between LigIV and XRCC4 is mediated by the linker region between the tandem BRCT domain at the C terminus of the ligase (Grawunder et al., 1998c; Sibanda et al., 2001). However, recent structural studies of the *S. cerevisiae* XRCC4 ortholog ligase interacting factor 1 (Lif1p) complex with the C-terminal BRCT domains of LigIV have demonstrated that both BRCT domains contributes to the Lif1p binding interface (Dore et al., 2006). Given the high degree of sequence conservation across residues involved in this interaction, it is likely that this mode of interaction has been conserved throughout the evolution. This mode of LX complex formation provides an explanation for the clinical phenotypes of certain patients with LigIV syndrome carrying mutations that produce C-terminal truncations of LigIV, such as R580X and R814X proteins. These mutations give rise to LigIV syndrome characterized by immunodeficiency and developmental delay (O'Driscoll et al., 2001).

The ligation reaction of the LX complex requires the formation of the ligase-adenylate complex. This modification occurs in a highly conserved motif, KYLGER (residues 273-278 in human LigIV), located in the N-terminal region of the ligase. The crucial role of this conserved motif for adenylation and ligation activity is underscored by the impact of mutations. A mutational change within the highly conserved motif encompassing the active site of LigIV was determined in 180BR cells, a radiosensitive cell line defective in DSB repair, which was derived from a leukaemia patient. 180BR cells carry a homozygous mutation R278H that impacts upon LigIV function reducing the activity to ~ 10% of wild-type levels (Badie et al., 1997; Girard et al., 2004; Riballo et al., 1999).

The ligation activity of the LX complex is influenced by the DNA-PK complex. Previous reports, indicated that the LX complex interacts with both components of DNA-PK, although there are conflicting results on the effects of these interactions and on the proteins involved. Chen and co-workers reported that DNA-PKcs stimulates LX intermolecular ligation probably by enhancing the association of DNA ends via protein-protein interactions (Chen et al., 2000). The same authors showed that Ku inhibits DNA joining by LX, although it does not prevent LX binding to DNA. Conversely, Ramsden and co-workers reported that Ku stimulates the intermolecular ligation of DNA fragments by eukaryotic DNA ligases (Ramsden and Gellert, 1998). Subsequently, McElhinny and colleagues demonstrated that Ku physically interacts with the LX complex and increases the initial ligation rate 20-fold. The same authors evidenced also that Ku is able to stimulate the ligation activity only of LigIV, since it does not interact with other mammalian ligases (Nick McElhinny et al., 2000). More recently, it has been shown that the efficiency of LX ligation is critically dependent upon the length of the DNA substrate and that the effect of Ku on LX ligation depends

on the stoichiometry of Ku-DNA complex, since inward translocation of Ku is essential to stimulate LX ligation (Kysela et al., 2003).

Studies with cells harboring aberrant Ku proteins and with *in vitro* expressed mutants showed that Ku70/80 interacts with DNA-PKcs through the C-terminal domain of Ku80 (Gell and Jackson, 1999; Han et al., 1996; Muller and Salles, 1997; Singleton et al., 1999). However, electron microscopy studies revealed that Ku makes extensive interactions with several regions of DNA-PKcs, including the HEAT repeats, their protruding claws and a region close to the kinase domain (Spagnolo et al., 2006). Consistent with this, analysis of the Ku-DNA-PKcs interaction with *in vitro* synthesized DNA-PKcs fragments demonstrated that Ku interacts with a region immediately N-terminal to the kinase domain (amino acids 3002-3850) (Jin et al., 1997). Moreover, protein interaction studies showed that LigIV interacts primarily with Ku and XRCC4 with DNA-PKcs (Hsu et al., 2002; Leber et al., 1998).

The role of nucleic acids in regulating the Ku-LX-DNA-PKcs interaction remains still unclear and controversial. Immunoprecipitation assays, reported in a first work, demonstrated that the interaction between Ku and LX is enhanced in the presence of DNA (Nick McElhinny et al., 2000). In agreement with these findings, Calsou and co-workers reported that interactions between Ku, DNA-PKcs and LX are mainly DNA dependent (Calsou et al., 2003). Conversely, Hsu and co-workers showed that LX associates with DNA-PK in a DNA independent manner (Hsu et al., 2002).

To gain further insight into the mechanism of assembly of the NHEJ complex, co-immunoprecipitation assays (co-ip) were performed using specific antibodies against Ku70/80, XRCC4 and LigIV. The role of nucleic acids in the complex formation was analysed and the interaction between Ku and LX was further characterized using a series of LigIV and Ku mutants. The impact of clinically relevant mutations in LigIV on the interaction with Ku was also evaluated. To investigate the role of DNA-PKcs in

the Ku-LX complex formation, interaction studies were performed in cells lacking the catalytic subunit of DNA-PK. Moreover, to assess the effect of the kinase activity of DNA-PK on NHEJ complex assembly, *in vitro* kinase assays were performed with anti-Ku immunoprecipitates.

3.3.2 Interaction between DNA-PK and LX in human cell extracts

To characterize the protein-protein interactions that occur between the main components of the NHEJ complex, co-ip experiments were performed using HeLa nuclear extracts and antibodies against three essential NHEJ factors, the Ku heterodimer, LigIV, and XRCC4. The identity of the co-immunoprecipitated proteins was established by Western blot analysis. Samples obtained using an antibody against the Ku heterodimer were also analysed by 8% SDS-PAGE stained with silver (Figure 3-16 B) and the proteins contained in some of the bands detected were identified by ESI-mass spectrometry analysis after in gel-digestion. Western blot and mass spectrometry analysis showed that Ku70/80, DNA-PKcs, and LigIV are present in the ip samples obtained using anti-Ku70/80 antibodies (Figure 3-16 A, lane 3; Figure 3-16 B, lane 1). Additionally, immunoprecipitates obtained using anti-XRCC4 and anti-LigIV antibodies efficiently retrieved DNA-PKcs and Ku (Figure 3-17, lane 3 and 6, respectively). Control experiments performed with IgG from normal mouse or rabbit serum and an antibody against an unrelated DNA binding protein did not recruit these proteins (Figure 3-16 A, lane 2; and 3-17, lane 2; Figure 3-18 lane 3) indicating that the results of the co-ip are not due to non-specific binding.

Whilst Hsu and co-workers showed that the assembly of these proteins is DNA independent, Calsou and co-workers reported that DNA is required to achieve co-ip of the NHEJ proteins (Calsou et al., 2003; Hsu et al., 2002). To address whether the co-associations observed are mediated by contaminating DNA present in the HeLa nuclear extracts, the effect of ethidium bromide (EtBr) was assayed. The DNA intercalating

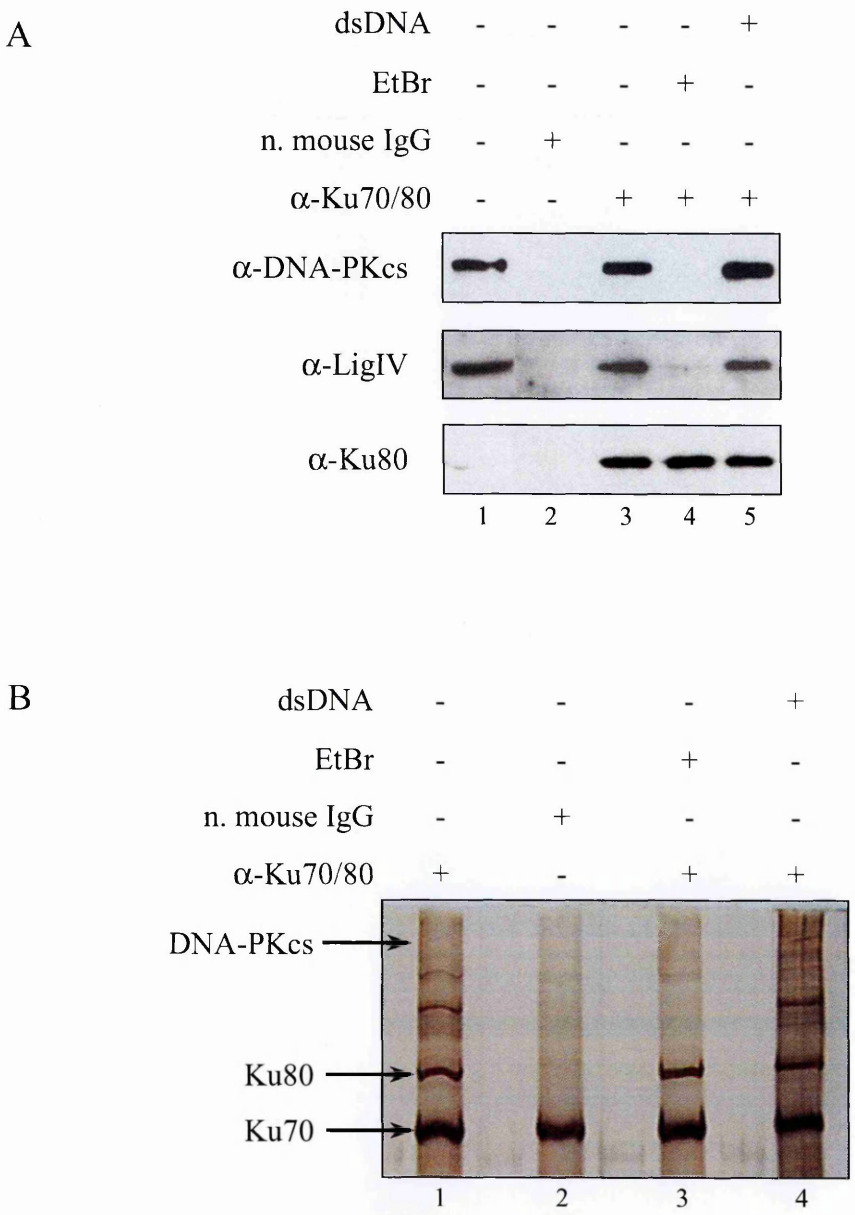

Figure 3-16 Co-ip assays performed with anti-Ku70/80 (α-Ku70/80) antibodies using HeLa nuclear extracts. **A**, 8 μg of HeLa nuclear extracts (lane 1), normal mouse IgG (lane 2) and α-Ku70/80 immunoprecipitates (lane 3-5) were examined by Western blotting with α-DNA-PK, α-LigIV and α-Ku80 antibodies. The co-ip assays with α-Ku70/80 antibodies were carried out with untreated extracts (lane 3), with extracts pre-incubated with EtBr (50 μg/ml) (lane 4) or supplemented with 10 μg/ml of a 75 bp ds blunt-ended oligonucleotide (lane 5). **B**, co-immunoprecipitated samples were also analysed by 8% SDS-PAGE gel silver stained. Immunoprecipitation reactions were performed with α-Ku70/80 antibodies (lane 1) and with normal mouse IgG (lane 2) using untreated extracts; with α-Ku70/80 antibodies using extracts pre-incubated with EtBr (50 μg/ml) (lane 3), or supplemented with 10 μg/ml of a 75 bp ds blunt-ended oligonucleotide (lane 4). Arrows indicate the bands that were analysed by ESI-MS after in-gel digestion.

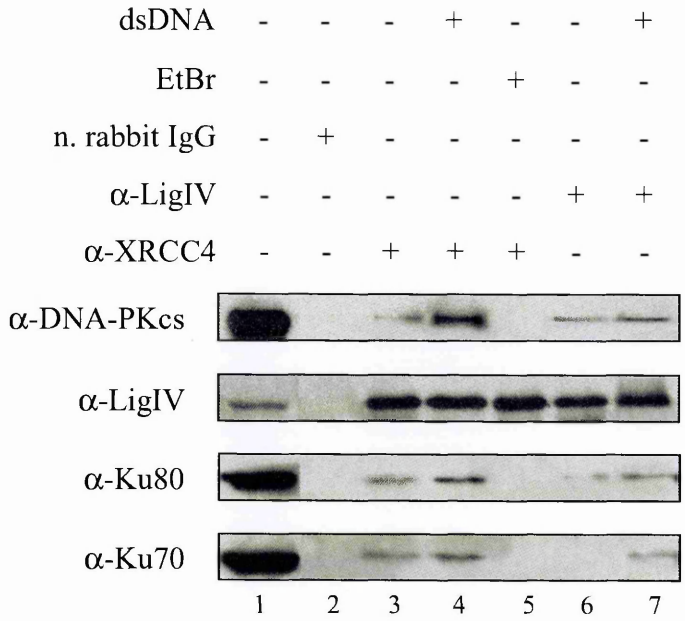

Figure 3-17 Co-ip assays performed with anti-XRCC4 (α-XRCC4) and anti-LigIV (α-LigIV) antibodies using HeLa nuclear extracts. 8 μg of HeLa nuclear extracts (lane 1), normal rabbit IgG (lane 2), α-XRCC4 (lane 3-5) and α-LigIV (lane 6, 7) immunoprecipitates were analysed by Western blotting. Co-ip reactions were performed with untreated nuclear extract (lane 3, 6), in the presence of 50 μg/ml EtBr (lane 5) or of 10 μg/ml of a 75 bp ds blunt-ended oligonucleotide (lane 4, 7).

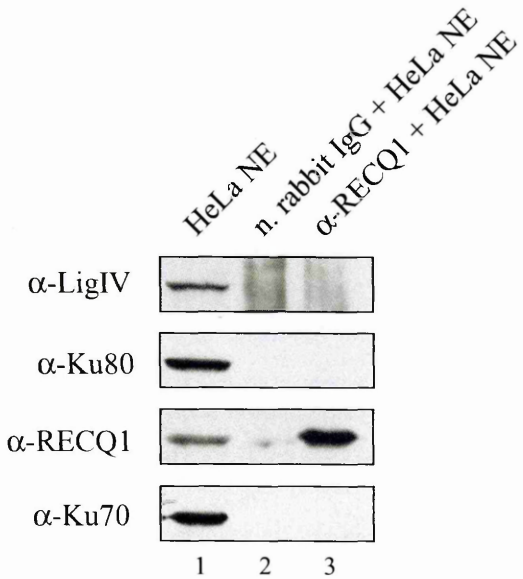

Figure 3-18 Co-ip assays performed with anti-RECQ1 (α-RECQ1) antibodies using HeLa nuclear extracts. 8 μg of HeLa nuclear extracts (lane 1), normal rabbit IgG (lane 2) and α-RECQ1 (lane 3) immunoprecipitates were analysed by Western blotting.

drug, EtBr, was added to the nuclear extracts to a final concentration of 50 μg/ml and maintained through all the co-ip steps. This concentration of EtBr was previously reported to affect the interaction between Ku, Oct-2 and a 110 kDa protein with DNA (Lai and Herr, 1992). Addition of EtBr almost completely disrupted the interaction between Ku, DNA-PKcs and LX, although it did not interfere with the formation of the Ku heterodimer nor of the LX complex (Figure 3-16 A, lane 4; Figure 3-17, lane 5). Conversely, co-ip assays using HeLa nuclear extracts supplemented with a 75 bp blunt-ended DNA fragment showed that the interaction between these proteins is slightly enhanced in the presence of DNA (Figure 3-16 A, lane 5; Figure 3-17, lane 4 and 7). Collectively, these data suggest that the Ku heterodimer forms a complex with LX and DNA-PKcs and that these interactions are DNA mediated, supporting the findings of Calsou and co-workers and McElhinny and co-workers (Calsou et al., 2003; Nick McElhinny et al., 2000). These results show that the DNA-PK and LX complexes can co-assemble in the presence of DNA. However, they do not demonstrate co-association of these proteins as an NHEJ complex since it is possible that the two complexes (DNA-PK and LX) may independently assemble on the DNA. Thus, the impact of cell lines lacking DNA-PKcs on the assembly of the remaining NHEJ proteins was analysed. Co-ip were performed using a human glioma cell line deficient for DNA-PKcs, M059J, and a control cell line, M059K. As shown in Figure 3-19, M059J and M059K extracts contain similar amounts of Ku and LX, whereas M059J extracts are completely devoid of DNA-PKcs (Figure 3-19, compare lane 2 and 3). The amount of LigIV retrieved by the anti-Ku70/80 antibodies in the absence of DNA-PKcs was considerably reduced compared to the control cells, but significant interaction remained (Figure 3-19, lane 5 and 6). These findings indicate that DNA-PKcs enhances the recruitment of LX at DNA ends. Since Ku, the DNA binding component of DNA-PK, remains present in the whole cell extracts and LX is expressed normally (Figure 3-19, lane 2 and 3), the

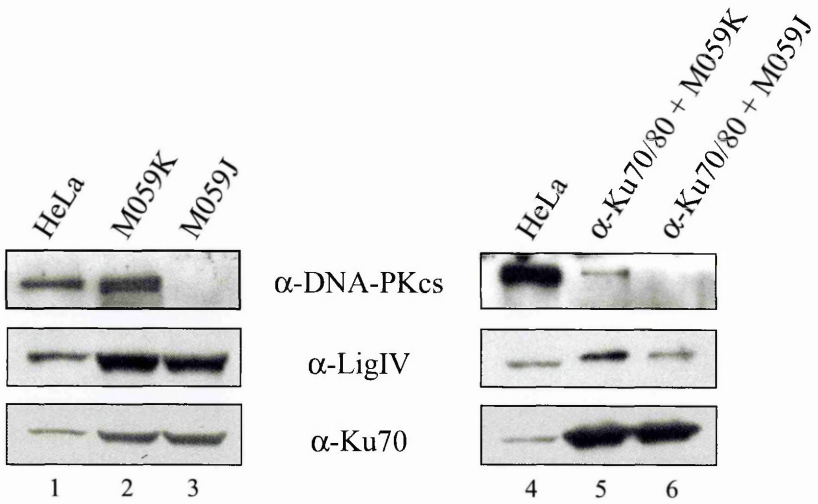

Figure 3-19 Co-ip assays performed with anti-Ku70/80 antibodies using DNA-PKcs-/- cell extracts. 6 μg of HeLa nuclear extracts (lane 1, 4), 25 μg of M059K (lane 2) and M059J, DNA-PKcs-/-, (lane 3) whole cell extracts were loaded as control. Immunoprecipitation assays with α-Ku70/80 antibodies were performed in M059K (lane 5) and M059J (lane 6) cells.

residual interaction observed shows that at least a component of LX is recruited to the DNA ends in a DNA-PKcs-independent manner. Additionally, EMSA experiments performed by other members of the Proteomics group (ICGEB, Trieste) showed that LX alone does not efficiently bind to DNA under the salt conditions used for these co-ip studies, further substantiating the notion that co-ip of LX with DNA-PK represents evidence for NHEJ complex assembly rather than non-interactive DNA binding. Moreover, these findings indicate that LX can interact with Ku bound at the DNA end and that this interaction is further enhanced by the presence of DNA-PKcs.

3.3.3 Interaction between recombinant Ku70/80 and LX

To gain further insight into the basis underlying the interaction between Ku and LX, co-ip assays were performed using recombinant proteins. The Ku heterodimer and LX complex were expressed individually in insect cells as described in the material and methods. The purity of the recombinant proteins was verified by SDS-PAGE gel stained with silver (Figure 3-20).

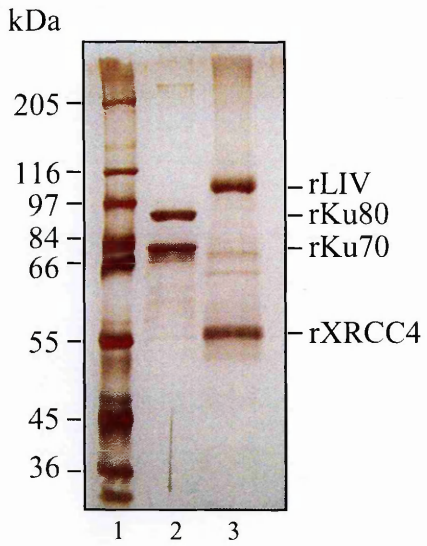

Figure 3-20 8% SDS-PAGE analysis of recombinant Ku and LX expressed using the baculovirus system. Silver-stained SDS-PAGE of broad-range molecular weight markers (lane 1), 0.8 μg of rKu70/80 (lane 2) and 0.8 μg of rLX (lane 3).

The expressed proteins were then mixed at a Ku:LX molar ratio of 2:1 and their ability to interact was examined by co-ip. LigIV was detectable in the immunoprecipitates obtained using anti-Ku70/80 antibodies (Figure 3-21 A, lane 4) while it was not detected in the co-ip samples obtained with normal mouse IgG (Figure 3-21 A, lane 3) or with anti-Ku70/80 antibodies incubated with LX alone (Figure 3-21 A, lane 6). These results were confirmed also using the anti-LigIV (Figure 3-21 C, lane 1) and anti-XRCC4 antibodies (Figure 3-21 C, lane 2). Ku was not detected in the ip samples performed using normal rabbit IgG (Figure 3-21 C, lane 3). The amount of LigIV that co-immunoprecipitated with Ku was slightly reduced upon addition of EtBr to the protein samples, suggesting that a fraction of recombinant proteins carried some DNA through the purification steps (Figure 3-21 A, lane 5). Since Ku70/80 is an abundant protein, while LX is expressed at more limiting amounts in cells, the Ku-LX interaction was also analysed using a Ku:LX molar ratio of about 7:1 (Figure 3-21 B). Addition of EtBr significantly reduced but did not abolish the Ku-LX interaction when a lower LX concentration was used in the co-ip (Figure 3-21 B, compare lane 4 and 5).

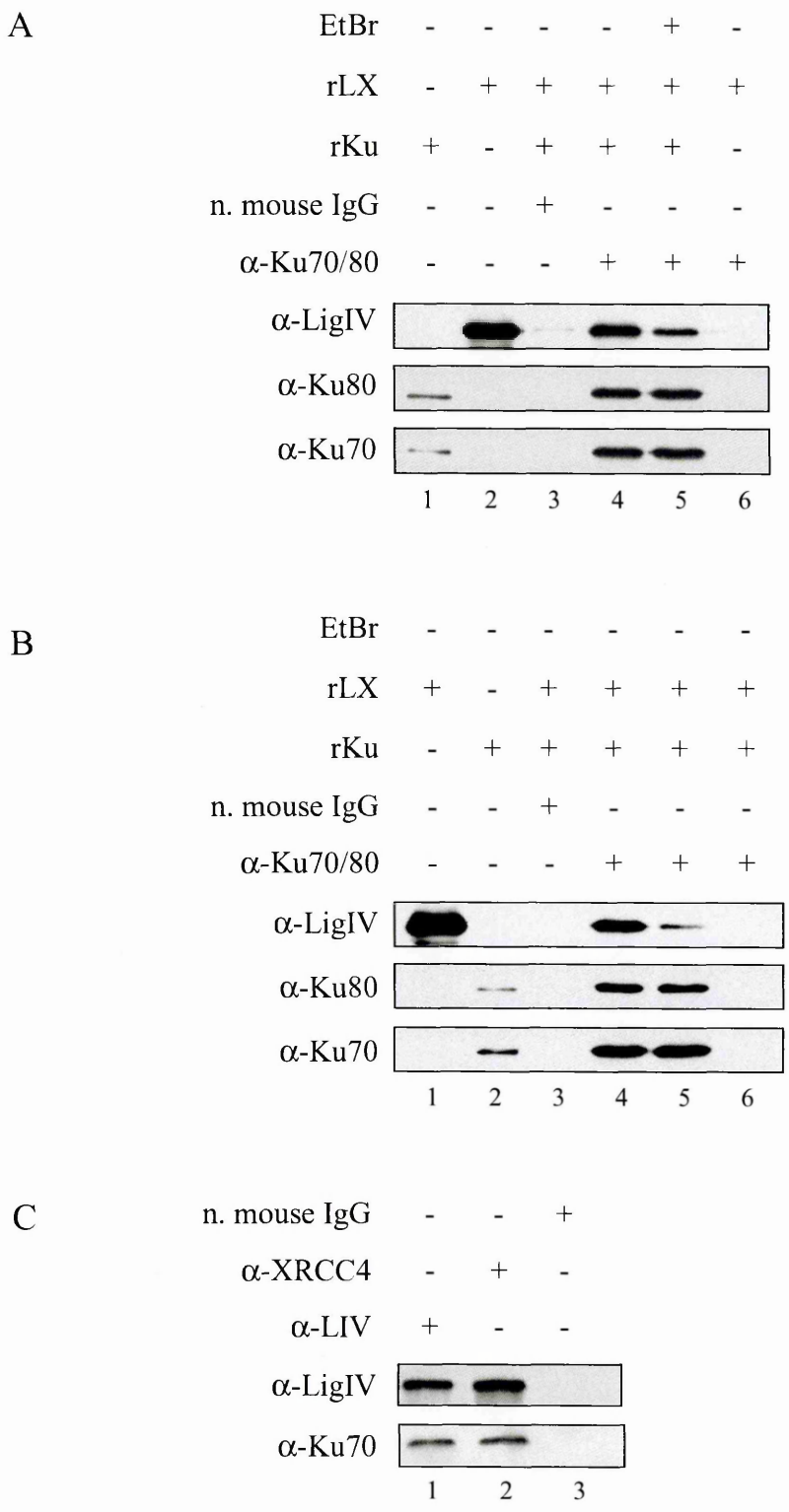

Figure 3-21 Analysis of the interaction between recombinant Ku and LX. **A**, 20 ng of rKu (lane 1) and of rLX (lane 2) were loaded as control. Co-ip assays were carried out with normal mouse IgG (lane 3) and with α-Ku70/80 (lane 4-6) antibodies incubated with 200 ng of rKu70/80 and 100 ng of rLX (lane 3-5) in the absence (lane 4) and in the presence (lane 5) of 50 μg/ml EtBr. A control reaction was performed by incubating the α-Ku70/80 antibodies with 100 ng of LX (lane 6). **B**, 20 ng of rLX (lane 1) and of rKu (lane 2) were loaded as control. Immunoprecipitates obtained with normal mouse IgG (lane 3) and with α-Ku70/80 (lane 4-6) antibodies incubated with 200 ng of rKu70/80 and 33 ng of rLX (lane 3-5) in the absence (lane 4) and in the presence (lane 5) of 50 μg/ml EtBr or with 33 ng of LX alone (lane 6). **C**, immunoprecipitation carried out with α-LigIV (lane 1), α-XRCC4 (lane 2) antibodies and normal rabbit IgG (lane 3) incubated with rKu and rLX.

These results provide evidence that Ku and LX interact in the absence of DNA-PKcs. In addition, experiments with EtBr suggest that the presence of nucleic acids favour the interaction between the Ku heterodimer and the LX complex.

3.3.4 Analysis of Ku and LX mutants

To map the regions of Ku and LX involved in their interaction, a series of mutant proteins (Figure 3-22 A and 3-24 A) were expressed using an *in vitro* translation system (Figure 3-22 B and 3-24 B). After incubation of the translation products (Figure

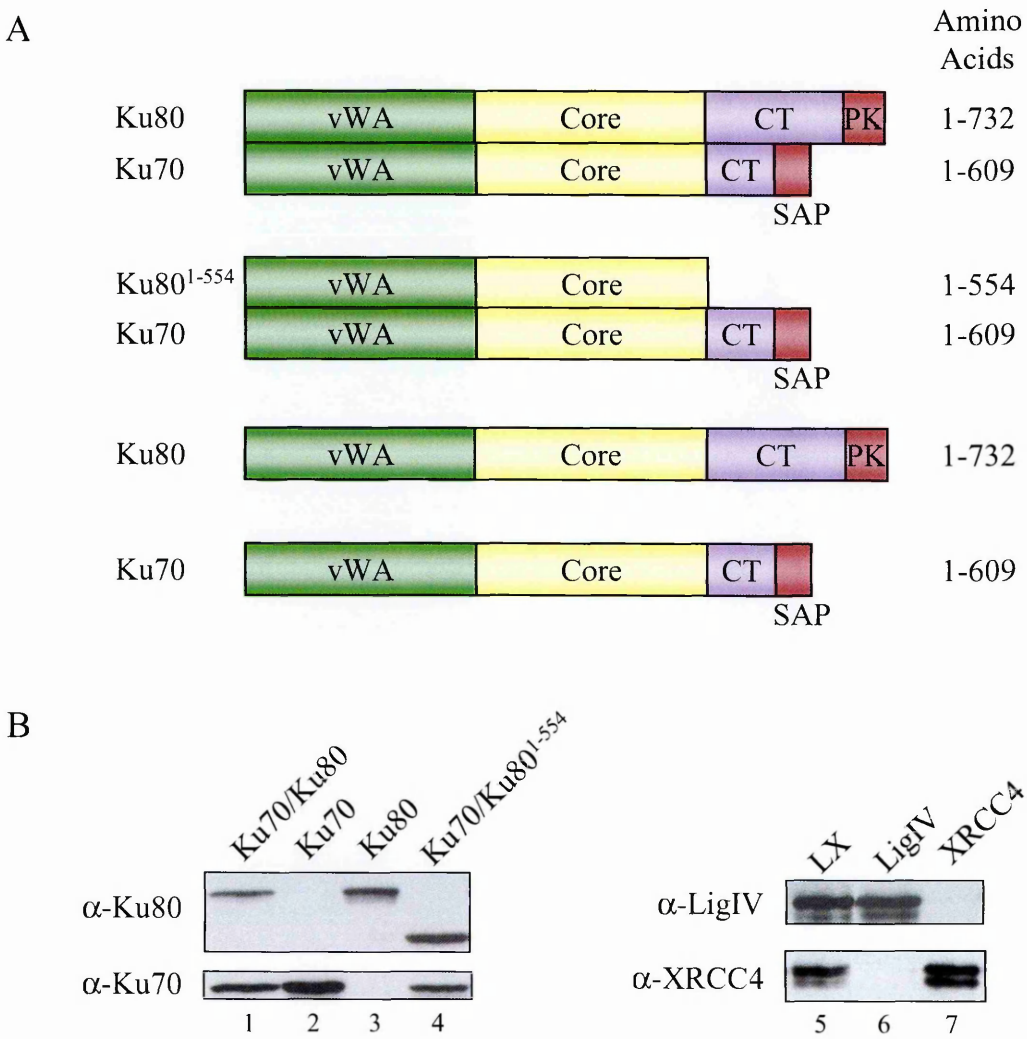

Figure 3-22 *In vitro* translated Ku70/80, Ku70, Ku80, Ku70/80$^{1-554}$, LigIV, XRCC4 and LX. **A**, graphic representation showing the domain organization of Ku70/80, Ku70/Ku80$^{1-554}$, Ku70 and Ku80. Ku proteins consist of the following regions: an N-terminal von Willebrand A domain (vWA), a central core domain (core) and a divergent C-terminal region (CT). In Ku80, the C-terminal region contains the DNA-PKcs binding domain (PK). In Ku70, the C-terminal region contains a SAP domain. **B**, Western blot analysis of *in vitro* translated Ku70/80 (lane1), Ku70 (lane 2), Ku80 (lane 3), Ku70/Ku80$^{1-554}$ (lane 4), LX (lane 5), LigIV (lane 6) and XRCC4 (lane 7).

3-22 B), proteins were immunoprecipitated with anti-XRCC4 antibodies and examined for the presence of Ku by Western blot analysis. Firstly, the interaction between the Ku heterodimer and LX was inhibited by the presence of EtBr, similarly to the findings obtained using the baculovirus expressed proteins (Figure 3-23, lane 1 and 2).

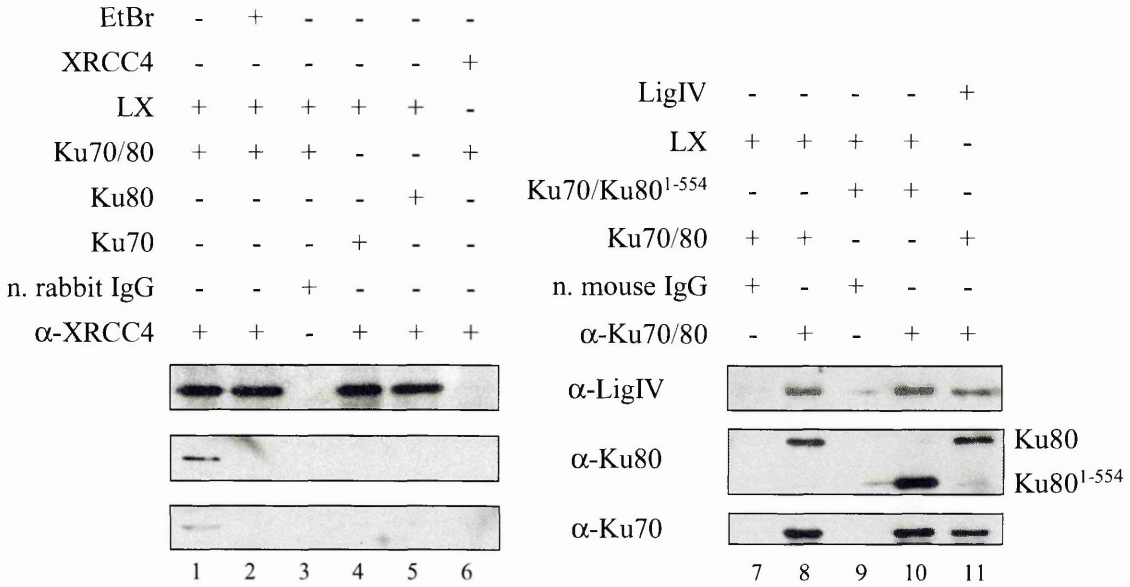

Figure 3-23 Co-ip assays with *in vitro* translated Ku70/80, Ku70, Ku80, Ku70/80$^{1-554}$, LigIV, XRCC4 and LX. On the left, co-ip assays using α-XRCC4 antibodies (lane 1, 2, 4-6) and normal rabbit IgG (lane 3) incubated with Ku70/80 and LX (lane 1-3), Ku70 and LX (lane 4), Ku80 and LX (lane 5), Ku70/80 and XRCC4 (lane 6). Co-ip assays using α-XRCC4 antibodies incubated with Ku70/80 and LX was also performed in the presence of 50 μg/ml EtBr (lane 2). On the right, co-ip assays with α-Ku70/80 antibodies (lane 8, 10-11) and normal mouse IgG (lane 7, 9) were performed after incubation of Ku70/80 with LX (lane 7, 8), Ku70/Ku80$^{1-554}$ with LX (lane 9, 10) and Ku70/80 with LigIV alone (lane 11).

Next, to investigate whether LX can interact with the separate subunits of the Ku heterodimer, *in vitro* translated LX was incubated with Ku70 or Ku80 alone. Neither subunit of Ku alone was retrieved by the anti-XRCC4 antibodies (Figure 3-23, lanes 4 and 5) indicating that Ku needs to be in its heterodimeric form to interact with LX (Figure 3-23, lane 1). The requirement for the C-terminal tail of Ku80 was also analysed using the deletion mutant Ku80$^{1-554}$. This region is dispensable for heterodimerization with Ku70, but is required for interaction of Ku with DNA-PKcs (Gell and Jackson, 1999; Han et al., 1996; Singleton et al., 1999). Moreover, recent structural studies have indicated that this region has an unique fold potentially serving

as a ligand binding pocket (Harris et al., 2004; Zhang et al., 2004). The $Ku80^{1-554}$ mutant was *in vitro* translated with Ku70, incubated with LX, and immunoprecipitated with anti-Ku antibodies. The amount of LX retrieved was similar to that co-immunoprecipitated in the presence of the wild type Ku70/80 indicating that the Ku80 C-terminus is dispensable for Ku-LX interaction (Figure 3-23, compare lane 8 and 10).

Then, it was tested whether XRCC4 and LigIV alone can interact with the Ku heterodimer. While XRCC4 alone did not interact with the Ku heterodimer (Figure 3-23, lane 6), *in vitro* translated LigIV co-immunoprecipitated with Ku70/80 (Figure 3-23, lane 11). However, the amount of LigIV retrieved by Ku in the absence of XRCC4 was less than that detected using the LX complex (Figure 3-23, compare lane 11 and 8). Thus, these data indicate that Ku preferentially interacts with the LigIV component of the LX complex and that this interaction is strengthened by the presence of XRCC4.

3.3.5 Analysis of LigIV deletion mutants

To map the region of LigIV responsible for interaction with Ku, a series of LigIV mutants were designed and expressed using the *in vitro* translation system (Figure 3-24 A). The adenylation dead mutant $LigIV^{K273G}$ carries a mutation in the adenylation site that abolishes adenylate complex formation (Kysela et al., 2003). The clinically relevant mutant $LigIV^{R814X}$ lacks the largest part of the second BRCT domain (O'Driscoll et al., 2001). $LigIV^{R814X}$ is significantly impaired in adenylation complex formation and retains ~10-15% residual ligation activity (Girard et al., 2004). $LigIV^{1-790}$, $LigIV^{1-748}$, $LigIV^{1-643}$ and $LigIV^{600-911}$ lack the last BRCT motif, the last BRCT and the linker region between the two BRCT, the two BRCT motifs, and the N-terminal catalytic domain, respectively (Figure 3-24 A). Wild type LigIV, LigIV mutants and XRCC4 were *in vitro* translated with a myc epitope fused in frame to their N termini (Figure 3-24 B). Western analysis with the anti-myc antibodies on the co-immunoprecipitated complexes showed that $LigIV^{1-790}$ and $LigIV^{600-911}$ mutants

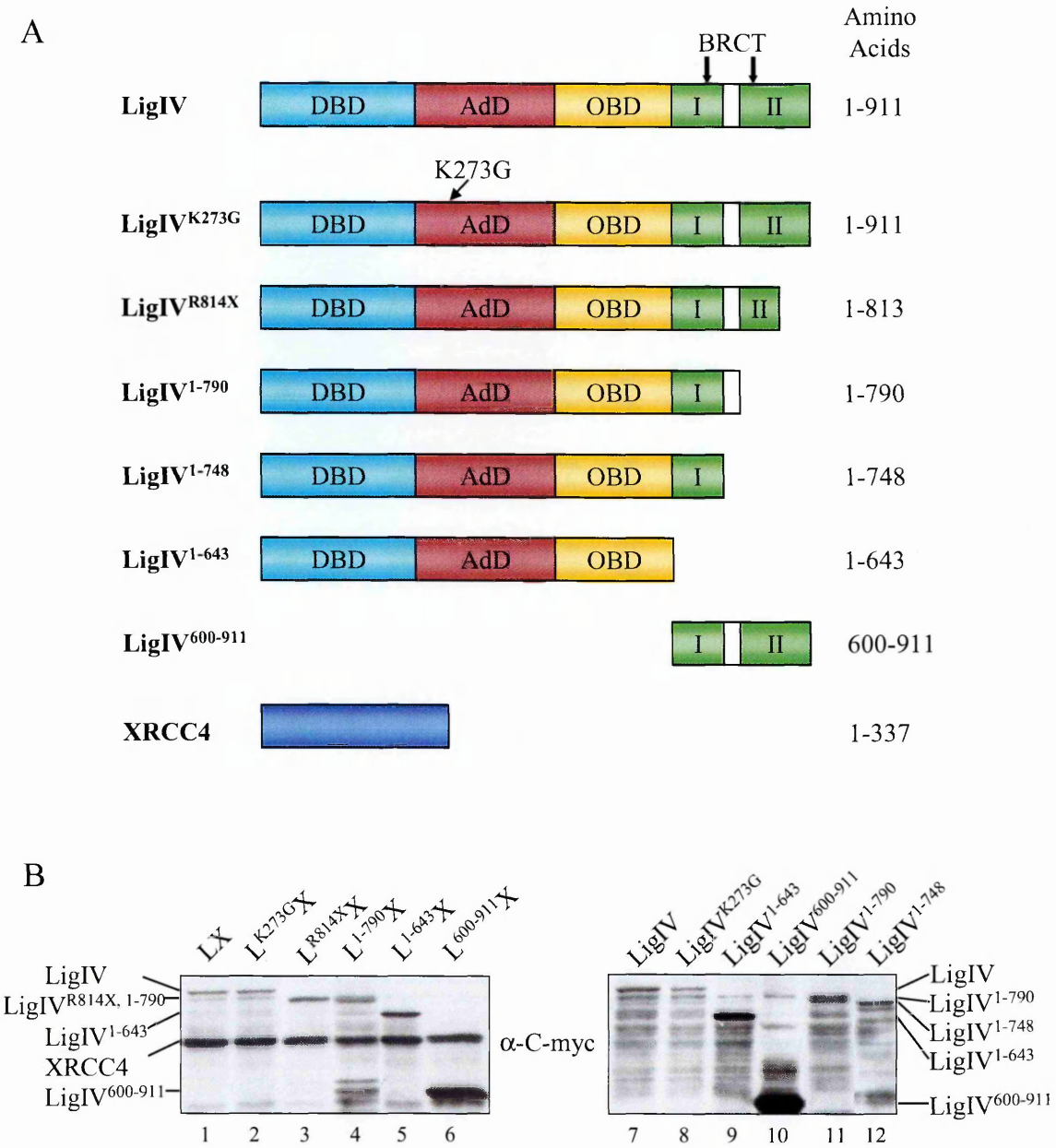

Figure 3-24 *In vitro* translated LX mutants. **A**, schematic representation of wild type LigIV, LigIV mutants and XRCC4. The DNA-binding domain (DBD), the adenylation domain (AdD) at the N-terminal, the oligo-binding domain (OBD) and the two BRCA-1 C-terminus (BRCT) domains of LigIV are shown. In LigIV ^{K273G} localization of the mutation is indicated. **B**, Western blot analysis of *in vitro* translated LX (lane 1), $L^{K273G}X$ (lane 2), $L^{R814X}X$ (lane 3), $L^{1-790}X$ (lane 4), $L^{1-643}X$ (lane 5), $L^{600-911}X$ (lane 6); LigIV (lane 7), $LigIV^{K273G}$ (lane 8), $LigIV^{1-643}$ (lane 9), $LigIV^{600-911}$ (lane 10), and $LigIV^{1-790}$ (lane 11), $LigIV^{1-748}$ (lane12).

interacted with the Ku heterodimer and that this occurred in the presence or absence of XRCC4 (Figure 3-25, lane 4, 6 and 10, 11). Also LigIV ^{R814X} expressed in the presence of XRCC4 interacted with Ku70/80 (Figure 3-25, lane 3). These results suggest that the region containing the BRCT motifs of LigIV is sufficient for the interaction with Ku.

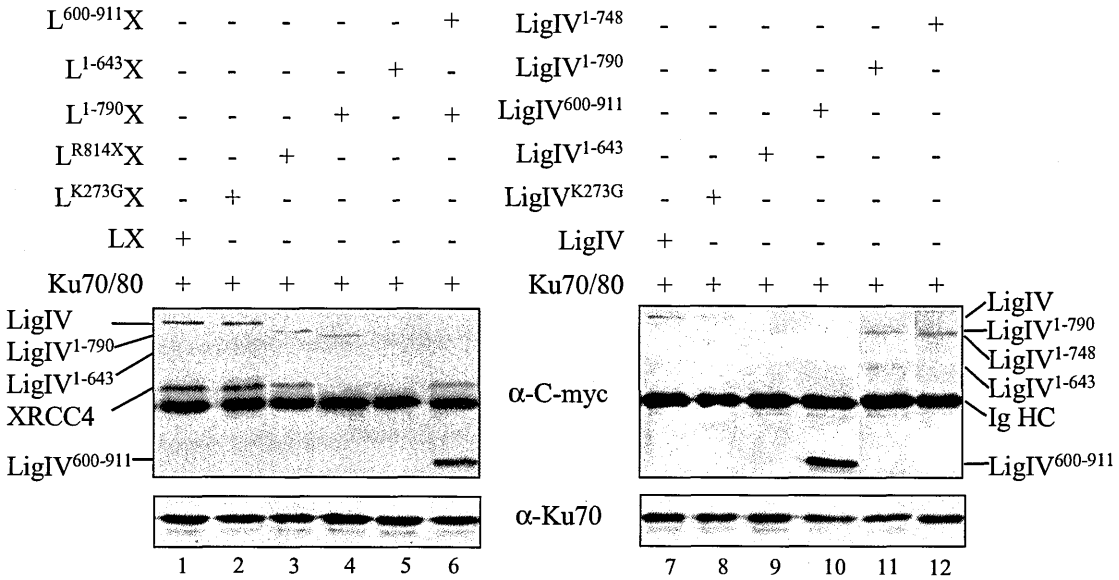

Figure 3-25 Analysis of the interaction between Ku and LX mutants. On the left, immunoprecipitates obtained using α-Ku70/80 antibodies after incubation of Ku70/80 with LX (lane 1), $L^{K273G}X$ (lane 2), $L^{R814X}X$ (lane 3), $L^{1-790}X$ (lane 4), $L^{1-643}X$ (lane 5) and with $L^{600-911}X$ (lane 6). On the right, immunoprecipitates obtained using α-Ku70/80 antibodies after incubation of Ku70/80 with LigIV (lane 7), $LigIV^{K273G}$ (lane 8), $LigIV^{1-643}$ (lane 9), $LigIV^{600-911}$ (lane 10), $LigIV^{1-790}$ (lane 11) and $LigIV^{1-748}$ (lane 12).

Furthermore, a LigIV mutant encompassing the N-terminal and the first BRCT domain (residues 1-790) of the ligase also interacted with Ku suggesting that the interaction may be mediated via the first BRCT domain. This mutant contains, however, also the linker region between the two BRCT motifs which was previously reported to be involved in XRCC4 binding (Grawunder et al., 1998c; Sibanda et al., 2001). Thus, another LigIV deletion mutant ($LigIV^{1-748}$) containing only the first BRCT motif was made to rule out the possibility that the XRCC4 binding region is involved in Ku binding (Figure 3-24 A). Western analysis showed that this mutant still interacted with the Ku heterodimer supporting the conclusion that the region encompassing the first BRCT domain of LigIV (644-748) is involved in Ku recognition (Figure 3-25, lane 12). Moreover, $LigIV^{1-643}$ did not interact with Ku, indicating that the region encompassing the active site of the enzyme is dispensable for the Ku-LX complex formation (Figure 3-25, lane 5 and 9). Additional experiments with the adenylation

dead LigIV^{K273G} showed efficient interaction with Ku (Figure 3-25, lane 2 and 8). Thus, LigIV adenylation is not required for the interaction with Ku, further supporting the conclusion that the active site of the ligase is not involved in the Ku-LX complex formation (Figure 3-25, lane 2, 5, 8 and 9). This result was confirmed by co-ip assays performed using HeLa nuclear extract. The immunocomplexes obtained with the anti-Ku70/80 antibodies were incubated with NaPPi and $MgCl_2$ to fully deadenylate the ligase. Analysis by Western blot did not show a significant change in the LigIV signal between the adenylated and de-adenylated samples (Figure 3-26, compare lane 2 and 3). In agreement with these findings, Ku interacted with the LigIV^{R278H} mutant in 180BR whole cell extracts as with wild type protein present in 1BR.3 whole cell extracts (Figure 3-27, lane 5 and 6).

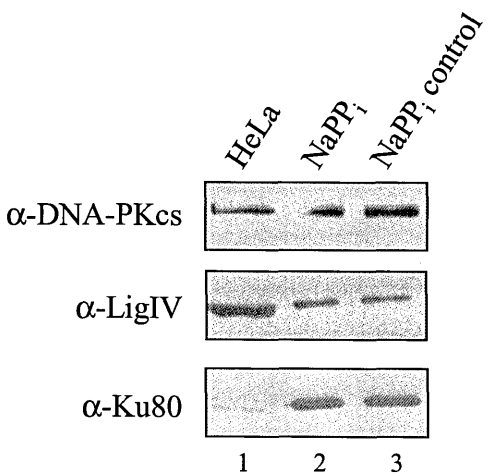

Figure 3-26 Analysis of the interaction between Ku and deadenylated LX. *In vitro* deadenylation assay of LX was performed on the α-Ku70/80 immunoprecipitates form HeLa nuclear extracts. Beads-associated proteins were incubated with (lane 2) or without (lane 3) NaPPi. 8 μg of HeLa nuclear extracts were loaded as control (lane 1).

In summary, these data show that the Ku heterodimer physically interacts with a region encompassing the two BRCT domains of LigIV and that adenylation of the ligase is dispensable for the binding of Ku to LX.

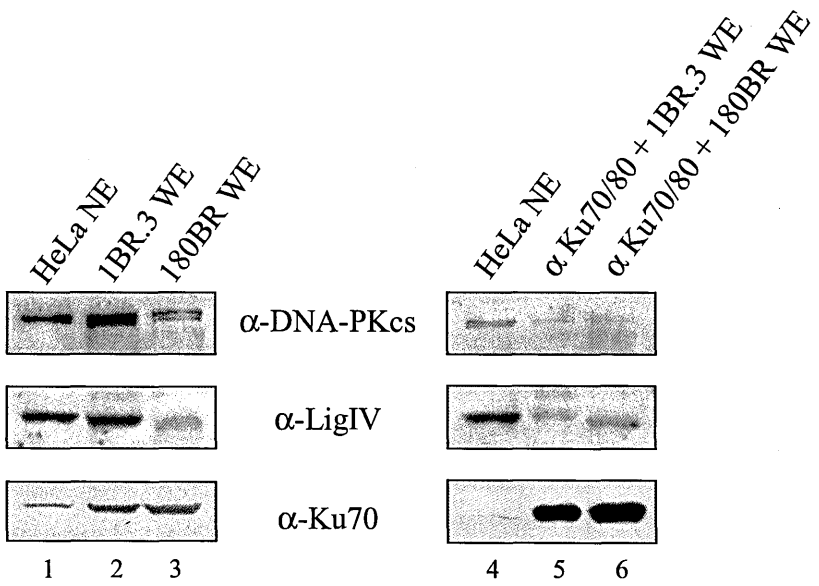

Figure 3-27 Co-ip assays using 180BR cell extracts. Immunoblotting of whole cell extracts (lane 2, 3) and immunoprecipitated samples (lane 5, 6) with α-Ku70/80 antibodies. 8 μg of HeLa nuclear extracts (lane 1, 4) and 25 μg of 1BR.3 (lane 2) and 180BR (lane 3) whole cell extracts were loaded as control.

3.3.6 Role of DNA-PKcs kinase activity

Although Ku and LX still interacted in the absence of DNA-PKcs *in vivo* and *in vitro* (Figures 3-19 and 3-21), data obtained with DNA-PKcs deficient cells suggested that DNA-PKcs enhances this interaction (Figure 3-19). Recent studies have shown that DNA-PKcs, Ku70, Ku80, XRCC4 and LigIV undergo DNA-PK dependent phosphorylation (Chan et al., 1999; Critchlow et al., 1997; Douglas et al., 2002; Wang et al., 2004). To assess the role of DNA-PKcs kinase activity and hence of the phosphorylation events on NHEJ complex assembly, *in vitro* kinase assays were performed using the anti-Ku immunoprecipitates from HeLa nuclear extracts. Preliminary experiments performed incubating the immunoprecipitated complex at different temperatures demonstrated that the complex is more stable at 25°C than at 30°C, thus the impact of phosphorylation was analysed following incubation at 25°C. After ip using anti-Ku antibodies, the immunocomplexes were incubated under conditions previously reported to be proficient for DNA-PKcs activity, in the presence of ATP and $MgCl_2$. Following washing of the beads, the integrity of the NHEJ complex

was examined. Reduced levels of DNA-PKcs and LigIV were observed after incubation of the ip samples in the presence of ATP, compared to the mock reaction lacking the nucleotide, suggesting that phosphorylation induces dissociation of the NHEJ complex (Figure 3-28, compare lane 1 and 2). The addition of dsDNA during the immunoprecipitation reaction did not influence these results. Inactivation of DNA-

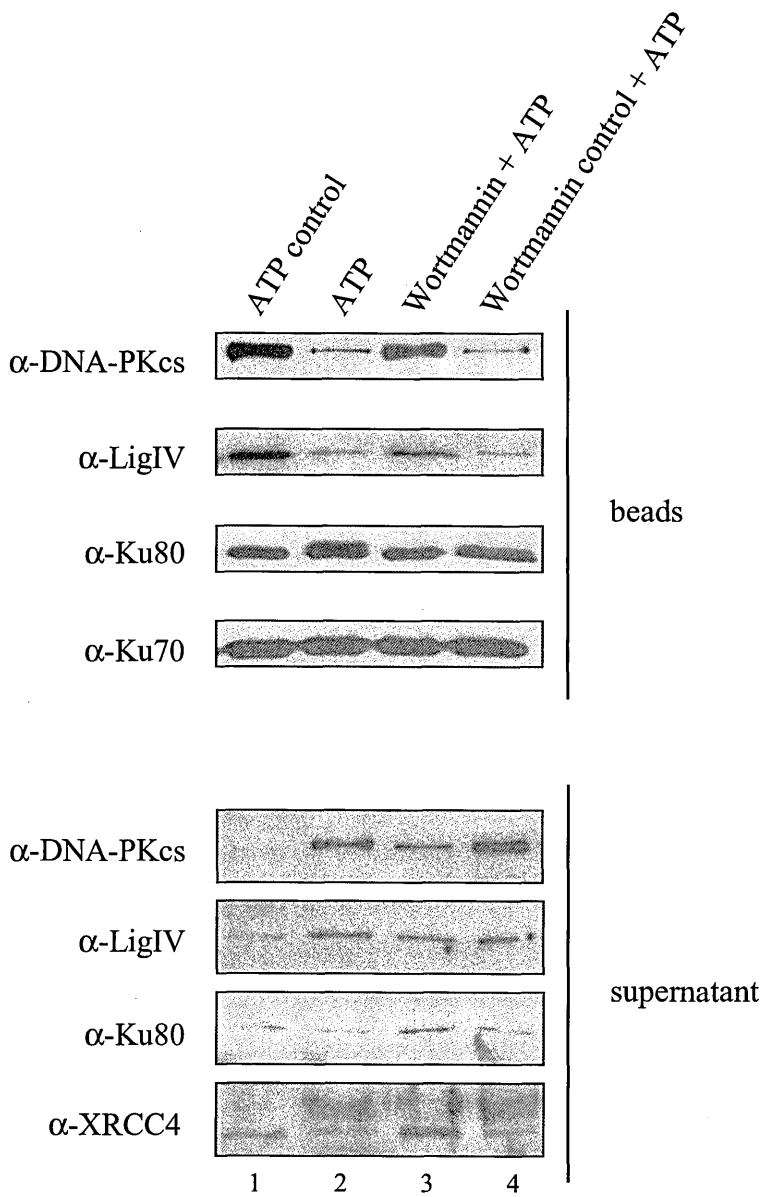

Figure 3-28 Role of DNA-PK kinase activity on the NHEJ complex. *In vitro* kinase assays were performed after immunoprecipitation with α-Ku70/80 antibodies. Immunocomplexes were incubated in the absence (lane 1) and in the presence (lane 2-4) of ATP. Beads-associated proteins were also preincubated with wortmannin (lane 3) or with wortmannin buffer (lane 4), prior to incubation with ATP. After incubation, beads were washed and the bound (beads) and unbound (supernatant) protein fractions were analysed by Western blotting.

PKcs kinase activity with wortmannin, a potent inhibitor of mammalian PI3-kinase, abolished the effect of phosphorylation on the stability of the DNA-PK/LX complex (Figure 3-28, lane 3 and 4). This data suggest that DNA-PKcs can induce the phosphorylation dependent disassembly of the NHEJ complex.

3.3.7 Effect of protein dephosphorylation

Since DNA-PK dependent phosphorylation of Ku70/80, LX and DNA-PKcs itself induced disassembly of the complex, it was examined whether treatment with a protein phosphatase could reverse the phosphorylation-induced effect on the NHEJ complex stability. HeLa nuclear extracts were incubated with λ-PPase prior to co-ip using the anti-Ku antibodies (Figure 3-29). Phosphatase treatment slightly enhanced the

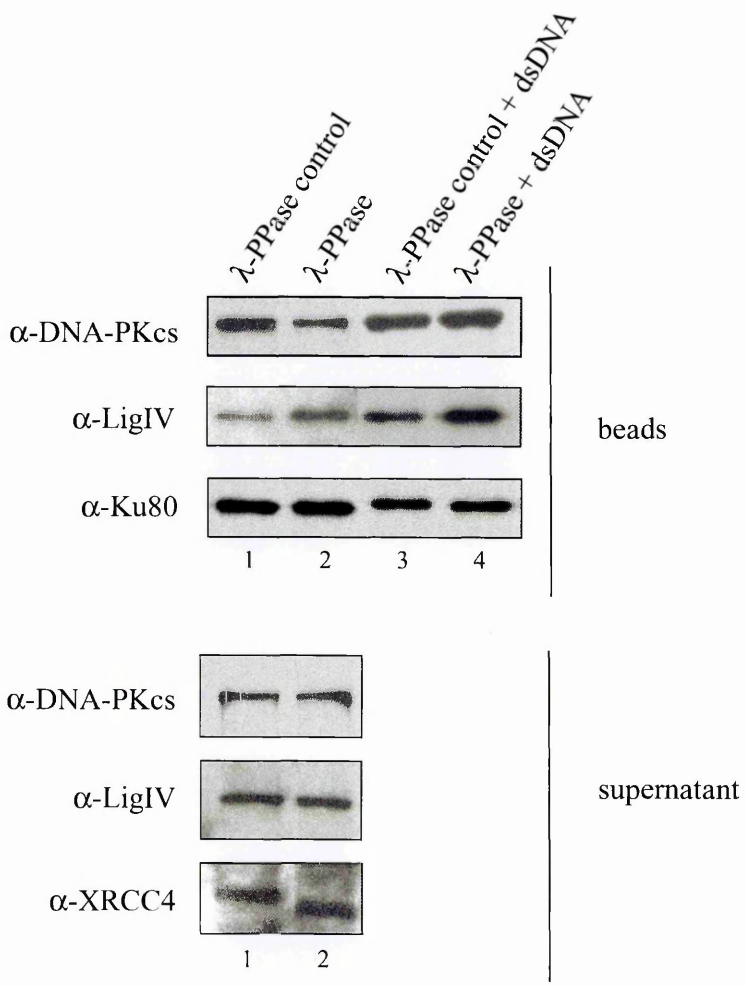

Figure 3-29 Effect of protein dephosphorylation on the NHEJ complex. HeLa nuclear extracts were treated with λ-PPase (lane 2, 4) in the absence (lane 2) and in the presence (lane 4) of 10 μg/ml of a 75bp dsDNA fragment prior to co-ip using α-Ku70/80 antibodies. After the co-ip, beads were washed and the bound (beads) and unbound (supernatant) protein fractions were analysed by Western blotting.

amount of LigIV present in the immunocomplex in absence or in the presence of an additional dsDNA oligonucleotide (Figure 3-29, compare lane 1 and 2, 3 and 4). On the contrary, the amount of DNA-PKcs after phosphatase treatment in the absence of additional DNA was slightly reduced. These results suggest that protein dephosphorylation diminishes dissociation of the NHEJ complex and that dephosphorylation favours the interaction between Ku and LX.

3.3.8 γ-H2AX analysis in Ku and DNA-PKcs deficient cells

The biochemical interaction studies described above provide evidence that DNA-PKcs facilitates the assembly of a NHEJ complex, but that it is not essential for the recruitment of Ku or LX to the DNA ends. To examine the requirement of each NHEJ component for DSB repair *in vivo*, γ-H2AX foci analysis was performed by members of the laboratory of Prof. Penny Jeggo, at the University of Sussex, UK. An early response to DSBs is phosphorylation of H2AX, called γ-H2AX when phosphorylated (see also general introduction). Analysis of γ-H2AX foci provides a quantitative procedure to monitor DSB induction and repair at low doses of γ-rays (Rogakou et al., 1998; Rothkamm and Lobrich, 2003). To avoid γ-H2AX foci formation at stalled replication forks, this assay was performed with non-replicating G0/G1 cells that were identified as non-BrdU labelled cells. Under such conditions after IR, γ-H2AX foci form primarily at DSBs. The time course of γ-H2AX foci formation and loss after 3 Gy γ-irradiation in non-BrdU labelled cells was examined in wild type, DNA-PKcs$^{-/-}$ and Ku80$^{-/-}$ MEFs (Figure 3-30). Foci were measured from 15 min following γ-irradiation, when the number of foci per cell was at a maximum. The number of foci per cell was slightly greater in repair defect MEFs, most likely because some DSB repair has already occurred during the first 15 min post irradiation in wild-type MEFs. At 2 h post-irradiation, the number of foci in the two repair defective cell

lines was higher compared with wild type cells indicating impaired DSB repair. Whilst the rate of DSB repair progressed very slowly in Ku80$^{-/-}$ MEFs, considerable residual DSB rejoining occurred in the DNA-PKcs$^{-/-}$ MEFs. A similar impaired rate of rejoining was also observed in control MEFs treated with a DNA-PKcs small molecule inhibitor (Riballo et al., 2004). Taken together, these results show that whilst loss of Ku substantially impairs rejoining, loss of DNA-PKcs has a milder impact consistent with the notion that for the majority of DSBs, DNA-PKcs facilitates but is not essential for NHEJ.

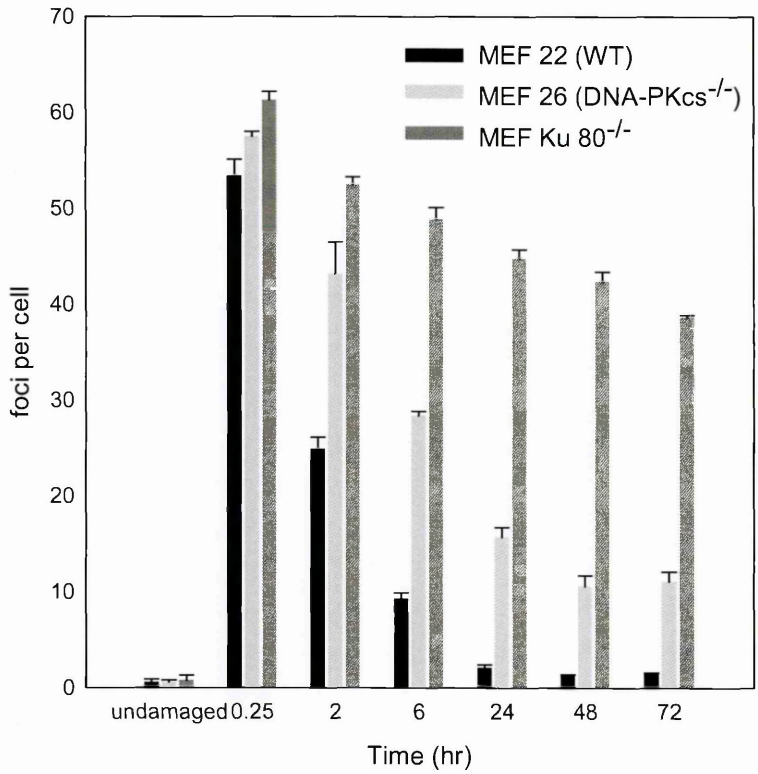

Figure 3-30 γ-H2AX analysis in wild type (MEF 22), DNA-PKcs-deficient (MEF 26) and Ku80-deficient (MEF Ku80$^{-/-}$) cells after 3 Gy irradiation. The mean number of foci per cell at various post irradiation times is shown. Data points were the mean of three independent experiments with SD indicated by error bars.

3.3.9 Conclusions

The studies reported in this chapter were performed to characterise the interaction between Ku and LX and to examine the role of DNA-PKcs in regulating the NHEJ complex assembly. Previous works have demonstrated that Ku and DNA-PKcs

interact with LX, although little is known on the domains that mediate their interaction and conflicting results are reported on the role of dsDNA in mediating the DNA-PK/LX complex assembly. One group reported that co-ip of LX with DNA-PK is DNA independent (Hsu et al., 2002), in contrast, two other groups found that this interaction is DNA dependent (Calsou et al., 2003; Nick McElhinny et al., 2000). Results reported here using HeLa nuclear extracts agree with the latter finding, demonstrating that the interaction between Ku, DNA-PKcs, and LX is markedly decreased in the presence of EtBr. LX cannot bind DNA under the salt concentrations used for the co-ip assays (data not shown and (Kysela et al., 2003; Marchetti et al., 2006)) strongly suggesting that the co-ip demonstrates assembly of a NHEJ complex rather than binding of the individual complexes to DNA. This suggestion is further substantiated by the finding that the Ku/LX complex formation is diminished in the absence of DNA-PKcs. Since DNA-PKcs does not affect the binding of Ku to DNA, this provides strong evidence that DNA-PKcs enhances complex assembly.

Experiments performed using DNA-PKcs deficient cells provided evidence for interaction between Ku and LX in the absence of DNA-PKcs. To gain insight into the basis underlying the Ku/LX interaction, co-ip assays were performed using recombinantly expressed proteins. These experiments demonstrated that Ku and LX interact in the absence of DNA-PKcs and that this interaction is not completely dependent on DNA, in agreement with the data reported by McElhinny and co-workers (Nick McElhinny et al., 2000). Indeed, experiments performed in the presence of EtBr showed that the interaction between Ku and LX is substantially reduced. Although an interaction between Ku and LX was detectable in the absence of DNA, dsDNA promoted the complex formation, expecially at low LX concentrations, probably by enhancing the affinity between the Ku heterodimer and the LX complex. This finding provides an explanation for the previous controversy concerning the role of DNA in

mediating the Ku-LX interaction and suggests that dsDNA induce a conformational change of these proteins that favour their mutual interaction. Further insight on the individual subunits of Ku and LX involved in the interaction emerged from the assays performed using the *in vitro* translated proteins. These studies show that the C-terminal domain of Ku80 responsible for the recruitment of DNA-PKcs is dispensable for the interaction with LX (Table 3-7). Moreover, Ku needs to be in its heterodimeric form in order to interact with LX. Experiments with the two separated components of the LX complex showed a direct interaction between Ku and LigIV (Table 3-7), which is strengthened by XRCC4. These findings are consistent with previous reports showing that Ku stimulates LigIV activity (Kysela et al., 2003; Nick McElhinny et al., 2000), while XRCC4 interacts with DNA-PKcs (Hsu et al., 2002). Studies performed with the *in vitro* expressed LX mutants demonstrate that the C-terminal tandem BRCT domain of LigIV is sufficient for Ku recognition. Furthermore, a construct encompassing the N-terminal catalytic domain and the first BRCT domain (residues 1-748) can also bind Ku providing evidence that the first BRCT domain may mediate this interaction. However, it is possible that binding is influenced by the protein conformation, which may not be entirely reproduced in these studies with deletion mutants. Indeed, previous studies showed that the region between the BRCT domains of LigIV was necessary and sufficient for binding LX (Grawunder et al., 1998c; Sibanda et al., 2001), but recent structural studies have shown that both BRCT domain also makes contacts with XRCC4 (Dore et al., 2006). Previous studies showed that the BRCT domains of XRCC1 (Levy et al., 2006), the terminal deoxynucleotidyl transferase (TdT) (Mahajan et al., 1999), DNA polymerase μ and λ are required for the interaction between these proteins and the Ku heterodimer (Ma et al., 2004). Whether all these BRCT containing proteins including LigIV, interact with the same region of Ku is however still unknown.

Table 3-7 Domains involved in the interaction between Ku70/80 and LX.

	LX	LIV	XRCC4	LX^{K273G}	LX^{R814X}	LX^{1-790}	LX^{1-748}	LX^{1-643}	$LX^{600-911}$
Ku70/80	yes	yes	no	yes	yes	yes	yes	no	yes
Ku70	no	-	-	-	-	-	-	-	-
Ku80	no	-	-	-	-	-	-	-	-
$Ku70/80^{1-554}$	yes	-	-	-	-	-	-	-	-

Yes indicates that an interaction has been detected by co-ip assays.
No indicates the absence of interaction.

In addition, experiments carried out with LX and LigIV mutants encompassing only the N-terminal catalytic domain (residues 1-643) demonstrated that the catalytic domain of the ligase is dispensable for the interaction with Ku. In agreement with these data, the adenylation status of LigIV does not impact upon this interaction.

The role of DNA-PKcs and its kinase activity in NHEJ is unclear. DNA-PKcs homologues have not been found in lower eukaryotes suggesting that the function of DNA-PKcs is not evolutionarily conserved and can potentially be dispensable for NHEJ. Co-ip assays performed with whole cell extracts of DNA-PKcs deficient cells substantiate previous findings demonstrating that DNA-PKcs facilitates but is not essential for the efficient recruitment of LX to broken DNA ends (Calsou et al., 2003; Hsu et al., 2002). These data suggest that DNA-PKcs acts as a scaffold and enhances the interaction between Ku and LX *in vivo*. In addition, γ-H2AX foci analysis performed on NHEJ defective cell lines in the laboratory of Prof. Penny Jeggo, demonstrates that substantial DSB rejoining occurs in the absence of DNA-PKcs, which is greater than that observed in the absence of Ku. Thus, suggesting that DNA-PKcs might have a regulatory role in NHEJ, making the process more efficient. Previous studies have shown that DNA-PK autophosphorylation results in its disassembly at the DNA end (Chan and Lees-Miller, 1996; Merkle et al., 2002). Analysis of the effect of DNA-PK phosphorylation on anti-Ku immunoprecipitates extend this to the NHEJ

complex. *In vitro* kinase assays performed on anti-Ku70/80 immunoprecipitates, show that a DNA-PKcs dependent phosphorylation event induces dissociation not only of DNA-PKcs from Ku bound to DNA end, but also of bound LX. This phosphorylation dependent disassembly could be either to a direct regulation of the Ku/LX interaction by protein phosphorylation or to the dissociation of the autophosphorylated form of DNA-PKcs from the NHEJ complex, which in turns induces the subsequent dissociation of LX. Dissociation from LX could be due to an impact of phosphorylation on either XRCC4 or LigIV. These findings suggest that DNA-PKcs kinase activity coordinates the temporal assembly and disassembly of all the NHEJ components at broken DNA ends. Interestingly, previous observations have shown that the phosphorylated form of XRCC4 does not bind to DNA (Modesti et al., 1999) and that the phosphorylation of LigIV negatively influence its stability (Wang et al., 2004). On the contrary, *in vivo* studies with Ku, XRCC4, and LX with mutated phosphorylation sites did not highlight any important role of DNA-PKcs phosphorylation for the NHEJ process. However, DNA-PKcs inactivated by point mutations in its kinase domain fails to complement the DSB repair defect of DNA-PKcs-deficient cells (Kienker et al., 2000; Kurimasa et al., 1999). These results suggest that only the simultaneous lack of phosphorylation on all the NHEJ components determine a detectable DSB repair defect. It is unclear, however, how DNA-PKcs manages to enhance complex assembly as well as dissociation through autophosphorylation. A challenging avenue for future studies will be to define the precise temporal ordering of these steps.

The work described in this chapter is contained in the following article:

Costantini S, Woodbine L, Andreoli L, Jeggo PA & Vindigni A. Interaction of the Ku heterodimer with the DNA ligase IV/Xrcc4 complex and its regulation by DNA-PK. *DNA repair 2007; in press.*

3.4 INTERACTION OF KU WITH OTHER DNA-REPAIR FACTORS

3.4.1 Introduction

Many factors are required to process DNA ends during NHEJ. For example, phosphatases or nucleotide kinases are necessary to remove or add phosphate groups, whilst polymerases or nucleases are required to extend or resect single-stranded overhangs. Artemis is a nuclease recently shown to be involved in NHEJ (Moshous et al., 2001). This protein interacts with DNA-PKcs which activates its 5'-3' endonuclease activity (Ma et al., 2002). The ability of Artemis to cleave hairpin structures suggested that this nuclease is the processing factor required during V(D)J recombination (Rooney et al., 2003). RECQ helicases play critical roles in maintaining genomic stability as evidenced by the hyper-recombination phenotype observed in *RECQ* mutants. RECQ1 is a human DNA helicase that belongs to this family (Bachrati and Hickson, 2003). Its biological importance cannot be clearly evaluated at present, because there is little information on the phenotypes of human *RECQ1* mutant cells. Werner syndrome protein (WRN) is another member of the RECQ helicase family that has both ATP-dependent helicase activity and 3'-5' exonuclease activity (Hickson, 2003). WRN defective cells show a mild radiosensitivity suggesting that this enzyme may be involved in NHEJ. This enzyme interacts with the DNA-PK complex and is phosphorylated by DNA-PK *in vitro* and *in vivo* (Karmakar et al., 2002a; Yannone et al., 2001). DNA-PK phosphorylation and association regulate WRN activity, suggesting physiological and functional interactions between WRN and the DNA-PK complex. Recent studies reported that WRN directly interacts with PARP-1, another factor implicated in DNA repair and in the cellular response to DNA damage (Adelfalk

et al., 2003; Lindahl et al., 1995; von Kobbe et al., 2003). PARP-1 is a nuclear factor, that poly(ADP-ribosyl)ates histones and other nuclear proteins, such as the Ku heterodimer (Ame et al., 2004; Li et al., 2004).

Another protein that might be involved in NHEJ is the heterotrimeric replication protein A (RPA), composed of three subunits of 70, 32 and 14 kDa. RPA is a single-stranded DNA-binding protein required for DNA replication and also for multiple DNA repair pathways including base excision repair, nucleotide excision repair, and DNA mismatch repair (Binz et al., 2004). In these pathways, RPA participates in damage recognition, excision, and re-synthesis reactions. Moreover, RPA is involved in multiple steps of the homologous recombination pathway. *In vitro* DSB rejoining assays demonstrated that RPA is not essential for NHEJ, but stimulates the rate of rejoining (Perrault et al., 2001), although its role in NHEJ is still not well defined. RPA is phosphorylated by DNA-PK in response to DNA damage. This phosphorylation event induces the dissociation of RPA from the Ku-DNA-PKcs complex and modulates the interactions of RPA with other proteins as well as its activity in DNA replication (Shao et al., 1999).

53BP1 is amongst the earliest proteins to be recruited into IR induced nuclear foci. Evidences for its role in NHEJ come from *in vitro* assays showing that it stimulates DNA end-joining (Iwabuchi et al., 2003) and, more recently, from genetic studies that demonstrated an epistatic relationship with other NHEJ factors (Nakamura et al., 2006; Riballo et al., 2004). Moreover, mice defective for this protein are radiosensitive, immune deficient, and predisposed to cancer (Morales et al., 2003).

The presence of these proteins in the NHEJ complex was investigated by Western blot analysis of the immunoprecipitated samples obtained with anti-Ku70/80 antibodies. Moreover, the effect of protein dephosphorylation on the interaction between Ku, WRN, and PARP-1 was evaluated by phosphatase treatment.

3.4.2 Search for novel Ku binding partners

The presence of Artemis in the samples immunoprecipitated with anti-Ku70/80 antibodies was analysed by conventional Western blot analysis (Figure 3-31 B, lane 1). However, under the reaction conditions used for the co-ip, Artemis was not found in the immunoprecipitated samples. Similarly, neither 53BP1 nor the helicase RECQ1 were found to associate with Ku (Figure 3-31 B, lane 1). Conversely, Western blot analysis revealed that Werner, PARP-1, and RPA are present in the immunoprecipitated samples (Figure 3-31 A, lane 3). Therefore, these results raise the possibility that Ku70/80 forms a complex with WRN, PARP-1, and RPA together with DNA-PKcs and LX in human extracts.

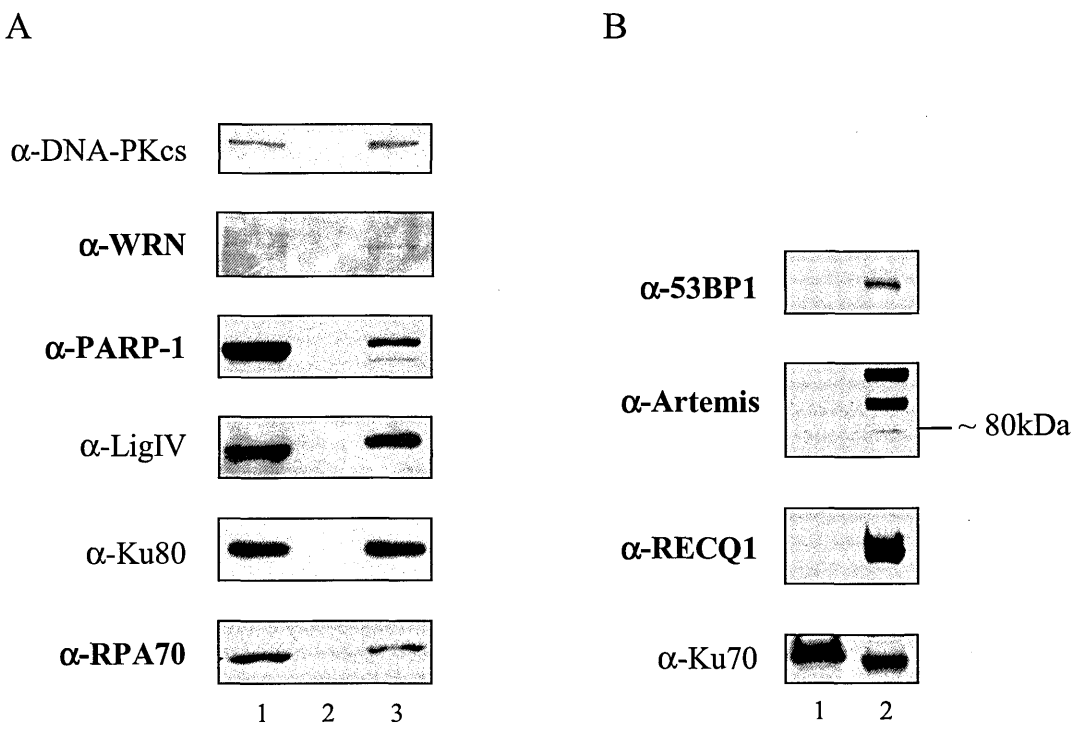

Figure 3-31 Co-ip assays with anti-Ku70/80 antibodies in HeLa nuclear extracts. 8 μg Hela nuclear extracts (**A,** lane 1 and **B,** lane 2), α-Ku70/80 (**A,** lane 3 and **B,** lane 1) and normal mouse IgG (**A**, lane 2) immunoprecipitates were analysed by Western blotting with α-WRN, α-PARP-1, α-RPA70, α-53BP1, α-Artemis, α-RECQ1, α-DNA-PKcs, α-LigIV, α-Ku80 and α-Ku70 antibodies.

3.4.3 Analysis of the Ku-RPA interaction using recombinant proteins

To further characterise the association between Ku and RPA, Far-Western analysis was performed using the purified recombinant proteins. Ku70/80 was expressed using the baculovirus expression system, while RPA was expressed using *E. coli*. Purified proteins were resolved by 10% SDS-PAGE and then transferred onto PVDF membrane (Figure 3-32 A). Proteins immobilized on the membrane were refolded and then incubated with RPA. After washes, Western blot analysis was performed using antibodies against the 70 kDa and the 32 kDa subunits of RPA.

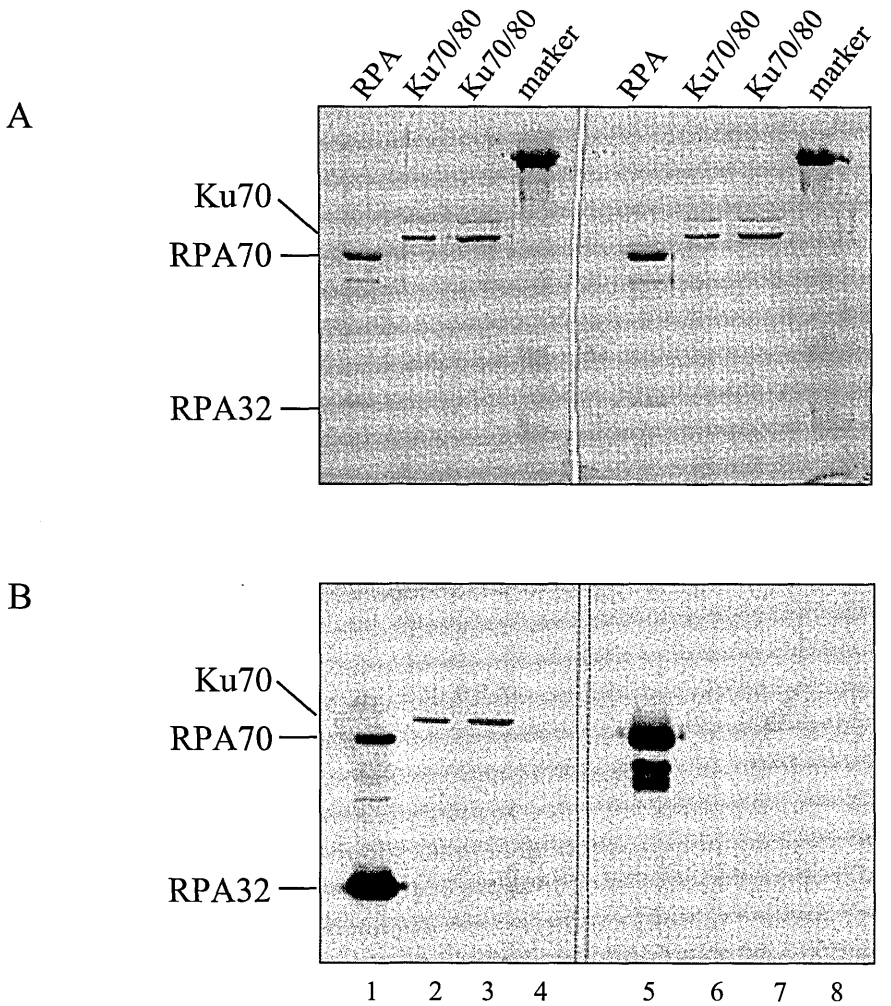

Figure 3-32 Far-Western analysis of the interaction between Ku70/80 and RPA. **A**, Coomassie-stained PVDF membrane. ~ 2 µg of rRPA were loaded in lane 1 and 5; ~ 1 µg of rKu was loaded in lane 2 and 6; 1.5 µg of rKu were loaded in lane 3 and 7; molecular weight markers were loaded in lane 4 and 8. **B**, immunoblotting after Far-Western analysis with α-RPA 32 (left side) and α-RPA 70 antibodies (right side).

Immunoblotting with anti-RPA32 detected a band corresponding to the 70 subunit of Ku and two bands corresponding to the 70 and 32 subunits of RPA. These results suggest that RPA interacts with the Ku70 subunit of the Ku heterodimer and that the full length human RPA interacts with the two separated subunits of the RPA complex (Figure 3-32 B, left side). Western blot analysis performed with anti-RPA70 subunit revealed only a band corresponding to the 70 subunit of RPA and lower bands that probably represent degradation products (Figure 3-32 B, right side). However, neither of the two subunits of Ku was visualized using this antibody, probably because the epitope recognized by the anti-RPA70 antibody is hidden or buried in the interaction.

3.4.4 Effect of protein dephosphorylation on the Ku/WRN/PARP-1 complex

The effect of DNA and protein phosphorylation on the interaction between Ku, WRN, and PARP-1 were analysed. To test the role of DNA, HeLa nuclear extracts were incubated with a 75 bp double-stranded oligonucleotide prior to co-ip with anti-Ku70/80 antibodies. Immunoblotting analysis indicated that DNA enhances the amount of PARP-1 retrieved by the anti-Ku70/80 antibodies (Figure 3-33, lane 4). To examine

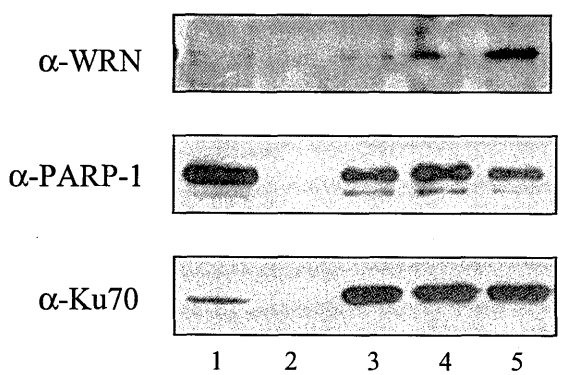

Figure 3-33 Effect of protein dephosphorylation on the Ku/WRN/PARP-1 complex. 8 µg Hela nuclear extracts were loaded as control (lane 1). Co-ip assays were performed with normal mouse IgG (lane 2) and α-Ku70/80 antibodies (lane 3-5) using untreated (lane 3) HeLa nuclear extracts, extracts in the presence of additional dsDNA (lane 4) and after λ-PPase treatment (lane 5).

the role of protein phosphorylation, HeLa nuclear extracts were treated with λ-PPase prior to the co-ip. As shown in Figure 3-33, lane 5, dephosphorylation significantly enhanced the association of Ku with WRN, while the amount of PARP-1 present in the complex did not change under these conditions.

3.4.5 Conclusions

Co-ip assays carried out in human nuclear extracts with anti-Ku70/80 antibodies showed that Ku forms a complex with WRN, PARP-1, and RPA. The interaction between Ku and RPA was further analysed by Far-Western analysis using purified proteins. This assay showed that Ku70 interacts with RPA. The interaction between Ku and RPA is not likely to be mediated by DNA, since the two separated subunits of Ku are not able to bind DNA. Indeed, preliminary EMSA experiments performed using the Ku70 subunit expressed with the baculovirus system showed that Ku70 alone is not able to bind DNA, in agreement with previous findings (Ono et al., 1994). The observation that RPA physically interacts with Ku70/80 is novel. Shao and co-workers, showed that the catalytic subunit of DNA-PK forms a complex with RPA and that RPA70 is required for this interaction (Shao et al., 1999). Moreover, the same authors reported that Ku is not required for the formation of the RPA/DNA-PKcs complex in an *in vitro* binding assay using purified proteins immunodepleted with anti-Ku70/80 antibodies, although this result did not exclude a direct interaction between Ku and RPA. DNA-PKcs has been reported to phosphorylate the 32 kDa subunit of RPA *in vitro* and *in vivo*. Therefore, it is likely that RPA interacts also with the regulatory subunit of the DNA-PK complex and the interaction between Ku70 and RPA might be needed to stabilise the interaction between DNA-PKcs and RPA.

In addition, co-ip assays indicated that Ku forms a complex with WRN in human cell extracts and, in agreement with previous findings, that also PARP-1 resides in this

complex (Li et al., 2004). The identification of WRN as one of the components of this complex is consistent with previous studies (Cooper et al., 2000; Li and Comai, 2000; Li and Comai, 2001), where it was established that Ku is a functional partner of WRN. PARP-1 is a factor implicated in the cellular response to DNA damage that has been reported to interact with WRN (Adelfalk et al., 2003; Lindahl et al., 1995; von Kobbe et al., 2003). *In vitro* assays with Ku70/80, WRN, and PARP-1 have shown that PARP-1 poly(ADP-ribosyl)ates Ku70/80, but not WRN and that this modification reduces the affinity of the Ku heterodimer for DNA, suggesting a functional interaction among these proteins (Li et al., 2004).

In the presence of additional dsDNA the amount of PARP-1 retrieved by the anti-Ku70/80 antibodies was significantly enhanced. Consistently, previous findings demonstrated that PARP-1 has a strong affinity for DSBs (Morrison et al., 1997) and that acts as a sensor of DNA damage (Burkle, 2001; de Murcia and Menissier de Murcia, 1994). The impact of proteins dephosphorylation on the WRN/PARP-1/Ku70/80 complex was also examined. Treatment of the nuclear extracts with λ-PPase prior to the co-ip significantly increased the amount of WRN present in the complex. Conversely, previous data with purified Ku70/80, DNA-PKcs, and WRN reported that the physical association among these proteins is unaffected by PP1 treatment (Karmakar et al., 2002a). This discrepancy might be due to the different experimental conditions and to the different activity of the phosphatases used in these assays. The same authors reported that dephosphorylation of WRN enhances both its exonuclease and helicase activity (Karmakar et al., 2002a). Therefore, the enhanced activity of WRN upon protein dephosphorylation could be related to its higher affinity for Ku that we detected. Indeed, Ku was shown to recruit WRN to DNA ends and to stimulate its exonuclease activity (Cooper et al., 2000; Li and Comai, 2000; Orren et al., 2001).

The interaction of WRN, PARP-1 and RPA with the key components of the NHEJ pathway suggests a possible role for these proteins in DNA repair. However, these are preliminary observations and further studies will be necessary to investigate their functional role in the NHEJ process.

4 GENERAL DISCUSSION

The Ku heterodimer is one of the main components of the NHEJ machinery. The aim of this thesis was to gain insight into the mechanism of interaction of Ku with nucleic acids and with the other NHEJ factors. More generally, these studies aimed to achieve a better understanding of the macromolecular interactions that regulate the NHEJ mechanism in cells. Our DNA binding studies demonstrate that Ku binds to DNA ends with very high affinity. The k_d value measured for the interaction of Ku70/80 with a blunt-ended dsDNA molecule of 25 bp is 0.5±0.01 nM in the presence of 220 mM NaCl (Arosio et al., 2004). Moreover, our salt dependence studies indicate that electrostatic interactions play a major role in the binding of Ku to DNA and that the k_d decreases approximately 60-fold as the salt concentration is lowered from 300 mM to 220 mM. Considering that the total intracellular ion concentration is roughly 150 mM, from the data obtained with salt-back titrations we can estimate that the k_d for the Ku-DNA interaction *in vivo* is in the order of 0.005 nM. This value is 600 fold higher than the k_d previously reported for the binding of DNA-PKcs to DNA. Indeed, SPR assays yielded an equilibrium dissociation constant of 3 nM for the binding of DNA-PKcs to a 35 bp ds oligonucleotide in a buffer containing 150 mM NaCl (West et al., 1998). However, the affinity of DNA-PKcs for DNA increases significantly in the presence of Ku, suggesting that Ku facilitates the recruitment of DNA-PKcs to DNA ends (Dvir et al., 1992; Gottlieb and Jackson, 1993; Suwa et al., 1994; West et al., 1998). Similarly, LX has very low intrinsic affinity for DNA and requires Ku to bind to DNA ends (Nick McElhinny et al., 2000). The high affinity of Ku for DNA, its ability to bind DNA ends regardless of their structure and its higher abundance in the mammalian cell nucleus compared to DNA-PKcs and LX, support a model where Ku is the first NHEJ protein that binds DNA ends at a DSB (Figure 4-1).

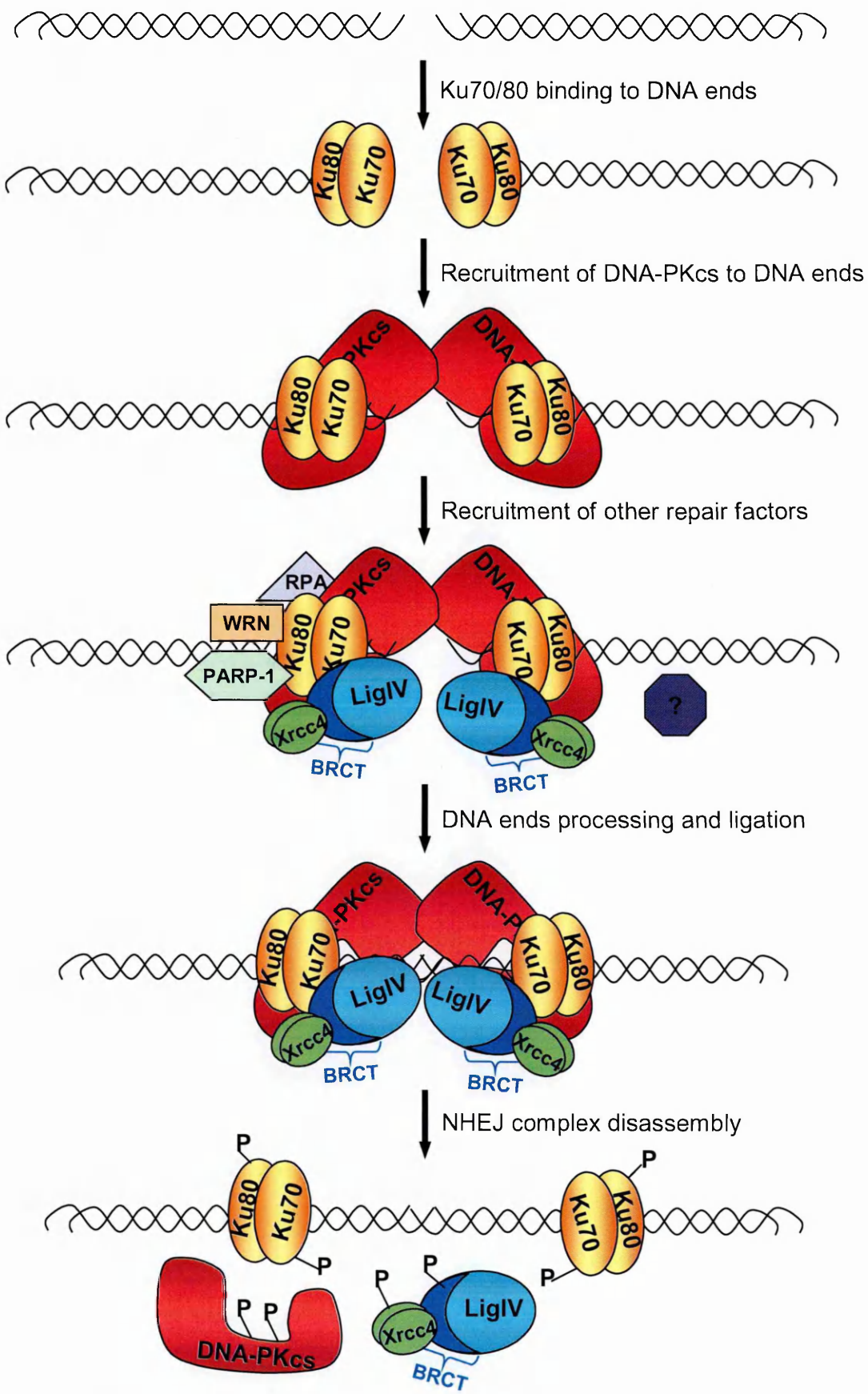

Figure 4-1 Proposed model for NHEJ. Ku70/80 (yellow) is the first protein of the NHEJ components that recognizes and binds to broken DNA ends. Once bound, Ku recruits DNA-PKcs (red) and translocates inward providing access to the DNA ends. The DNA-PK complex then recruits LX (blue and green). Ku interacts with the BRCT domains of LigIV, while DNA-PKcs interacts with XRCC4. Other repair factors, such as WRN (pink), PARP-1 (light green), and RPA (light violet) are also recruited. After DNA ends processing and ligation, DNA-PKcs mediated phosphorylation induces the dissociation of the NHEJ complex.

Our fluorescence emission spectra of Ku bound to a 25 bp DNA duplex suggest that DNA-binding might induce a conformational change of the C-terminal domain of Ku80 and/or of the N-terminal region of Ku70. A conformational change of the C-terminal region of Ku80 might be necessary for the subsequent recruitment of DNA-PKcs to the DNA ends. Interestingly, our protein-protein interaction studies reported in section 3.3.2 demonstrate that DNA is required for the DNA-PK complex formation, suggesting that Ku and/or DNA-PKcs need to change their conformation in order to interact. A previous report showed, however, that DNA-PKcs can bind to a Ku/DNA complex using a DNA duplex of 18 bp (West et al., 1998). Since Ku covers approximately 20-25 bp when bound to DNA, this result suggests that is the Ku heterodimer rather than DNA-PKcs that needs to change its conformation and that protein-protein interactions mediate the binding of DNA-PKcs to Ku. A conformational change in the N-terminal domain of Ku70 might instead regulate the binding of the Ku heterodimer with DNA. Indeed, the crystal structure showed that the N-terminal region of Ku70 borders the DNA binding site of Ku, even though the last 33 amino acids at the N terminus were not modelled in the 3D structure. These N-terminal residues are acidic and may provide an electrostatic or steric block to the DNA entrance in the Ku ring.

Our analysis of the stoichiometry of Ku binding to DNA duplexes containing 1, 2, or 3 heterodimers, shows that Ku covers about 20-25 bp when bound to dsDNA. Moreover, the same analysis performed with a DNA duplex of 60 bp with a gap of 20 nucleotides in the middle demonstrates that Ku does not bind to DNA single-stranded regions, in contrast to a previous work where it was shown that Ku can bind to circular duplex molecules containing a single-stranded region (Falzon et al., 1993). The observation that Ku is able to bind closed circular DNA molecules is also in contrast with the crystallographic data which show that the Ku ring requires DNA ends to bind the DNA molecule. However, the results obtained with circular DNA duplexes could

be explained considering that Ku is able to bind secondary structures formed by the DNA duplex and to structures formed by transient strand separation or stem-loop formation in the presence of a gap.

Analysis of the interaction of Ku with DNA duplexes longer than 42 bp demonstrates that more than one Ku heterodimer binds to long DNA molecules. However, once bound, Ku can slide freely along the dsDNA chain and its presence on the duplex does not favour or impair the binding of additional heterodimers to the same dsDNA break. Indeed, both the overlapping and the non-overlapping model applied to analyse the binding of Ku to DNA yield similar conclusions and demonstrate the absence of cooperative interaction among the Ku molecules binding to DNA. This is in agreement with a model where Ku, once bound to DNA ends, recruits other enzymes required for the processing of the DNA ends. In this view, the absence of positive cooperativity would prevent clustering of Ku heterodimers at the DNA ends. Instead, Ku molecules would easily slide to internal positions of the DNA molecule allowing the binding of other factors. Previous DNA binding studies using LX demonstrated that inward translocation of Ku along the DNA molecule is essential to Ku stimulation of LX activity (Kysela et al., 2003). Moreover, electron microscopy studies of the DNA-PK complex bound to DNA showed that Ku is located inside the DNA molecule, while DNA-PKcs remains bound to the DNA end (Spagnolo et al., 2006). In agreement with the observation that Ku could also function as a recruitment platform for other repair factors to the sites of damage, protein-protein interactions studies reported in section 3.3.2 and 3.4.2 show that LX, WRN, PARP-1, and RPA also co-immunoprecipitated with DNA-PK using human nuclear extracts (Figure 4-1).

Co-ip assays performed in M059J, DNA-PKcs-/-, cells showed that DNA-PKcs is necessary for the efficient recruitment of LX on DNA. Moreover, co-ip assays with anti-XRCC4 antibodies using human cell extracts demonstrated that the DNA-PKcs/LX

interaction is DNA dependent, thus excluding the possibility that a DNA-PKcs/LX complex exists in solution without DNA and suggesting that Ku first recruits DNA-PKcs and then the DNA-PK complex binds LX (Figure 4-1). Previous studies reported that XRCC4 interacts with DNA-PKcs (Hsu et al., 2002). Our *in vitro* studies with recombinant Ku and LX demonstrate that these complexes physically interact and that DNA enhances their affinity. Addition of EtBr significantly reduces this interaction. These results suggest that although a direct interaction between Ku and LX is still detectable in the absence of DNA, nucleic acids favour or stabilize the interaction between the Ku heterodimer and the LX complex probably by inducing a conformational change of these proteins. Studies with Ku and LX mutants demonstrate that the Ku heterodimer interacts with the C-terminal region of LigIV encompassing the tandem BRCT domain and that residues 643-748, including the first BRCT motif, are necessary to mediate this interaction. Interestingly, LigIV is the only eukaryotic ligase that contains two BRCT domains at the C-terminal tail and previous work reported that Ku does not interact with other eukaryotic ligases, supporting our conclusion that Ku recognition of LigIV is mediated via its tandem BRCT domain. The interaction of Ku with the ligase and of DNA-PKcs with XRCC4 is probably required to stabilise the DNA-PK-LX complex at the DNA ends.

The formation of the DNA-PKcs/Ku/DNA complex activates the kinase activity of DNA-PKcs, which in turn results in DNA-PKcs autophosphorylation as well as in the phosphorylation of other NHEJ components. Our *in vitro* kinase assays demonstrate that a DNA-PKcs-dependent phosphorylation event induces the disassembly of the DNA-PK/LX complex. Dissociation of this complex could be due to an impact of phosphorylation on the single NHEJ components or to a further impact of DNA-PKcs autophosphorylation. This phosphorylation event might be necessary for the unloading of the NHEJ factors once the ligation step is completed or might induce a recycling of

the repair factors necessary for the proper processing of the DNA ends prior to ligation. Previous studies showed that complete autophosphorylation induces dissociation of DNA-PKcs from Ku and DNA (Chan and Lees-Miller, 1996; Merkle et al., 2002). A current model for DNA-PKcs phosphorylation proposes that this kinase undergoes a series of autophosphorylation events that induce conformational changes necessary to regulate access of DNA ends to repair factors (Cui et al., 2005). DNA-PKcs autophosphorylation at the cluster 2609-2647 is required for LX ligation, but is not sufficient for DNA-PKcs dissociation (Block et al., 2004; Ding et al., 2003; Reddy et al., 2004). Subsequent phosphorylation of cluster 2023-2056 of DNA-PKcs might induce a conformational change that probably promotes interaction with LX (Cui et al., 2005). Conversely, *in vitro* phosphorylation assays of Ku70/80 or LX alone indicated that phosphorylation of these factors is not required for DNA end-joining, suggesting that these modifications might be necessary only after the ligation step is completed. However, the effect of the simultaneous phosphorylation of the Ku heterodimer, LX, and DNA-PKcs on DNA end-joining has never been examined. Further studies are required to define the precise temporal ordering of these steps and the impact of each phosphorylation events on the NHEJ mechanism.

In summary, the work included in this thesis provides novel important information on the macromolecular interactions that regulate the NHEJ mechanism in cells and additional evidence on the role of protein phosphorylation on the NHEJ complex disassembly. The results obtained open new challenging avenues to understand the temporal order that regulate the assembly and disassembly of the NHEJ complex on DNA ends as well as the role of newly discovered factors whose precise function has not been elucidated.

4.1 FUTURE DIRECTIONS

Results reported in section 3.3 showed that the DNA-PK holoenzyme both facilitates the recruitment of LX and induces the dissolution of the NHEJ complex. In the future it will be interesting to analyse how this is regulated and whether there are additional factors enhancing the dissociation of the complex *in vivo*. Thus, the effect of the kinase activity of DNA-PK on the NHEJ complex could be analysed in cells defective in NHEJ. Moreover, it will be necessary to investigate whether complex disassembly is a consequence of the phosphorylation of DNA-PKcs, Ku70/80, LigIV and XRCC4 or if it is simply a consequence of the dissociation of the phosphorylated form of the catalytic subunit of DNA-PK. Next, it will be important to determine whether the phosphorylation of residues in Ku and LX, already known to be targets of DNA-PKcs, are responsible for the dissociation of the NHEJ complex. In particular, the interaction between LigIV phosphomimetic mutants at Thr 650, Ser 668 and Ser 672 and the Ku heterodimer should be examined both *in vitro* using recombinant proteins and *in vivo* using cells transfected with mutants.

Preliminary co-ip experiments reported in section 3.4.2 showed that Ku forms a complex with RPA, WRN, and PARP-1. The role of these Ku binding partners in NHEJ has not been established yet. Therefore, in order to investigate whether these proteins are required for NHEJ, analysis of γ-H2AX foci should be performed using cells that lack or are depleted for these factors. Next, to analyse if the interaction between these new potential NHEJ factors and Ku is induced by DNA damage, co-ip assays could be performed using cell extracts after treating the cells with DSBs inducing agents, such as bleomicin or ionizing radiation. In addition, novel quantitative mass spectrometry methods could be useful to quantify these interactions. The results obtained *in vitro* could also be confirmed *in vivo* by immunofluorescence or fluorescence resonance energy transfer (FRET) analysis in transfected cells.

A lot of efforts will be required in the future in order to completely elucidate the NHEJ pathway and to further characterise all the proteins involved.

ACKNOWLEDGEMENTS

I would like to sincerely thank my supervisor, Dr. Alessandro Vindingi, for his fundamental guidance and support throughout the time of my Ph.D..

I wish also to express a sincere thanks to my second supervisor, Prof. Penny Jeggo, for her valuable suggestions, irreplaceable discussions and to provide me many DNA plasmids and cell lines.

Thanks go to all the people in ICGEB who gave me kind help and above all to the members of the Proteomics Group, for their professional support and for having created a friendly and cheerful atmosphere in the lab. In particular, I would like to thank Daniele Arosio to whom I owe all my knowledge about biophysics. Raffaella Klima and Federico Odreman who helped me on my first steps in molecular biology. Cui Sheng for his scientific and everyday life advices. Lucia Andreoli for all the challenging discussions we had. Maria Elena Lopez for her kindness and help on growing all the cell lines. Caterina Marchetti for her advises on several experiments. Laura Muzzolini for her fundamental support and concrete help during the writing of this thesis.

I wish to express my gratitude to Dr. Patrizia Polverino de Laureto and Prof. Angelo Fontana who introduced me into scientific research.

A special thanks go to Marco for his comforting and reassuring trust in me, his patience and for being always close to me.

Finally, I wish to express a heartfelt thanks to my parents, my brother, Francesca, Lisa and my friends for always supporting me with their love.

BIBLIOGRAPHY

Adelfalk, C., Kontou, M., Hirsch-Kauffmann, M. and Schweiger, M. (2003) Physical and functional interaction of the Werner syndrome protein with poly-ADP ribosyl transferase. *FEBS Lett*, **554**, 55-58.

Ahnesorg, P., Smith, P. and Jackson, S.P. (2006) XLF interacts with the XRCC4-DNA ligase IV complex to promote DNA nonhomologous end-joining. *Cell*, **124**, 301-313.

Allen, C., Kurimasa, A., Brenneman, M.A., Chen, D.J. and Nickoloff, J.A. (2002) DNA-dependent protein kinase suppresses double-strand break-induced and spontaneous homologous recombination. *Proc Natl Acad Sci U S A*, **99**, 3758-3763.

Ame, J.C., Spenlehauer, C. and de Murcia, G. (2004) The PARP superfamily. *Bioessays*, **26**, 882-893.

Anderson, C.F. and Record, M.T., Jr. (1995) Salt-nucleic acid interactions. *Annu Rev Phys Chem*, **46**, 657-700.

Anderson, C.F., Record, M.T., Jr. and Hart, P.A. (1978) Sodium-23 NMR studies of cation-DNA interactions. *Biophys Chem*, **7**, 301-316.

Anderson, C.W. and Carter, T.H. (1996) The DNA-activated protein kinase-DNA-PK. In Jessberger, R. and Lieber, M.R. (eds.), *Molecular analysis of DNA rearrangements in the immune system.*, Springer-Verlag, Heidelberg, Germany, pp. 91-112.

Anderson, C.W., Dunn, J.J., Freimuth, P.I., Galloway, A.M. and Allalunis-Turner, M.J. (2001) Frameshift mutation in PRKDC, the gene for DNA-PKcs, in the DNA repair-defective, human, glioma-derived cell line M059J. *Radiat Res*, **156**, 2-9.

Anderson, C.W. and Lees-Miller, S.P. (1992) The nuclear serine/threonine protein kinase DNA-PK. *Crit Rev Eukaryot Gene Expr*, **2**, 283-314.

Aravind, L. and Koonin, E.V. (2001) Prokaryotic homologs of the eukaryotic DNA-end-binding protein Ku, novel domains in the Ku protein and prediction of a prokaryotic double-strand break repair system. *Genome Res*, **11**, 1365-1374.

Arosio, D., Costantini, S., Kong, Y. and Vindigni, A. (2004) Fluorescence anisotropy studies on the Ku-DNA interaction: anion and cation effects. *J Biol Chem*, **279**, 42826-42835.

Arosio, D., Cui, S., Ortega, C., Chovanec, M., Di Marco, S., Baldini, G., Falaschi, A. and Vindigni, A. (2002) Studies on the mode of Ku interaction with DNA. *J Biol Chem*, **277**, 9741-9748.

Ausubel, F.M., Brent, R., Kingston, R.E., Moore D.D., Seidman, J.G., Smith, J.A., Struhl, K. (1994) *Current Protocols in Molecular Biology*. John Wiley & Sons, Inc., USA.

Bachrati, C.Z. and Hickson, I.D. (2003) RecQ helicases: suppressors of tumorigenesis and premature aging. *Biochem J*, **374**, 577-606.

Badie, C., Goodhardt, M., Waugh, A., Doyen, N., Foray, N., Calsou, P., Singleton, B., Gell, D., Salles, B., Jeggo, P., Arlett, C.F. and Malaise, E.P. (1997) A DNA double-strand break defective fibroblast cell line (180BR) derived from a radiosensitive patient represents a new mutant phenotype. *Cancer Res*, **57**, 4600-4607.

Barnes, D.E., Stamp, G., Rosewell, I., Denzel, A. and Lindahl, T. (1998) Targeted disruption of the gene encoding DNA ligase IV leads to lethality in embryonic mice. *Curr Biol*, **8**, 1395-1398.

Bassing, C.H. and Alt, F.W. (2004) The cellular response to general and programmed DNA double strand breaks. *DNA Repair (Amst)*, **3**, 781-796.

Bassing, C.H., Chua, K.F., Sekiguchi, J., Suh, H., Whitlow, S.R., Fleming, J.C., Monroe, B.C., Ciccone, D.N., Yan, C., Vlasakova, K., Livingston, D.M., Ferguson, D.O., Scully, R. and Alt, F.W. (2002) Increased ionizing radiation sensitivity and genomic instability in the absence of histone H2AX. *Proc Natl Acad Sci U S A*, **99**, 8173-8178.

Baumann, P. and West, S.C. (1998) DNA end-joining catalyzed by human cell-free extracts. *Proc Natl Acad Sci U S A*, **95**, 14066-14070.

Bekker-Jensen, S., Lukas, C., Melander, F., Bartek, J. and Lukas, J. (2005) Dynamic assembly and sustained retention of 53BP1 at the sites of DNA damage are controlled by Mdc1/NFBD1. *J Cell Biol*, **170**, 201-211.

Belli, M., Sapora, O. and Tabocchini, M.A. (2002) Molecular targets in cellular response to ionizing radiation and implications in space radiation protection. *J Radiat Res (Tokyo)*, **43 Suppl**, S13-19.

Binz, S.K., Sheehan, A.M. and Wold, M.S. (2004) Replication protein A phosphorylation and the cellular response to DNA damage. *DNA Repair (Amst)*, **3**, 1015-1024.

Blier, P.R., Griffith, A.J., Craft, J. and Hardin, J.A. (1993) Binding of Ku protein to DNA. Measurement of affinity for ends and demonstration of binding to nicks. *J Biol Chem*, **268**, 7594-7601.

Block, W.D., Yu, Y., Merkle, D., Gifford, J.L., Ding, Q., Meek, K. and Lees-Miller, S.P. (2004) Autophosphorylation-dependent remodeling of the DNA-dependent protein kinase catalytic subunit regulates ligation of DNA ends. *Nucleic Acids Res*, **32**, 4351-4357.

Boskovic, J., Rivera-Calzada, A., Maman, J.D., Chacon, P., Willison, K.R., Pearl, L.H. and Llorca, O. (2003) Visualization of DNA-induced conformational changes in the DNA repair kinase DNA-PKcs. *Embo J*, **22**, 5875-5882.

Bosotti, R., Isacchi, A. and Sonnhammer, E.L. (2000) FAT: a novel domain in PIK-related kinases. *Trends Biochem Sci*, **25**, 225-227.

Brewerton, S.C., Dore, A.S., Drake, A.C., Leuther, K.K. and Blundell, T.L. (2004) Structural analysis of DNA-PKcs: modelling of the repeat units and insights into the detailed molecular architecture. *J Struct Biol*, **145**, 295-306.

Bryans, M., Valenzano, M.C. and Stamato, T.D. (1999) Absence of DNA ligase IV protein in XR-1 cells: evidence for stabilization by XRCC4. *Mutat Res*, **433**, 53-58.

Buck, D., Malivert, L., de Chasseval, R., Barraud, A., Fondaneche, M.C., Sanal, O., Plebani, A., Stephan, J.L., Hufnagel, M., le Deist, F., Fischer, A., Durandy, A., de Villartay, J.P. and Revy, P. (2006) Cernunnos, a novel nonhomologous end-joining factor, is mutated in human immunodeficiency with microcephaly. *Cell*, **124**, 287-299.

Bujalowski, W. and Lohman, T.M. (1987) Limited co-operativity in protein-nucleic acid interactions. A thermodynamic model for the interactions of Escherichia coli single strand binding protein with single-stranded nucleic acids in the "beaded", (SSB)65 mode. *J Mol Biol*, **195**, 897-907.

Bujalowski, W. and Lohman, T.M. (1989) Negative co-operativity in Escherichia coli single strand binding protein-oligonucleotide interactions. II. Salt, temperature and oligonucleotide length effects. *J Mol Biol*, **207**, 269-288.

Bujalowski, W., Lohman, T.M. and Anderson, C.F. (1989) On the cooperative binding of large ligands to a one-dimensional homogeneous lattice: the generalized three-state lattice model. *Biopolymers*, **28**, 1637-1643.

Burkle, A. (2001) PARP-1: a regulator of genomic stability linked with mammalian longevity. *Chembiochem*, **2**, 725-728.

Burma, S., Chen, B.P., Murphy, M., Kurimasa, A. and Chen, D.J. (2001) ATM phosphorylates histone H2AX in response to DNA double-strand breaks. *J Biol Chem*, **276**, 42462-42467.

Cai, Q.Q., Plet, A., Imbert, J., Lafage-Pochitaloff, M., Cerdan, C. and Blanchard, J.M. (1994) Chromosomal location and expression of the genes coding for Ku p70 and p80 in human cell lines and normal tissues. *Cytogenet Cell Genet*, **65**, 221-227.

Calsou, P., Delteil, C., Frit, P., Drouet, J. and Salles, B. (2003) Coordinated assembly of Ku and p460 subunits of the DNA-dependent protein kinase on DNA ends is necessary for XRCC4-ligase IV recruitment. *J Mol Biol*, **326**, 93-103.

Cary, R.B., Peterson, S.R., Wang, J., Bear, D.G., Bradbury, E.M. and Chen, D.J. (1997) DNA looping by Ku and the DNA-dependent protein kinase. *Proc Natl Acad Sci U S A*, **94**, 4267-4272.

Celeste, A., Petersen, S., Romanienko, P.J., Fernandez-Capetillo, O., Chen, H.T., Sedelnikova, O.A., Reina-San-Martin, B., Coppola, V., Meffre, E., Difilippantonio, M.J., Redon, C., Pilch, D.R., Olaru, A., Eckhaus, M., Camerini-Otero, R.D., Tessarollo, L., Livak, F., Manova, K., Bonner, W.M., Nussenzweig, M.C. and Nussenzweig, A. (2002) Genomic instability in mice lacking histone H2AX. *Science*, **296**, 922-927.

Chan, D.W., Chen, B.P., Prithivirajsingh, S., Kurimasa, A., Story, M.D., Qin, J. and Chen, D.J. (2002) Autophosphorylation of the DNA-dependent protein kinase catalytic subunit is required for rejoining of DNA double-strand breaks. *Genes Dev*, **16**, 2333-2338.

Chan, D.W. and Lees-Miller, S.P. (1996) The DNA-dependent protein kinase is inactivated by autophosphorylation of the catalytic subunit. *J Biol Chem*, **271**, 8936-8941.

Chan, D.W., Ye, R., Veillette, C.J. and Lees-Miller, S.P. (1999) DNA-dependent protein kinase phosphorylation sites in Ku 70/80 heterodimer. *Biochemistry*, **38**, 1819-1828.

Chappell, C., Hanakahi, L.A., Karimi-Busheri, F., Weinfeld, M. and West, S.C. (2002) Involvement of human polynucleotide kinase in double-strand break repair by non-homologous end joining. *Embo J*, **21**, 2827-2832.

Chen, L., Trujillo, K., Sung, P. and Tomkinson, A.E. (2000) Interactions of the DNA ligase IV-XRCC4 complex with DNA ends and the DNA-dependent protein kinase. *J Biol Chem*, **275**, 26196-26205.

Chernikova, S.B., Wells, R.L. and Elkind, M.M. (1999) Wortmannin sensitizes mammalian cells to radiation by inhibiting the DNA-dependent protein kinase-mediated rejoining of double-strand breaks. *Radiat Res*, **151**, 159-166.

Chou, C.H., Wang, J., Knuth, M.W. and Reeves, W.H. (1992) Role of a major autoepitope in forming the DNA binding site of the p70 (Ku) antigen. *J Exp Med*, **175**, 1677-1684.

Convery, E., Shin, E.K., Ding, Q., Wang, W., Douglas, P., Davis, L.S., Nickoloff, J.A., Lees-Miller, S.P. and Meek, K. (2005) Inhibition of homologous recombination by variants of the catalytic subunit of the DNA-dependent protein kinase (DNA-PKcs). *Proc Natl Acad Sci U S A*, **102**, 1345-1350.

Cooper, M.P., Machwe, A., Orren, D.K., Brosh, R.M., Ramsden, D. and Bohr, V.A. (2000) Ku complex interacts with and stimulates the Werner protein. *Genes Dev*, **14**, 907-912.

Critchlow, S.E., Bowater, R.P. and Jackson, S.P. (1997) Mammalian DNA double-strand break repair protein XRCC4 interacts with DNA ligase IV. *Curr Biol*, **7**, 588-598.

Cui, X., Yu, Y., Gupta, S., Cho, Y.M., Lees-Miller, S.P. and Meek, K. (2005) Autophosphorylation of DNA-dependent protein kinase regulates DNA end processing and may also alter double-strand break repair pathway choice. *Mol Cell Biol*, **25**, 10842-10852.

d'Adda di Fagagna, F., Hande, M.P., Tong, W.M., Roth, D., Lansdorp, P.M., Wang, Z.Q. and Jackson, S.P. (2001) Effects of DNA nonhomologous end-joining factors on telomere length and chromosomal stability in mammalian cells. *Curr Biol*, **11**, 1192-1196.

d'Adda di Fagagna, F., Teo, S.H. and Jackson, S.P. (2004) Functional links between telomeres and proteins of the DNA-damage response. *Genes Dev*, **18**, 1781-1799.

de Murcia, G. and Menissier de Murcia, J. (1994) Poly(ADP-ribose) polymerase: a molecular nick-sensor. *Trends Biochem Sci*, **19**, 172-176.

de Vries, E., van Driel, W., Bergsma, W.G., Arnberg, A.C. and van der Vliet, P.C. (1989) HeLa nuclear protein recognizing DNA termini and translocating on DNA forming a regular DNA-multimeric protein complex. *J Mol Biol*, **208**, 65-78.

DeFazio, L.G., Stansel, R.M., Griffith, J.D. and Chu, G. (2002) Synapsis of DNA ends by DNA-dependent protein kinase. *Embo J*, **21**, 3192-3200.

Di Cera, E. and Kong, Y. (1996) Theory of multivalent binding in one and two-dimensional lattices. *Biophysical Chemistry*, **61**, 107-124.

Ding, Q., Reddy, Y.V., Wang, W., Woods, T., Douglas, P., Ramsden, D.A., Lees-Miller, S.P. and Meek, K. (2003) Autophosphorylation of the catalytic subunit of the DNA-dependent protein kinase is required for efficient end processing during DNA double-strand break repair. *Mol Cell Biol*, **23**, 5836-5848.

Dore, A.S., Furnham, N., Davies, O.R., Sibanda, B.L., Chirgadze, D.Y., Jackson, S.P., Pellegrini, L. and Blundell, T.L. (2006) Structure of an Xrcc4-DNA ligase IV yeast ortholog complex reveals a novel BRCT interaction mode. *DNA Repair (Amst)*, **5**, 362-368.

Dou, S.X., Wang, P.Y., Xu, H.Q. and Xi, X.G. (2004) The DNA binding properties of the Escherichia coli RecQ helicase. *J Biol Chem*, **279**, 6354-6363.

Douglas, P., Gupta, S., Morrice, N., Meek, K. and Lees-Miller, S.P. (2005) DNA-PK-dependent phosphorylation of Ku70/80 is not required for non-homologous end joining. *DNA Repair (Amst)*, **4**, 1006-1018.

Douglas, P., Sapkota, G.P., Morrice, N., Yu, Y., Goodarzi, A.A., Merkle, D., Meek, K., Alessi, D.R. and Lees-Miller, S.P. (2002) Identification of in vitro and in vivo phosphorylation sites in the catalytic subunit of the DNA-dependent protein kinase. *Biochem J*, **368**, 243-251.

Dragan, A.I., Klass, J., Read, C., Churchill, M.E., Crane-Robinson, C. and Privalov, P.L. (2003) DNA binding of a non-sequence-specific HMG-D protein is entropy driven with a substantial non-electrostatic contribution. *J Mol Biol*, **331**, 795-813.

Dudas, A. and Chovanec, M. (2004) DNA double-strand break repair by homologous recombination. *Mutat Res*, **566**, 131-167.

Dvir, A., Peterson, S.R., Knuth, M.W., Lu, H. and Dynan, W.S. (1992) Ku autoantigen is the regulatory component of a template-associated protein kinase that phosphorylates RNA polymerase II. *Proc Natl Acad Sci U S A*, **89**, 11920-11924.

Dynan, W.S. and Yoo, S. (1998) Interaction of Ku protein and DNA-dependent protein kinase catalytic subunit with nucleic acids. *Nucleic Acids Res*, **26**, 1551-1559.

Errami, A., Smider, V., Rathmell, W.K., He, D.M., Hendrickson, E.A., Zdzienicka, M.Z. and Chu, G. (1996) Ku86 defines the genetic defect and restores X-ray resistance and V(D)J recombination to complementation group 5 hamster cell mutants. *Mol Cell Biol*, **16**, 1519-1526.

Espejel, S., Franco, S., Sgura, A., Gae, D., Bailey, S.M., Taccioli, G.E. and Blasco, M.A. (2002) Functional interaction between DNA-PKcs and telomerase in telomere length maintenance. *Embo J*, **21**, 6275-6287.

Falzon, M., Fewell, J.W. and Kuff, E.L. (1993) EBP-80, a transcription factor closely resembling the human autoantigen Ku, recognizes single- to double-strand transitions in DNA. *J Biol Chem*, **268**, 10546-10552.

Ferguson, D.O. and Alt, F.W. (2001) DNA double strand break repair and chromosomal translocation: lessons from animal models. *Oncogene*, **20**, 5572-5579.

Fernandez-Capetillo, O., Lee, A., Nussenzweig, M. and Nussenzweig, A. (2004) H2AX: the histone guardian of the genome. *DNA Repair (Amst)*, **3**, 959-967.

Ferrari, M.E., Bujalowski, W. and Lohman, T.M. (1994) Co-operative binding of Escherichia coli SSB tetramers to single-stranded DNA in the (SSB)35 binding mode. *J Mol Biol*, **236**, 106-123.

Finnie, N.J., Gottlieb, T.M., Blunt, T., Jeggo, P.A. and Jackson, S.P. (1995) DNA-dependent protein kinase activity is absent in xrs-6 cells: implications for site-specific recombination and DNA double-strand break repair. *Proc Natl Acad Sci U S A*, **92**, 320-324.

Frank, K.M., Sekiguchi, J.M., Seidl, K.J., Swat, W., Rathbun, G.A., Cheng, H.L., Davidson, L., Kangaloo, L. and Alt, F.W. (1998) Late embryonic lethality and impaired V(D)J recombination in mice lacking DNA ligase IV. *Nature*, **396**, 173-177.

Friedman, R.A. and Manning, G.S. (1984) Polyelectrolyte effects on site-binding equilibria with application to the intercalation of drugs into DNA. *Biopolymers*, **23**, 2671-2714.

Fujimori, A., Araki, R., Fukumura, R., Ohhata, T., Takahashi, H., Kawahara, A., Tatsumi, K. and Abe, M. (2000) Identification of four highly conserved regions in DNA-PKcs. *Immunogenetics*, **51**, 965-973.

Gao, Y., Sun, Y., Frank, K.M., Dikkes, P., Fujiwara, Y., Seidl, K.J., Sekiguchi, J.M., Rathbun, G.A., Swat, W., Wang, J., Bronson, R.T., Malynn, B.A., Bryans, M., Zhu, C., Chaudhuri, J., Davidson, L., Ferrini, R., Stamato, T., Orkin, S.H., Greenberg, M.E. and Alt, F.W. (1998) A critical role for DNA end-joining proteins in both lymphogenesis and neurogenesis. *Cell*, **95**, 891-902.

Gell, D. and Jackson, S.P. (1999) Mapping of protein-protein interactions within the DNA-dependent protein kinase complex. *Nucleic Acids Res*, **27**, 3494-3502.

Getts, R.C. and Stamato, T.D. (1994) Absence of a Ku-like DNA end binding activity in the xrs double-strand DNA repair-deficient mutant. *J Biol Chem*, **269**, 15981-15984.

Gilley, D., Tanaka, H., Hande, M.P., Kurimasa, A., Li, G.C., Oshimura, M. and Chen, D.J. (2001) DNA-PKcs is critical for telomere capping. *Proc Natl Acad Sci U S A*, **98**, 15084-15088.

Girard, P.M., Kysela, B., Harer, C.J., Doherty, A.J. and Jeggo, P.A. (2004) Analysis of DNA ligase IV mutations found in LIG4 syndrome patients: the impact of two linked polymorphisms. *Hum Mol Genet*, **13**, 2369-2376.

Gottlieb, T.M. and Jackson, S.P. (1993) The DNA-dependent protein kinase: requirement for DNA ends and association with Ku antigen. *Cell*, **72**, 131-142.

Grawunder, U., Wilm, M., Wu, X., Kulesza, P., Wilson, T.E., Mann, M. and Lieber, M.R. (1997) Activity of DNA ligase IV stimulated by complex formation with XRCC4 protein in mammalian cells. *Nature*, **388**, 492-495.

Grawunder, U., Zimmer, D., Fugmann, S., Schwarz, K. and Lieber, M.R. (1998a) DNA ligase IV is essential for V(D)J recombination and DNA double-strand break repair in human precursor lymphocytes. *Mol Cell*, **2**, 477-484.

Grawunder, U., Zimmer, D., Kulesza, P. and Lieber, M.R. (1998b) Requirement for an interaction of XRCC4 with DNA ligase IV for wild-type V(D)J recombination and DNA double-strand break repair in vivo. *J Biol Chem*, **273**, 24708-24714.

Grawunder, U., Zimmer, D. and Leiber, M.R. (1998c) DNA ligase IV binds to XRCC4 via a motif located between rather than within its BRCT domains. *Curr Biol*, **8**, 873-876.

Griffith, A.J., Blier, P.R., Mimori, T. and Hardin, J.A. (1992) Ku polypeptides synthesized in vitro assemble into complexes which recognize ends of double-stranded DNA. *J Biol Chem*, **267**, 331-338.

Griffith, J.D., Lindsey-Boltz, L.A. and Sancar, A. (2002) Structures of the human Rad17-replication factor C and checkpoint Rad 9-1-1 complexes visualized by glycerol spray/low voltage microscopy. *J Biol Chem*, **277**, 15233-15236.

Gu, Y., Jin, S., Gao, Y., Weaver, D.T. and Alt, F.W. (1997) Ku70-deficient embryonic stem cells have increased ionizing radiosensitivity, defective DNA end-binding activity, and inability to support V(D)J recombination. *Proc Natl Acad Sci U S A*, **94**, 8076-8081.

Gupta, S. and Meek, K. (2005) The leucine rich region of DNA-PKcs contributes to its innate DNA affinity. *Nucleic Acids Res*, **33**, 6972-6981.

Ha, J.H., Capp, M.W., Hohenwalter, M.D., Baskerville, M. and Record, M.T., Jr. (1992) Thermodynamic stoichiometries of participation of water, cations and anions in specific and non-specific binding of lac repressor to DNA. Possible thermodynamic origins of the "glutamate effect" on protein-DNA interactions. *J Mol Biol*, **228**, 252-264.

Hammarsten, O. and Chu, G. (1998) DNA-dependent protein kinase: DNA binding and activation in the absence of Ku. *Proc Natl Acad Sci U S A*, **95**, 525-530.

Han, Z., Johnston, C., Reeves, W.H., Carter, T., Wyche, J.H. and Hendrickson, E.A. (1996) Characterization of a Ku86 variant protein that results in altered DNA binding and diminished DNA-dependent protein kinase activity. *J Biol Chem*, **271**, 14098-14104.

Hanakahi, L.A., Bartlet-Jones, M., Chappell, C., Pappin, D. and West, S.C. (2000) Binding of inositol phosphate to DNA-PK and stimulation of double-strand break repair. *Cell*, **102**, 721-729.

Hanakahi, L.A. and West, S.C. (2002) Specific interaction of IP6 with human Ku70/80, the DNA-binding subunit of DNA-PK. *Embo J*, **21**, 2038-2044.

Harris, R., Esposito, D., Sankar, A., Maman, J.D., Hinks, J.A., Pearl, L.H. and Driscoll, P.C. (2004) The 3D solution structure of the C-terminal region of Ku86 (Ku86CTR). *J Mol Biol*, **335**, 573-582.

Hartley, K.O., Gell, D., Smith, G.C., Zhang, H., Divecha, N., Connelly, M.A., Admon, A., Lees-Miller, S.P., Anderson, C.W. and Jackson, S.P. (1995) DNA-dependent protein kinase catalytic subunit: a relative of phosphatidylinositol 3-kinase and the ataxia telangiectasia gene product. *Cell*, **82**, 849-856.

Hefferin, M.L. and Tomkinson, A.E. (2005) Mechanism of DNA double-strand break repair by non-homologous end joining. *DNA Repair (Amst)*, **4**, 639-648.

Henricksen, L.A., Umbricht, C.B. and Wold, M.S. (1994) Recombinant replication protein A: expression, complex formation, and functional characterization. *J Biol Chem*, **269**, 11121-11132.

Hickson, I.D. (2003) RecQ helicases: caretakers of the genome. *Nat Rev Cancer*, **3**, 169-178.

Hoeijmakers, J.H. (2001) Genome maintenance mechanisms for preventing cancer. *Nature*, **411**, 366-374.

Hoppe, B.S., Jensen, R.B. and Kirchgessner, C.U. (2000) Complementation of the radiosensitive M059J cell line. *Radiat Res*, **153**, 125-130.

Hsu, H.L., Gilley, D., Blackburn, E.H. and Chen, D.J. (1999) Ku is associated with the telomere in mammals. *Proc Natl Acad Sci U S A*, **96**, 12454-12458.

Hsu, H.L., Yannone, S.M. and Chen, D.J. (2002) Defining interactions between DNA-PK and ligase IV/XRCC4. *DNA Repair (Amst)*, **1**, 225-235.

Huang, J. and Dynan, W.S. (2002) Reconstitution of the mammalian DNA double-strand break end-joining reaction reveals a requirement for an Mre11/Rad50/NBS1-containing fraction. *Nucleic Acids Res*, **30**, 667-674.

Hunter, T. (1995) When is a lipid kinase not a lipid kinase? When it is a protein kinase. *Cell*, **83**, 1-4.

Iliakis, G., Wang, Y., Guan, J. and Wang, H. (2003) DNA damage checkpoint control in cells exposed to ionizing radiation. *Oncogene*, **22**, 5834-5847.

Inamdar, K.V., Pouliot, J.J., Zhou, T., Lees-Miller, S.P., Rasouli-Nia, A. and Povirk, L.F. (2002) Conversion of phosphoglycolate to phosphate termini on 3' overhangs of DNA double strand breaks by the human tyrosyl-DNA phosphodiesterase hTdp1. *J Biol Chem*, **277**, 27162-27168.

Iwabuchi, K., Basu, B.P., Kysela, B., Kurihara, T., Shibata, M., Guan, D., Cao, Y., Hamada, T., Imamura, K., Jeggo, P.A., Date, T. and Doherty, A.J. (2003) Potential role for 53BP1 in DNA end-joining repair through direct interaction with DNA. *J Biol Chem*, **278**, 36487-36495.

Jackson, S.P. (2002) Sensing and repairing DNA double-strand breaks. *Carcinogenesis*, **23**, 687-696.

Jeggo, P. and O'Neill, P. (2002) The Greek Goddess, Artemis, reveals the secrets of her cleavage. *DNA Repair (Amst)*, **1**, 771-777.

Jeggo, P.A. (1998) DNA breakage and repair. *Adv Genet*, **38**, 185-218.

Jeggo, P.A., Tesmer, J. and Chen, D.J. (1991) Genetic analysis of ionising radiation sensitive mutants of cultured mammalian cell lines. *Mutat Res*, **254**, 125-133.

Jin, S., Kharbanda, S., Mayer, B., Kufe, D. and Weaver, D.T. (1997) Binding of Ku and c-Abl at the kinase homology region of DNA-dependent protein kinase catalytic subunit. *J Biol Chem*, **272**, 24763-24766.

Johnson, A. and O'Donnell, M. (2005) DNA ligase: getting a grip to seal the deal. *Curr Biol*, **15**, R90-92.

Junop, M.S., Modesti, M., Guarne, A., Ghirlando, R., Gellert, M. and Yang, W. (2000) Crystal structure of the Xrcc4 DNA repair protein and implications for end joining. *Embo J*, **19**, 5962-5970.

Karmakar, P., Piotrowski, J., Brosh, R.M., Jr., Sommers, J.A., Miller, S.P., Cheng, W.H., Snowden, C.M., Ramsden, D.A. and Bohr, V.A. (2002a) Werner protein is a target of DNA-dependent protein kinase in vivo and in vitro, and its catalytic activities are regulated by phosphorylation. *J Biol Chem*, **277**, 18291-18302.

Karmakar, P., Snowden, C.M., Ramsden, D.A. and Bohr, V.A. (2002b) Ku heterodimer binds to both ends of the Werner protein and functional interaction occurs at the Werner N-terminus. *Nucleic Acids Res*, **30**, 3583-3591.

Keeney, S. and Neale, M.J. (2006) Initiation of meiotic recombination by formation of DNA double-strand breaks: mechanism and regulation. *Biochem Soc Trans*, **34**, 523-525.

Khanna, K.K. and Jackson, S.P. (2001) DNA double-strand breaks: signaling, repair and the cancer connection. *Nat Genet*, **27**, 247-254.

Kienker, L.J., Shin, E.K. and Meek, K. (2000) Both V(D)J recombination and radioresistance require DNA-PK kinase activity, though minimal levels suffice for V(D)J recombination. *Nucleic Acids Res*, **28**, 2752-2761.

Koch, C.A., Agyei, R., Galicia, S., Metalnikov, P., O'Donnell, P., Starostine, A., Weinfeld, M. and Durocher, D. (2004) Xrcc4 physically links DNA end processing by polynucleotide kinase to DNA ligation by DNA ligase IV. *Embo J*, **23**, 3874-3885.

Koike, M. (2002) Dimerization, translocation and localization of Ku70 and Ku80 proteins. *J Radiat Res (Tokyo)*, **43**, 223-236.

Kong, Y. (2001) A simple method for evaluating partition functions of linear polymers. *J Phys Chem B*, **105**, 10111-10114.

Kowalczykowski, S.C., Lonberg, N., Newport, J.W. and von Hippel, P.H. (1981) Interactions of bacteriophage T4-coded gene 32 protein with nucleic acids. I. Characterization of the binding interactions. *J Mol Biol*, **145**, 75-104.

Kuil, M.E., van Amerongen, H., van der Vliet, P.C. and van Grondelle, R. (1989) Complex formation between the adenovirus DNA-binding protein and single-stranded poly(rA). Cooperativity and salt dependence. *Biochemistry*, **28**, 9795-9800.

Kurimasa, A., Kumano, S., Boubnov, N.V., Story, M.D., Tung, C.S., Peterson, S.R. and Chen, D.J. (1999) Requirement for the kinase activity of human DNA-dependent protein kinase catalytic subunit in DNA strand break rejoining. *Mol Cell Biol*, **19**, 3877-3884.

Kysela, B., Doherty, A.J., Chovanec, M., Stiff, T., Ameer-Beg, S.M., Vojnovic, B., Girard, P.M. and Jeggo, P.A. (2003) Ku stimulation of DNA ligase IV-dependent ligation requires inward movement along the DNA molecule. *J Biol Chem*, **278**, 22466-22474.

Laemmli, U.K. (1970) Cleavage of structural proteins during the assembly of the head of bacteriophage T4. *Nature*, **227**, 680-685.

Lai, J.S. and Herr, W. (1992) Ethidium bromide provides a simple tool for identifying genuine DNA-independent protein associations. *Proc Natl Acad Sci U S A*, **89**, 6958-6962.

Leber, R., Wise, T.W., Mizuta, R. and Meek, K. (1998) The XRCC4 gene product is a target for and interacts with the DNA-dependent protein kinase. *J Biol Chem*, **273**, 1794-1801.

Lee, K.J., Huang, J., Takeda, Y. and Dynan, W.S. (2000) DNA ligase IV and XRCC4 form a stable mixed tetramer that functions synergistically with other repair factors in a cell-free end-joining system. *J Biol Chem*, **275**, 34787-34796.

Lees-Miller, S.P., Godbout, R., Chan, D.W., Weinfeld, M., Day, R.S., 3rd, Barron, G.M. and Allalunis-Turner, J. (1995) Absence of p350 subunit of DNA-activated protein kinase from a radiosensitive human cell line. *Science*, **267**, 1183-1185.

Levy, N., Martz, A., Bresson, A., Spenlehauer, C., de Murcia, G. and Menissier-de Murcia, J. (2006) XRCC1 is phosphorylated by DNA-dependent protein kinase in response to DNA damage. *Nucleic Acids Res*, **34**, 32-41.

Li, B. and Comai, L. (2000) Functional interaction between Ku and the werner syndrome protein in DNA end processing. *J Biol Chem*, **275**, 28349-28352.

Li, B. and Comai, L. (2001) Requirements for the nucleolytic processing of DNA ends by the Werner syndrome protein-Ku70/80 complex. *J Biol Chem*, **276**, 9896-9902.

Li, B., Navarro, S., Kasahara, N. and Comai, L. (2004) Identification and biochemical characterization of a Werner's syndrome protein complex with Ku70/80 and poly(ADP-ribose) polymerase-1. *J Biol Chem*, **279**, 13659-13667.

Li, Z., Otevrel, T., Gao, Y., Cheng, H.L., Seed, B., Stamato, T.D., Taccioli, G.E. and Alt, F.W. (1995) The XRCC4 gene encodes a novel protein involved in DNA double-strand break repair and V(D)J recombination. *Cell*, **83**, 1079-1089.

Lieber, M.R., Ma, Y., Pannicke, U. and Schwarz, K. (2003) Mechanism and regulation of human non-homologous DNA end-joining. *Nat Rev Mol Cell Biol*, **4**, 712-720.

Lin, F.L., Sperle, K. and Sternberg, N. (1984) Model for homologous recombination during transfer of DNA into mouse L cells: role for DNA ends in the recombination process. *Mol Cell Biol*, **4**, 1020-1034.

Lindahl, T., Satoh, M.S., Poirier, G.G. and Klungland, A. (1995) Post-translational modification of poly(ADP-ribose) polymerase induced by DNA strand breaks. *Trends Biochem Sci*, **20**, 405-411.

Lohman, T.M. and Bujalowski, W. (1991) Thermodynamic methods for model-independent determination of equilibrium binding isotherms for protein-DNA interactions: spectroscopic approaches to monitor binding. *Methods Enzymol*, **208**, 258-290.

Lohman, T.M. and Mascotti, D.P. (1992) Thermodynamics of ligand-nucleic acid interactions. *Methods Enzymol*, **212**, 400-424.

Lohman, T.M., Overman, L.B., Ferrari, M.E. and Kozlov, A.G. (1996) A highly salt-dependent enthalpy change for Escherichia coli SSB protein-nucleic acid binding due to ion-protein interactions. *Biochemistry*, **35**, 5272-5279.

Ma, Y. and Lieber, M.R. (2001) DNA length-dependent cooperative interactions in the binding of Ku to DNA. *Biochemistry*, **40**, 9638-9646.

Ma, Y. and Lieber, M.R. (2002) Binding of inositol hexakisphosphate (IP6) to Ku but not to DNA-PKcs. *J Biol Chem*, **277**, 10756-10759.

Ma, Y., Lu, H., Tippin, B., Goodman, M.F., Shimazaki, N., Koiwai, O., Hsieh, C.L., Schwarz, K. and Lieber, M.R. (2004) A biochemically defined system for mammalian nonhomologous DNA end joining. *Mol Cell*, **16**, 701-713.

Ma, Y., Pannicke, U., Schwarz, K. and Lieber, M.R. (2002) Hairpin opening and overhang processing by an Artemis/DNA-dependent protein kinase complex in nonhomologous end joining and V(D)J recombination. *Cell*, **108**, 781-794.

Mahajan, K.N., Gangi-Peterson, L., Sorscher, D.H., Wang, J., Gathy, K.N., Mahajan, N.P., Reeves, W.H. and Mitchell, B.S. (1999) Association of terminal deoxynucleotidyl transferase with Ku. *Proc Natl Acad Sci U S A*, **96**, 13926-13931.

Mahajan, K.N., Nick McElhinny, S.A., Mitchell, B.S. and Ramsden, D.A. (2002) Association of DNA polymerase mu (pol mu) with Ku and ligase IV: role for pol mu in end-joining double-strand break repair. *Mol Cell Biol*, **22**, 5194-5202.

Marchetti, C., Walker, S.A., Odreman, F., Vindigni, A., Doherty, A.J. and Jeggo, P. (2006) Identification of a novel motif in DNA ligases exemplified by DNA ligase IV. *DNA Repair (Amst)*, **5**, 788-798.

Martin, I.V. and MacNeill, S.A. (2002) ATP-dependent DNA ligases. *Genome Biol*, **3**, REVIEWS3005.

Maryon, E. and Carroll, D. (1991) Characterization of recombination intermediates from DNA injected into Xenopus laevis oocytes: evidence for a nonconservative mechanism of homologous recombination. *Mol Cell Biol*, **11**, 3278-3287.

Mathieu, N., Pirzio, L., Freulet-Marriere, M.A., Desmaze, C. and Sabatier, L. (2004) Telomeres and chromosomal instability. *Cell Mol Life Sci*, **61**, 641-656.

McGhee, J.D. and von Hippel, P.H. (1974) Theoretical aspects of DNA-protein interactions: co-operative and non-co-operative binding of large ligands to a one-dimensional homogeneous lattice. *J Mol Biol*, **86**, 469-489.

Menetski, J.P. and Kowalczykowski, S.C. (1985) Interaction of recA protein with single-stranded DNA. Quantitative aspects of binding affinity modulation by nucleotide cofactors. *J Mol Biol*, **181**, 281-295.

Merkle, D., Douglas, P., Moorhead, G.B., Leonenko, Z., Yu, Y., Cramb, D., Bazett-Jones, D.P. and Lees-Miller, S.P. (2002) The DNA-dependent protein kinase interacts with DNA to form a protein-DNA complex that is disrupted by phosphorylation. *Biochemistry*, **41**, 12706-12714.

Mickelsen, S., Snyder, C., Trujillo, K., Bogue, M., Roth, D.B. and Meek, K. (1999) Modulation of terminal deoxynucleotidyltransferase activity by the DNA-dependent protein kinase. *J Immunol*, **163**, 834-843.

Mimori, T., Akizuki, M., Yamagata, H., Inada, S., Yoshida, S. and Homma, M. (1981) Characterization of a high molecular weight acidic nuclear protein recognized by autoantibodies in sera from patients with polymyositis-scleroderma overlap. *J Clin Invest*, **68**, 611-620.

Mimori, T. and Hardin, J.A. (1986) Mechanism of interaction between Ku protein and DNA. *J Biol Chem*, **261**, 10375-10379.

Mimori, T., Hardin, J.A. and Steitz, J.A. (1986) Characterization of the DNA-binding protein antigen Ku recognized by autoantibodies from patients with rheumatic disorders. *J Biol Chem*, **261**, 2274-2278.

Mizuta, R., Cheng, H.L., Gao, Y. and Alt, F.W. (1997) Molecular genetic characterization of XRCC4 function. *Int Immunol*, **9**, 1607-1613.

Mochan, T.A., Venere, M., DiTullio, R.A., Jr. and Halazonetis, T.D. (2004) 53BP1, an activator of ATM in response to DNA damage. *DNA Repair (Amst)*, **3**, 945-952.

Modesti, M., Hesse, J.E. and Gellert, M. (1999) DNA binding of Xrcc4 protein is associated with V(D)J recombination but not with stimulation of DNA ligase IV activity. *Embo J*, **18**, 2008-2018.

Modesti, M., Junop, M.S., Ghirlando, R., van de Rakt, M., Gellert, M., Yang, W. and Kanaar, R. (2003) Tetramerization and DNA ligase IV interaction of the DNA double-strand break repair protein XRCC4 are mutually exclusive. *J Mol Biol*, **334**, 215-228.

Morales, J.C., Xia, Z., Lu, T., Aldrich, M.B., Wang, B., Rosales, C., Kellems, R.E., Hittelman, W.N., Elledge, S.J. and Carpenter, P.B. (2003) Role for the BRCA1 C-terminal repeats (BRCT) protein 53BP1 in maintaining genomic stability. *J Biol Chem*, **278**, 14971-14977.

Morrison, C., Smith, G.C., Stingl, L., Jackson, S.P., Wagner, E.F. and Wang, Z.Q. (1997) Genetic interaction between PARP and DNA-PK in V(D)J recombination and tumorigenesis. *Nat Genet*, **17**, 479-482.

Moshous, D., Callebaut, I., de Chasseval, R., Corneo, B., Cavazzana-Calvo, M., Le Deist, F., Tezcan, I., Sanal, O., Bertrand, Y., Philippe, N., Fischer, A. and de Villartay, J.P. (2001) Artemis, a novel DNA double-strand break repair/V(D)J recombination protein, is mutated in human severe combined immune deficiency. *Cell*, **105**, 177-186.

Muller, C. and Salles, B. (1997) Regulation of DNA-dependent protein kinase activity in leukemic cells. *Oncogene*, **15**, 2343-2348.

Nakamura, K., Sakai, W., Kawamoto, T., Bree, R.T., Lowndes, N.F., Takeda, S. and Taniguchi, Y. (2006) Genetic dissection of vertebrate 53BP1: a major role in non-homologous end joining of DNA double strand breaks. *DNA Repair (Amst)*, **5**, 741-749.

Nick McElhinny, S.A., Havener, J.M., Garcia-Diaz, M., Juarez, R., Bebenek, K., Kee, B.L., Blanco, L., Kunkel, T.A. and Ramsden, D.A. (2005) A gradient of template dependence defines distinct biological roles for family X polymerases in nonhomologous end joining. *Mol Cell*, **19**, 357-366.

Nick McElhinny, S.A., Snowden, C.M., McCarville, J. and Ramsden, D.A. (2000) Ku recruits the XRCC4-ligase IV complex to DNA ends. *Mol Cell Biol*, **20**, 2996-3003.

Niida, H. and Nakanishi, M. (2006) DNA damage checkpoints in mammals. *Mutagenesis*, **21**, 3-9.

Nussenzweig, A., Chen, C., da Costa Soares, V., Sanchez, M., Sokol, K., Nussenzweig, M.C. and Li, G.C. (1996) Requirement for Ku80 in growth and immunoglobulin V(D)J recombination. *Nature*, **382**, 551-555.

O'Driscoll, M., Cerosaletti, K.M., Girard, P.M., Dai, Y., Stumm, M., Kysela, B., Hirsch, B., Gennery, A., Palmer, S.E., Seidel, J., Gatti, R.A., Varon, R., Oettinger, M.A., Neitzel, H., Jeggo, P.A. and Concannon, P. (2001) DNA ligase IV mutations identified in patients exhibiting developmental delay and immunodeficiency. *Mol Cell*, **8**, 1175-1185.

O'Driscoll, M. and Jeggo, P. (2002) Immunological disorders and DNA repair. *Mutat Res*, **509**, 109-126.

O'Driscoll, M. and Jeggo, P.A. (2006) The role of double-strand break repair - insights from human genetics. *Nat Rev Genet*, **7**, 45-54.

Ono, M., Tucker, P.W. and Capra, J.D. (1994) Production and characterization of recombinant human Ku antigen. *Nucleic Acids Res*, **22**, 3918-3924.

Orren, D.K., Machwe, A., Karmakar, P., Piotrowski, J., Cooper, M.P. and Bohr, V.A. (2001) A functional interaction of Ku with Werner exonuclease facilitates digestion of damaged DNA. *Nucleic Acids Res*, **29**, 1926-1934.

Overman, L.B., Bujalowski, W. and Lohman, T.M. (1988) Equilibrium binding of Escherichia coli single-strand binding protein to single-stranded nucleic acids in the (SSB)65 binding mode. Cation and anion effects and polynucleotide specificity. *Biochemistry*, **27**, 456-471.

Overman, L.B. and Lohman, T.M. (1994) Linkage of pH, anion and cation effects in protein-nucleic acid equilibria. Escherichia coli SSB protein-single stranded nucleic acid interactions. *J Mol Biol*, **236**, 165-178.

Paillard, S. and Strauss, F. (1991) Analysis of the mechanism of interaction of simian Ku protein with DNA. *Nucleic Acids Res*, **19**, 5619-5624.

Pang, D., Yoo, S., Dynan, W.S., Jung, M. and Dritschilo, A. (1997) Ku proteins join DNA fragments as shown by atomic force microscopy. *Cancer Res*, **57**, 1412-1415.

Pascal, J.M., O'Brien, P.J., Tomkinson, A.E. and Ellenberger, T. (2004) Human DNA ligase I completely encircles and partially unwinds nicked DNA. *Nature*, **432**, 473-478.

Patel, G.a.J.N.C. (1995) The baculovirus expression system. In Glover, D.M.a.H., B.D. (ed.), *DNA cloning 2*, Vol. II, pp. 205-244.

Paull, T.T. and Gellert, M. (1998) The 3' to 5' exonuclease activity of Mre 11 facilitates repair of DNA double-strand breaks. *Mol Cell*, **1**, 969-979.

Paull, T.T., Rogakou, E.P., Yamazaki, V., Kirchgessner, C.U., Gellert, M. and Bonner, W.M. (2000) A critical role for histone H2AX in recruitment of repair factors to nuclear foci after DNA damage. *Curr Biol*, **10**, 886-895.

Pergola, F., Zdzienicka, M.Z. and Lieber, M.R. (1993) V(D)J recombination in mammalian cell mutants defective in DNA double-strand break repair. *Mol Cell Biol*, **13**, 3464-3471.

Perrault, R., Cheong, N., Wang, H. and Iliakis, G. (2001) RPA facilitates rejoining of DNA double-strand breaks in an in vitro assay utilizing genomic DNA as substrate. *Int J Radiat Biol*, **77**, 593-607.

Pfeiffer, P., Thode, S., Hancke, J. and Vielmetter, W. (1994) Mechanisms of overlap formation in nonhomologous DNA end joining. *Mol Cell Biol*, **14**, 888-895.

Poltoratsky, V.P., Shi, X., York, J.D., Lieber, M.R. and Carter, T.H. (1995) Human DNA-activated protein kinase (DNA-PK) is homologous to phosphatidylinositol kinases. *J Immunol*, **155**, 4529-4533.

Pouget, J.P. and Mather, S.J. (2001) General aspects of the cellular response to low- and high-LET radiation. *Eur J Nucl Med*, **28**, 541-561.

Povirk, L.F. (1996) DNA damage and mutagenesis by radiomimetic DNA-cleaving agents: bleomycin, neocarzinostatin and other enediynes. *Mutat Res*, **355**, 71-89.

Ramsden, D.A. and Gellert, M. (1998) Ku protein stimulates DNA end joining by mammalian DNA ligases: a direct role for Ku in repair of DNA double-strand breaks. *Embo J*, **17**, 609-614.

Rathmell, W.K. and Chu, G. (1994) A DNA end-binding factor involved in double-strand break repair and V(D)J recombination. *Mol Cell Biol*, **14**, 4741-4748.

Rebuzzini, P., Lisa, A., Giulotto, E. and Mondello, C. (2004) Chromosomal end-to-end fusions in immortalized mouse embryonic fibroblasts deficient in the DNA-dependent protein kinase catalytic subunit. *Cancer Lett*, **203**, 79-86.

Reddy, Y.V., Ding, Q., Lees-Miller, S.P., Meek, K. and Ramsden, D.A. (2004) Non-homologous end joining requires that the DNA-PK complex undergo an autophosphorylation-dependent rearrangement at DNA ends. *J Biol Chem*, **279**, 39408-39413.

Riballo, E., Critchlow, S.E., Teo, S.H., Doherty, A.J., Priestley, A., Broughton, B., Kysela, B., Beamish, H., Plowman, N., Arlett, C.F., Lehmann, A.R., Jackson, S.P. and Jeggo, P.A. (1999) Identification of a defect in DNA ligase IV in a radiosensitive leukaemia patient. *Curr Biol*, **9**, 699-702.

Riballo, E., Kuhne, M., Rief, N., Doherty, A., Smith, G.C., Recio, M.J., Reis, C., Dahm, K., Fricke, A., Krempler, A., Parker, A.R., Jackson, S.P., Gennery, A., Jeggo, P.A. and Lobrich, M. (2004) A pathway of double-strand break rejoining dependent upon ATM, Artemis, and proteins locating to gamma-H2AX foci. *Mol Cell*, **16**, 715-724.

Rich, T., Allen, R.L. and Wyllie, A.H. (2000) Defying death after DNA damage. *Nature*, **407**, 777-783.

Richardson, C. and Jasin, M. (2000a) Coupled homologous and nonhomologous repair of a double-strand break preserves genomic integrity in mammalian cells. *Mol Cell Biol*, **20**, 9068-9075.

Richardson, C. and Jasin, M. (2000b) Frequent chromosomal translocations induced by DNA double-strand breaks. *Nature*, **405**, 697-700.

Rivera-Calzada, A., Maman, J.D., Spagnolo, L., Pearl, L.H. and Llorca, O. (2005) Three-dimensional structure and regulation of the DNA-dependent protein kinase catalytic subunit (DNA-PKcs). *Structure*, **13**, 243-255.

Robins, P. and Lindahl, T. (1996) DNA ligase IV from HeLa cell nuclei. *J Biol Chem*, **271**, 24257-24261.

Rogakou, E.P., Boon, C., Redon, C. and Bonner, W.M. (1999) Megabase chromatin domains involved in DNA double-strand breaks in vivo. *J Cell Biol*, **146**, 905-916.

Rogakou, E.P., Pilch, D.R., Orr, A.H., Ivanova, V.S. and Bonner, W.M. (1998) DNA double-stranded breaks induce histone H2AX phosphorylation on serine 139. *J Biol Chem*, **273**, 5858-5868.

Rooney, S., Alt, F.W., Lombard, D., Whitlow, S., Eckersdorff, M., Fleming, J., Fugmann, S., Ferguson, D.O., Schatz, D.G. and Sekiguchi, J. (2003) Defective DNA repair and increased genomic instability in Artemis-deficient murine cells. *J Exp Med*, **197**, 553-565.

Rooney, S., Sekiguchi, J., Zhu, C., Cheng, H.L., Manis, J., Whitlow, S., DeVido, J., Foy, D., Chaudhuri, J., Lombard, D. and Alt, F.W. (2002) Leaky Scid phenotype associated with defective V(D)J coding end processing in Artemis-deficient mice. *Mol Cell*, **10**, 1379-1390.

Rosenzweig, K.E., Youmell, M.B., Palayoor, S.T. and Price, B.D. (1997) Radiosensitization of human tumor cells by the phosphatidylinositol3-kinase inhibitors wortmannin and LY294002 correlates with inhibition of DNA-dependent protein kinase and prolonged G2-M delay. *Clin Cancer Res*, **3**, 1149-1156.

Roth, D.B., Porter, T.N. and Wilson, J.H. (1985) Mechanisms of nonhomologous recombination in mammalian cells. *Mol Cell Biol*, **5**, 2599-2607.

Roth, D.B. and Wilson, J.H. (1985) Relative rates of homologous and nonhomologous recombination in transfected DNA. *Proc Natl Acad Sci U S A*, **82**, 3355-3359.

Roth, D.B. and Wilson, J.H. (1986) Nonhomologous recombination in mammalian cells: role for short sequence homologies in the joining reaction. *Mol Cell Biol*, **6**, 4295-4304.

Rothkamm, K. and Lobrich, M. (2003) Evidence for a lack of DNA double-strand break repair in human cells exposed to very low x-ray doses. *Proc Natl Acad Sci U S A*, **100**, 5057-5062.

Rouse, J. and Jackson, S.P. (2002) Interfaces between the detection, signaling, and repair of DNA damage. *Science*, **297**, 547-551.

Saintigny, Y., Delacote, F., Vares, G., Petitot, F., Lambert, S., Averbeck, D. and Lopez, B.S. (2001) Characterization of homologous recombination induced by replication inhibition in mammalian cells. *Embo J*, **20**, 3861-3870.

Sankaranarayanan, K. and Wassom, J.S. (2005) Ionizing radiation and genetic risks XIV. Potential research directions in the post-genome era based on knowledge of repair of radiation-induced DNA double-strand breaks in mammalian somatic cells and the origin of deletions associated with human genomic disorders. *Mutat Res*, **578**, 333-370.

Schultz, L.B., Chehab, N.H., Malikzay, A. and Halazonetis, T.D. (2000) p53 binding protein 1 (53BP1) is an early participant in the cellular response to DNA double-strand breaks. *J Cell Biol*, **151**, 1381-1390.

Senear, D.F. and Batey, R. (1991) Comparison of operator-specific and nonspecific DNA binding of the lambda cI repressor: [KCl] and pH effects. *Biochemistry*, **30**, 6677-6688.

Shao, R.G., Cao, C.X., Zhang, H., Kohn, K.W., Wold, M.S. and Pommier, Y. (1999) Replication-mediated DNA damage by camptothecin induces phosphorylation of RPA by DNA-dependent protein kinase and dissociates RPA:DNA-PK complexes. *Embo J*, **18**, 1397-1406.

Shiloh, Y. (2003) ATM and related protein kinases: safeguarding genome integrity. *Nat Rev Cancer*, **3**, 155-168.

Sibanda, B.L., Critchlow, S.E., Begun, J., Pei, X.Y., Jackson, S.P., Blundell, T.L. and Pellegrini, L. (2001) Crystal structure of an Xrcc4-DNA ligase IV complex. *Nat Struct Biol*, **8**, 1015-1019.

Singleton, B.K., Priestley, A., Steingrimsdottir, H., Gell, D., Blunt, T., Jackson, S.P., Lehmann, A.R. and Jeggo, P.A. (1997) Molecular and biochemical characterization of xrs mutants defective in Ku80. *Mol Cell Biol*, **17**, 1264-1273.

Singleton, B.K., Torres-Arzayus, M.I., Rottinghaus, S.T., Taccioli, G.E. and Jeggo, P.A. (1999) The C terminus of Ku80 activates the DNA-dependent protein kinase catalytic subunit. *Mol Cell Biol*, **19**, 3267-3277.

Sonoda, E., Hochegger, H., Saberi, A., Taniguchi, Y. and Takeda, S. (2006) Differential usage of non-homologous end-joining and homologous recombination in double strand break repair. *DNA Repair (Amst)*.

Spagnolo, L., Rivera-Calzada, A., Pearl, L.H. and Llorca, O. (2006) Three-dimensional structure of the human DNA-PKcs/Ku70/Ku80 complex assembled on DNA and its implications for DNA DSB repair. *Mol Cell*, **22**, 511-519.

Stewart, G.S., Wang, B., Bignell, C.R., Taylor, A.M. and Elledge, S.J. (2003) MDC1 is a mediator of the mammalian DNA damage checkpoint. *Nature*, **421**, 961-966.

Stiff, T., O'Driscoll, M., Rief, N., Iwabuchi, K., Lobrich, M. and Jeggo, P.A. (2004) ATM and DNA-PK function redundantly to phosphorylate H2AX after exposure to ionizing radiation. *Cancer Res*, **64**, 2390-2396.

Suwa, A., Hirakata, M., Takeda, Y., Jesch, S.A., Mimori, T. and Hardin, J.A. (1994) DNA-dependent protein kinase (Ku protein-p350 complex) assembles on double-stranded DNA. *Proc Natl Acad Sci U S A*, **91**, 6904-6908.

Taccioli, G.E., Gottlieb, T.M., Blunt, T., Priestley, A., Demengeot, J., Mizuta, R., Lehmann, A.R., Alt, F.W., Jackson, S.P. and Jeggo, P.A. (1994) Ku80: product of the XRCC5 gene and its role in DNA repair and V(D)J recombination. *Science*, **265**, 1442-1445.

Taccioli, G.E., Rathbun, G., Oltz, E., Stamato, T., Jeggo, P.A. and Alt, F.W. (1993) Impairment of V(D)J recombination in double-strand break repair mutants. *Science*, **260**, 207-210.

Takata, M., Sasaki, M.S., Sonoda, E., Morrison, C., Hashimoto, M., Utsumi, H., Yamaguchi-Iwai, Y., Shinohara, A. and Takeda, S. (1998) Homologous recombination and non-homologous end-joining pathways of DNA double-

strand break repair have overlapping roles in the maintenance of chromosomal integrity in vertebrate cells. *Embo J*, **17**, 5497-5508.

Thacker, J. and Wilkinson, R.E. (1991) The genetic basis of resistance to ionising radiation damage in cultured mammalian cells. *Mutat Res*, **254**, 135-142.

Thompson, L.H. and Jeggo, P.A. (1995) Nomenclature of human genes involved in ionizing radiation sensitivity. *Mutat Res*, **337**, 131-134.

Tomkinson, A.E., Vijayakumar, S., Pascal, J.M. and Ellenberger, T. (2006) DNA ligases: structure, reaction mechanism, and function. *Chem Rev*, **106**, 687-699.

Trujillo, K.M., Yuan, S.S., Lee, E.Y. and Sung, P. (1998) Nuclease activities in a complex of human recombination and DNA repair factors Rad50, Mre11, and p95. *J Biol Chem*, **273**, 21447-21450.

Tuteja, N., Tuteja, R., Ochem, A., Taneja, P., Huang, N.W., Simoncsits, A., Susic, S., Rahman, K., Marusic, L., Chen, J. and et al. (1994) Human DNA helicase II: a novel DNA unwinding enzyme identified as the Ku autoantigen. *Embo J*, **13**, 4991-5001.

Valerie, K. and Povirk, L.F. (2003) Regulation and mechanisms of mammalian double-strand break repair. *Oncogene*, **22**, 5792-5812.

van Attikum, H. and Gasser, S.M. (2005) The histone code at DNA breaks: a guide to repair? *Nat Rev Mol Cell Biol*, **6**, 757-765.

Van Dyck, E., Stasiak, A.Z., Stasiak, A. and West, S.C. (2001) Visualization of recombination intermediates produced by RAD52-mediated single-strand annealing. *EMBO Rep*, **2**, 905-909.

van Gent, D.C., Hoeijmakers, J.H. and Kanaar, R. (2001) Chromosomal stability and the DNA double-stranded break connection. *Nat Rev Genet*, **2**, 196-206.

Vanasse, G.J., Concannon, P. and Willerford, D.M. (1999) Regulated genomic instability and neoplasia in the lymphoid lineage. *Blood*, **94**, 3997-4010.

von Hippel, P.H. and Schleich, T. (1969) *Biological Macromolecules*. Marcel Dekker, Inc., New York.

von Kobbe, C., Harrigan, J.A., May, A., Opresko, P.L., Dawut, L., Cheng, W.H. and Bohr, V.A. (2003) Central role for the Werner syndrome protein/poly(ADP-ribose) polymerase 1 complex in the poly(ADP-ribosyl)ation pathway after DNA damage. *Mol Cell Biol*, **23**, 8601-8613.

Walker, J.R., Corpina, R.A. and Goldberg, J. (2001) Structure of the Ku heterodimer bound to DNA and its implications for double-strand break repair. *Nature*, **412**, 607-614.

Wang, Y.G., Nnakwe, C., Lane, W.S., Modesti, M. and Frank, K.M. (2004) Phosphorylation and regulation of DNA ligase IV stability by DNA-dependent protein kinase. *J Biol Chem*, **279**, 37282-37290.

Ward, I.M. and Chen, J. (2001) Histone H2AX is phosphorylated in an ATR-dependent manner in response to replicational stress. *J Biol Chem*, **276**, 47759-47762.

Wei, Y.F., Robins, P., Carter, K., Caldecott, K., Pappin, D.J., Yu, G.L., Wang, R.P., Shell, B.K., Nash, R.A., Schar, P. and et al. (1995) Molecular cloning and expression of human cDNAs encoding a novel DNA ligase IV and DNA ligase III, an enzyme active in DNA repair and recombination. *Mol Cell Biol*, **15**, 3206-3216.

West, R.B., Yaneva, M. and Lieber, M.R. (1998) Productive and nonproductive complexes of Ku and DNA-dependent protein kinase at DNA termini. *Mol Cell Biol*, **18**, 5908-5920.

West, S.C. (2003) Molecular views of recombination proteins and their control. *Nat Rev Mol Cell Biol*, **4**, 435-445.

Weterings, E. and van Gent, D.C. (2004) The mechanism of non-homologous end-joining: a synopsis of synapsis. *DNA Repair (Amst)*, **3**, 1425-1435.

Wood, R.D., Mitchell, M. and Lindahl, T. (2005) Human DNA repair genes, 2005. *Mutat Res*, **577**, 275-283.

Woodbury, C.P., Jr. (1981) Free-sliding ligands: an alternative model of DNA-protein interactions. *Biopolymers*, **20**, 2225-2241.

Wyman, C., Ristic, D. and Kanaar, R. (2004) Homologous recombination-mediated double-strand break repair. *DNA Repair (Amst)*, **3**, 827-833.

Yaneva, M., Kowalewski, T. and Lieber, M.R. (1997) Interaction of DNA-dependent protein kinase with DNA and with Ku: biochemical and atomic-force microscopy studies. *Embo J*, **16**, 5098-5112.

Yannone, S.M., Roy, S., Chan, D.W., Murphy, M.B., Huang, S., Campisi, J. and Chen, D.J. (2001) Werner syndrome protein is regulated and phosphorylated by DNA-dependent protein kinase. *J Biol Chem*, **276**, 38242-38248.

Yoo, S., Kimzey, A. and Dynan, W.S. (1999) Photocross-linking of an oriented DNA repair complex. Ku bound at a single DNA end. *J Biol Chem*, **274**, 20034-20039.

Zhang, Z., Hu, W., Cano, L., Lee, T.D., Chen, D.J. and Chen, Y. (2004) Solution structure of the C-terminal domain of Ku80 suggests important sites for protein-protein interactions. *Structure*, **12**, 495-502.

Zhao, J., Wang, J., Chen, D.J., Peterson, S.R. and Trewhella, J. (1999) The solution structure of the DNA double-stranded break repair protein Ku and its complex with DNA: a neutron contrast variation study. *Biochemistry*, **38**, 2152-2159.

Zhu, C., Bogue, M.A., Lim, D.S., Hasty, P. and Roth, D.B. (1996) Ku86-deficient mice exhibit severe combined immunodeficiency and defective processing of V(D)J recombination intermediates. *Cell*, **86**, 379-389.